DESIGN AND SYNTHESIS OF CHIRAL LIGANDS AND THEIR APPLICATION IN TRANSITION METAL-CATALYZED ASYMMETRIC HYDROGENATIONS

By

SHAODONG LIU

A dissertation submitted to the

Graduated School-New Brunswick

Rutgers, The State University of New Jersey

In Partial Fulfillment of the Requirements

For the degree of

Doctor of Philosophy

Graduate Program in Chemistry and Chemical Biology

Written under the direction of

Professor Xumu Zhang

And approved by

_____

_____

_____

_____

New Brunswick, New Jersey

October, 2016

ABSTRACT OF THE DISSERTATION

DESIGN AND SYNTHESIS OF CHIRAL LIGANDS AND THEIR APPLICATION IN TRANSITION METAL-CATALYZED ASYMMETRIC HYDROGENATIONS

By SHAODONG LIU

Dissertation Director:

Professor Xumu Zhang

Transition metal catalyzed hydrogenations are among the most powerful and direct approaches for the synthesis of organic molecules. During the past half century, chiral ligands have been extensively studied in transition metal catalyzed transformations. Development of new chiral ligands, efficient catalyst systems and their applications in the reduction of various prochiral unsaturated substrates are the focus of this dissertation.

In chapter 1, novel chiral tridentate f-amphox ligands were designed and synthesized. Two chiral wings in the ligands form a chiral pocket which introduces the chirality in the asymmetric hydrogenation. Tridentate f-amphox ligand has formed a highly enantioselective Iridium catalyst for direct

hydrogenation of β-aryl β-ketoesters (up to 99% ee) and 3-oxo-3-arylpropionic acid ethyl esters (up to 99% ee) with high turnover number (up to 1,000,000). In chapter 2, I focus on the highly enantioselective direct reductive amination of aromatic ketone. With phenylhydrazide as the nitrogen source, various chiral hydrazides were synthesized in excellent enantioselectivities and yields. In chapter 3, a highly efficient enantioselective hydrogenation of *N*-alkyl-2-arylpyridinium salts was discussed. This work provides the unique example of using a chiral phosphole-based ligand for highly efficient asymmetric catalysis. The mechanism of this transformation was studied and a mechanistic cycle was proposed.

ACKNOLEDGEMENTS

I express my deep sense of gratitude to my supervisor, Professor Xumu Zhang, whose encouragement, guidance, advices, valuable comments and support enabled me to accomplish my Ph.D. study and this dissertation at Rutgers-The state University of New Jersey, New Brunswick. Sharing his knowledge, experience, perspective and enthusiasm helped me to open my mind not only to chemistry but also to the whole world.

I wish to thank my committee members, Professor Leslie Jimenez, Professor Alan Goldman, Professor Kai Hultzsch and Professor Longqin Hu for their time and valuable discussions.

I would like to thank Dr. Mingxin Chang for his generous help when I just join Zhang group as a freshman. Dr. Chang and I composed Chapter two together. I wish to thank my collaborators Dr. Yuhua Huang and Dr. Yonggang Chen in Merck. Dr. Huang helped me to compose part of Chapter three. I would like to thank all other former and current group members in Zhang group for their help in the past five years, including Dr. Bonan Cao, Dr. Kexuan Huang, Dr. Tian Sun, Dr. Xin Zheng, Mr. Bin Qian, Mr. Jialin Wen, and Mr. Renchang Tan. I would like to thank all visiting students and visiting scholars in Zhang group for sharing ideas and offering valuable suggestions, including Dr. Qingyang Zhao, Dr. Tanglin Liu, Dr. Shengkun Li, Ms. Lin Yao, Mr. Yang Hu, Dr. Hao Xu, and Dr. Hongfei Lu. I would also like to thank undergraduate

student Song Kim who shared a good time with me to conduct reactions together and discuss chemistry.

I would like to express my special thanks to my parents: Yongsheng Liu and Wentan Shao. Their love encourages me to persuade Ph.D. degree. Last but not least, thanks are to my wife, Changyao. She is the one that has always been there devoting her endless love and cheering me up through the good and bad times.

Dedication

To my daughter, Katherine.

Table of Contents

List of Tables

List of Figures

Chapter 1

Design and Synthesis of Novel Chiral Tridentate Ligands and Their Applications in Asymmetric Hydrogenation

1.1 Introduction

Phosphorus ligands development for asymmetric hydrogenation

Among all the catalytic asymmetric methodologies to chiral compounds, homogeneous transition metal-catalyzed asymmetric hydrogenation plays a particularly important role. During the past half century, the asymmetric catalytic technology has become the most desirable and practical method for producing enantiopure chemicals, due to the fast increasing demand of pharmaceutical drugs, agrochemicals and other fine chemicals.[1] Because of its high efficiency and atom economy, homogeneous asymmetric hydrogenation becomes one of the most reliable and investigated methods.[2]

In 1939, the first report of homogeneous Rh-catalyzed hydrogenation published by Iguchi. In the 1960s, Knowles[3a] and Horner[3b] first reported that the enantioselective hydrogenation of prochiral double bonds is possible by using chiral versions of Wilkinson's catalyst. Since then, the development of methods to prepare chiral phosphine ligands has never stopped. To date, hundreds of chiral phosphine ligands have been created for asymmetric hydrogenation. We have to mention some of them because of their long-lasting impact on the history of asymmetric hydrogenation.

In the early 1970s, Kagan developed the first C_2-symmetric chelating bisphosphine DIOP (**1**). [4] (Figure 1-1-1) This work showed that a chelating ligand with backbone chirality is capable of inducing high enantioselectivity without *P*-chirality. Meanwhile, Knowles continued to develop an improved *P*-chiral bidentate ligand DIPAMP (**2**) which led to the first industrial scale synthesis of L-DOPA via asymmetric hydrogenation.[5] In 1980, A major breakthrough was made by Noyori and co-workers when they carried out pioneering studies on axially chiral BINAP (**3**).[6] The Ru-BINAP catalytic system was confirmed to show unprecedented substrate scope for both functionalized olefins and functionalized ketones.[6] Later, a Ru-BINAP-diamine system was discovered to show extremely high activity and selectivity to unfunctionalized simple ketones through a novel bifunctional mechanism.[6] Parallel to Noyori's research, significant progress was also made in the synthesis many efficient chiral phosphorus ligands for the Rh-catalyzed asymmetric hydrogenation. In 1991, Burk developed conformationally rigid electron-rich bis(phospholane) DuPhos (**4**) and BPE (**5**) for Rh-catalyzed hydrogenation of various functional olefins.[7] Those ligands could change their chiral environment through structural modification of the R group. A C_1-symmetric planar chiral ferrocene-based Josiphos (**6**) ligand was also developed later by Togni.[8] With modification of the two different chelating phosphine parts, a large ligand series has been prepared to fit the steric and electronic requirements of different substrates.[8b] Novel *P*-chiral trialkyl

phosphine ligands such as BisP*(7) were also reported to with impressive results by Imamoto.[9]

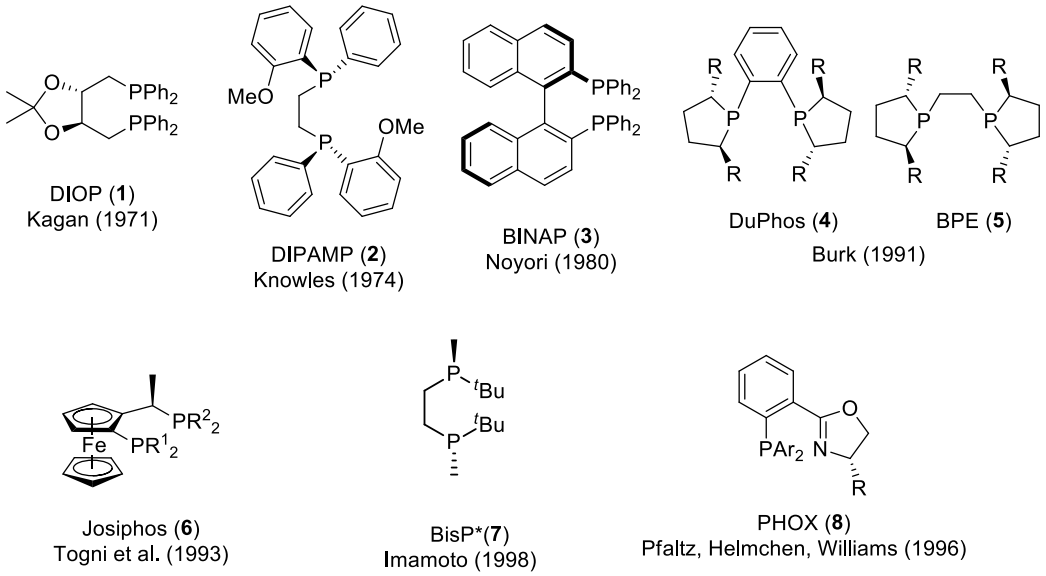

Figure 1.1. Historically important ligands for asymmetric hydrogenation

For Ir-catalyzed hydrogenation, the most important class of chiral modular ligands is P, N-ligand PHOX (**8**) developed by Pfaltz and others, which was designed to mimic Crabtree's catalyst for the hydrogenation of multi-substituted olefins.[10] Its two chelating donors are both sterically and electronically tunable, allowing Ir-catalyzed asymmetric hydrogenation of imines and unfunctionalized olefins to afford excellent enantioselectivities.

Although lots of asymmetric hydrogenations have been studied, mechanism of asymmetric hydrogenation was rarely studied. The generally accepted mechanism of Rh-catalyzed asymmetric hydrogenation of enamides was proposed by Halpern[11] and Brown[12] in the 1980s, which was established

by using Rh-catalysts generated from ligands such as DIPAMP and ChiraPhos. The so-called “unsaturated” mechanism is depicted in Figure 1-1-2 and encompasses four elemental steps:

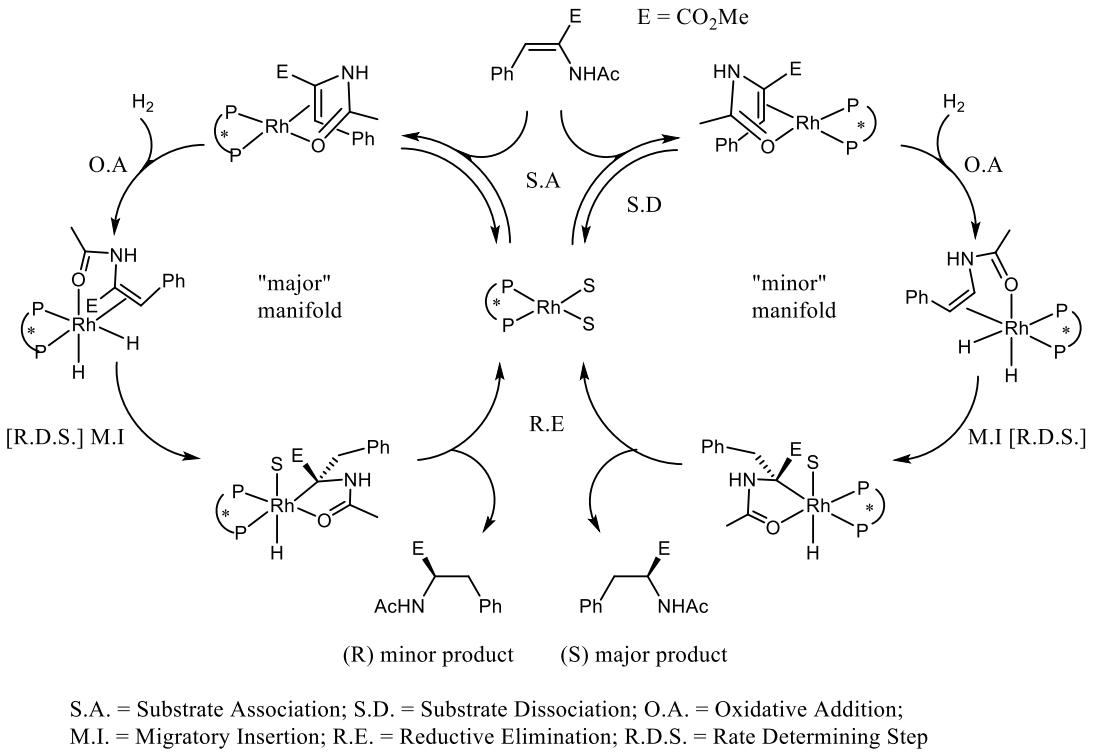

Figure 1.2. “Unsaturated” mechanism of Rh-catalyzed asymmetric hydrogenation.

(a) Reversible binding of the substrate to the catalyst affording a mixture of two diastereomeric Rh-substrate complexes. One of them is predominant as the major isomer; (b) irreversible oxidative addition of H_2 to the Rh-substrate complex, in which two manifolds are available from the diastereomeric Rh-substrate complexes; (c) irreversible migratory insertion of the alkene which is the rate determining step， providing a Rh-hydridoalkyl complex; and (d) irreversible reductive elimination leading to the product and regenerating the catalyst. The enantioselectivity in this reaction is confirmed to originate not

from the predominance of the major diastereomeric Rh-substrate complex, but from the much higher relative reactivity toward H_2 of the minor complex, which eventually gives the product with the experimentally observed configuration.

A chiral ligand toolbox has been developed by Zhang's lab. Different types of ligands have been designed and synthesized, including p-chiral ligands, bisphospholane, DIOP type ligands, PN ligands, ferrocene-based ligands, ligands with axial chirality and bifunctional ligands.

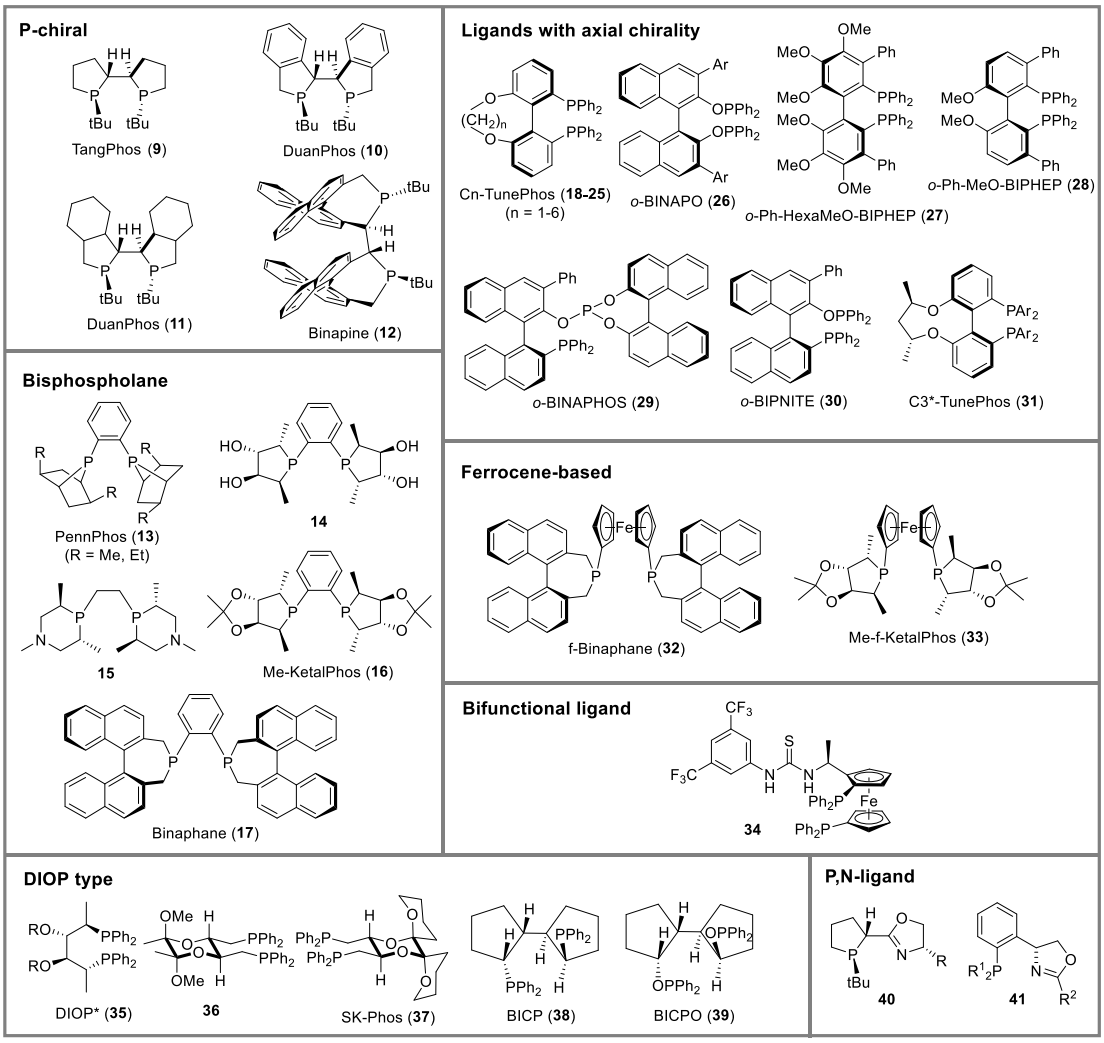

Figure 1.3. A chiral bidentate ligand toolbox developed by Zhang's lab

Despite over thousands of chiral diphosphines have been made, only a few of these ligands afforded the efficiency and selectivity required for commercial applications. There is no universal catalyst which gives both high enantioselectivity and activities for many substrates. Therefore, the discovery of new chiral ligands is greatly needed. Introducing these chiral ligands commercially will make a major and direct impact in asymmetric hydrogenation and other reactions.

1.2 Design and synthesis of novel chiral tridentate PNN ligands

1.2.1 Background of Tridentate Ligands with NH Moiety

Although traditional phosphine ligands have shown great potential in asymmetric hydrogenation, in many catalysts, the M-NH system has shown to be a key moiety for achieving high catalytic activity and excellent enantioselectivities in the hydrogenation of ketones. Extensive research by Noyori's group has resulted in a promising Ru(II)-TsDPEN (N-(p-tolylsulfonyl)-1, 2-diphenylethylene-diamine) transferring hydrogenation catalyst, $RuCl_2$(bisphosphine)(diamine) direct hydrogenation catalyst[13] and other related systems for reducing aromatic ketones. They suggest that a NH moiety in the ligand can undergo hydrogen bonding to a ketone substrate.

Following this breakthrough, a number of papers have published for both asymmetric transfer hydrogenation and direct hydrogenation of ketones.

Although bidentate ligands-metal catalyzed asymmetric reduction of ketones is one of the most fundamental organic transformations. Chiral tridentate ligands generally form a deeper chiral concave pocket around the metal center than the corresponding chiral bidentate ligands which may leads to better enantioselectivity. An example is the chiral bis(oxazolinyl)pyridine ligand (pybox) developed by Nishiyama, which has been successfully applied to numerous asymmetric reactions.[14] The two substituents on the oxazoline rings of pybox form a highly enantioselective “chiral fence”, which can effectively differentiate the *re* and *si* faces of many substrates.

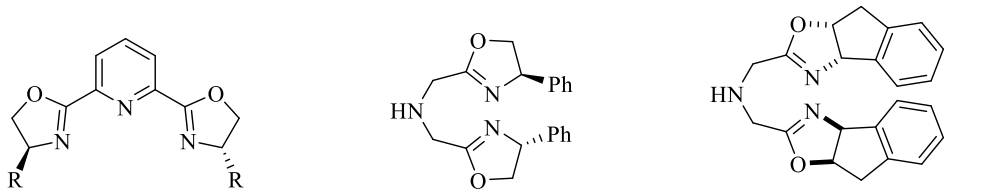

Figure 1.4. Examples of tridentate ligands.

Combine NH moiety and tridentate concept together, in 1998, Zhang designed and synthesized bis(oxazolinylmethyl)amine (Ambox) ligand, and successfully applied the in-situ generated Ru(II)-ph-Ambox complex in the asymmetric transfer hydrogenation (ATH) of simple ketones achieving high enantioselectivities.[15] In 2007, indan-ambox was prepared in our group and it

was successfully applied in direct asymmetric hydrogenation of simple ketones achieving high enantioselectivities and decent activity.[16]

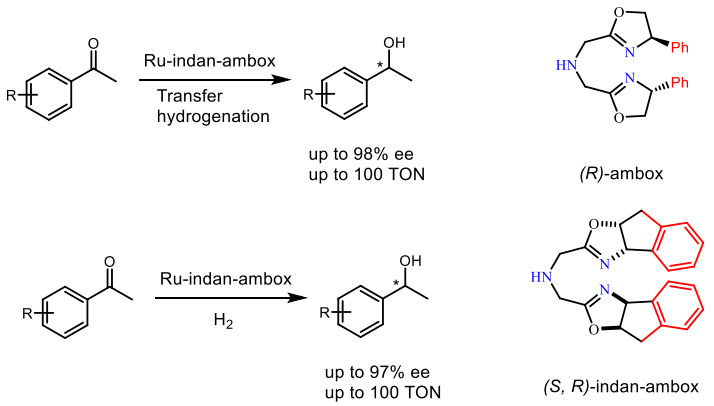

Figure 1.5. Applications of tridentate ligands with NH moiety.

By replacing the pyridine backbone of pybox with a secondary amine (NH) group, a similar six-membered cyclic transition state as suggested by Noyori[13] and highly enantioselective hydrogenation and transfer hydrogenation of simple ketones can be realized.

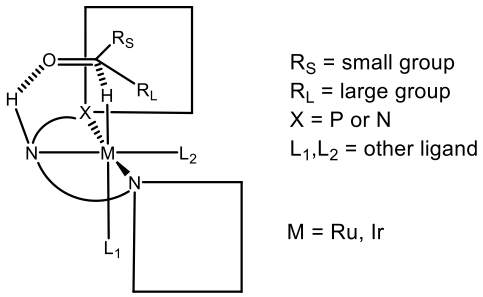

Figure 1.6. Proposed transition state of tridentate ligands with NH moiety.

In 2011, Zhou has made a breakthrough using catalysts with Ir-NH species for hydrogenation of ketones in an Ir-SpiroPAP system.[17] Excellent ee's and

turnovers have been achieved. Slight drawback is that the ligand synthesis is tedious. In 2012, Zhou applied this system to the hydrogenation of β-alkyl β-ketoesters.[18]

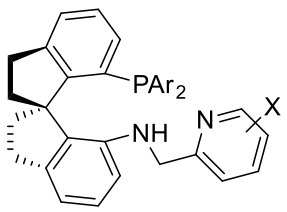

45a Ar = C_6H_3, X = H
45b Ar = 3,5-$(Me)_2C_6H_3$, X = H
45c Ar = 3,5-$(t\text{Bu})_2C_6H_3$, X = H
45d Ar = 3,5-$(t\text{Bu})_2C_6H_3$, X = 6-Me
45e Ar = 3,5-$(t\text{Bu})_2C_6H_3$, X = 6-Et
45f Ar = 3,5-$(t\text{Bu})_2C_6H_3$, X = 5,6-$(CH)_4$
45g Ar = 3,5-$(t\text{Bu})_2C_6H_3$, X = 3-Me
45h Ar = 3,5-$(t\text{Bu})_2C_6H_3$, X = 4-*t*Bu

Figure 1.7. SpiroPAP ligands.

1.2.2 Ferrocene Based Ligands

Chiral ferrocenylphosphines, which have planar chirality due to 1,2-unsymmetrically substituted ferrocene structure[19] and also have various functional groups such as an amino or a hydroxyl group, have been found to give rise to a high asymmetric induction in several transition metal catalyzed asymmetric reactions, such as hydrogenation of olefins, ketones, and imines.[20]

The ferrocene-based diphosphines are one of the most promising ligands in the enantioselective hydrogenation due to their unique structural advantages: 1) strong electron donating property of ferrocene ring; 2) ferrocene part is vertical to the metal-diphosphine planar, and 3) modifications of ferrocene-based phosphine ligands are easier.

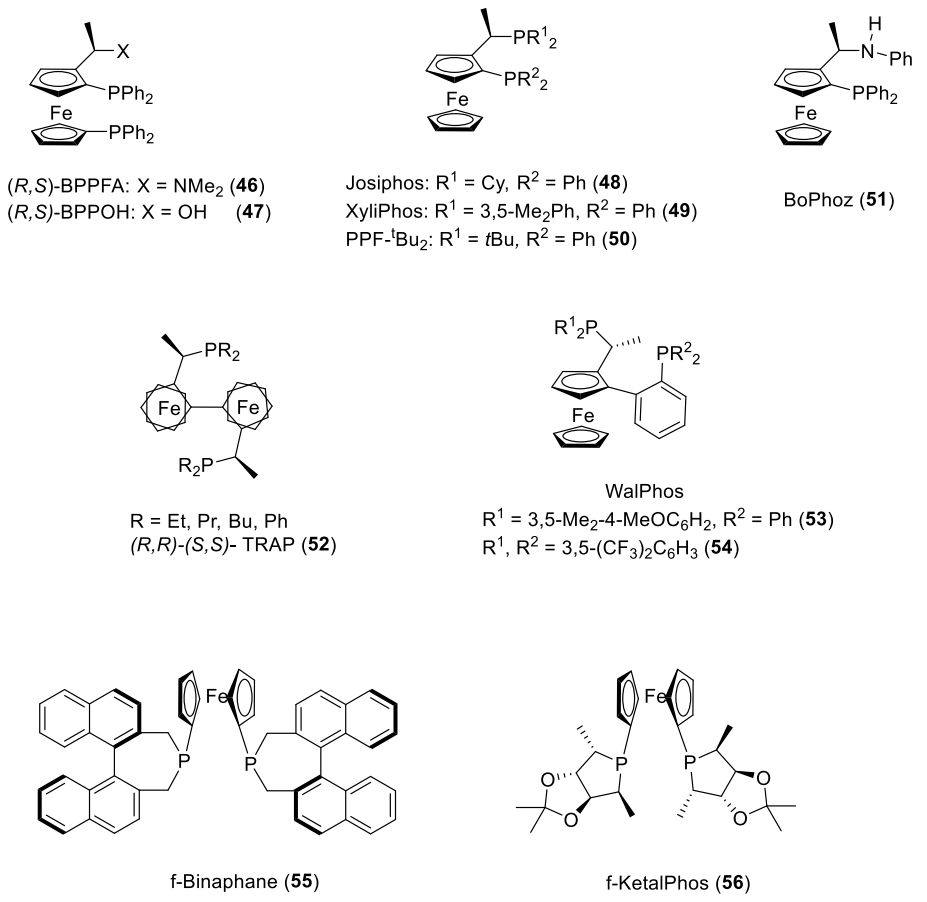

Figure 1.8. Ferrocene-based chiral ligands.

A typical strategy to synthesize ferrocene based chiral ligands is starting with chiral Ugi amine. Ferrocene can be aminomethylated with formaldehyde and dimethylamine in the presence of acid.[21] Tertiary amine was converted through its methiodide to the corresponding primary alcohol. Alcohol was then converted to its corresponding aldehyde with MnO_2. The reaction of aldehyde with dimethylamine and sodium cyanide will form aminonitrile. The aminonitrile was shown to react with methylmagnesium iodide to form tertiary amine, racemic Ugi amine.[22] The resolution of racemic Ugi amine with tartaric acid could provide corresponding chiral Ugi amine.

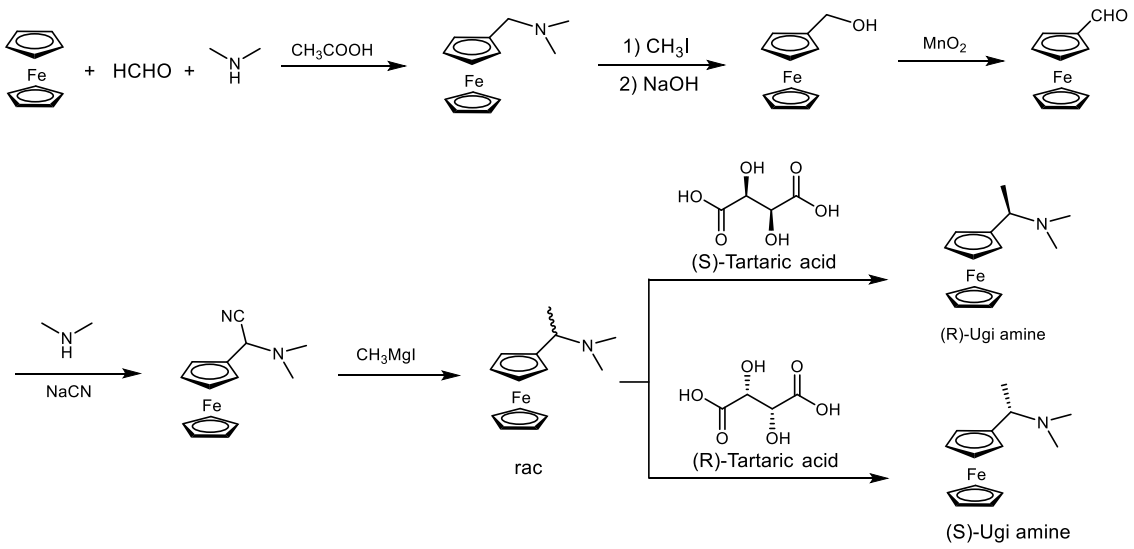

Figure 1.9. Synthesis of Ugi-amine.

Lithilation of Ugi amine with butyllithium produces a 96:4 mixture. Using (*R*)-Ugi amine as an example, it will form 96% (*R*)-(*S*) intermediate and 4% (*R*)-(*R*) intermediate. Subsequent treatment with phosphinechloride will provide corresponding PPFA. Recrystallization of this mixture will offer optical pure phosphine ligand.[19]

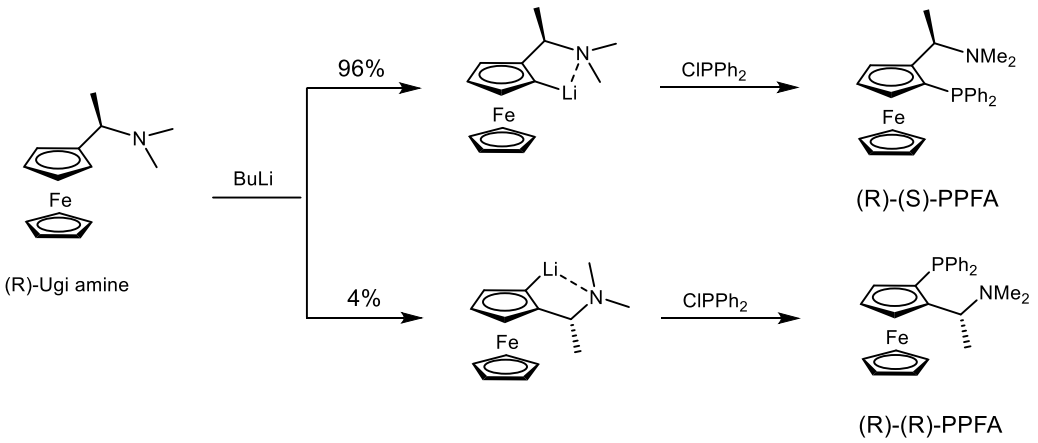

Figure 1.10. Introducing phosphine to Ugi-amine.

1.2.3 Oxazoline Based Tridentate Ligands

In 1998, Zhang designed and synthesized bis(oxazolinylmethyl)amine (Ambox) ligand.[15] Ambox contains two chiral oxazolines as two “wings” which are used to define the chiral environment. The reaction of iminodiacetonitrile with methanol and HCl gas afforded imidate. The HCl gas was generated by adding conc. HCl dropwise to conc. H_2SO_4. Then chiral amino alcohols were added to imidate under inert atmosphere to form corresponding ambox.

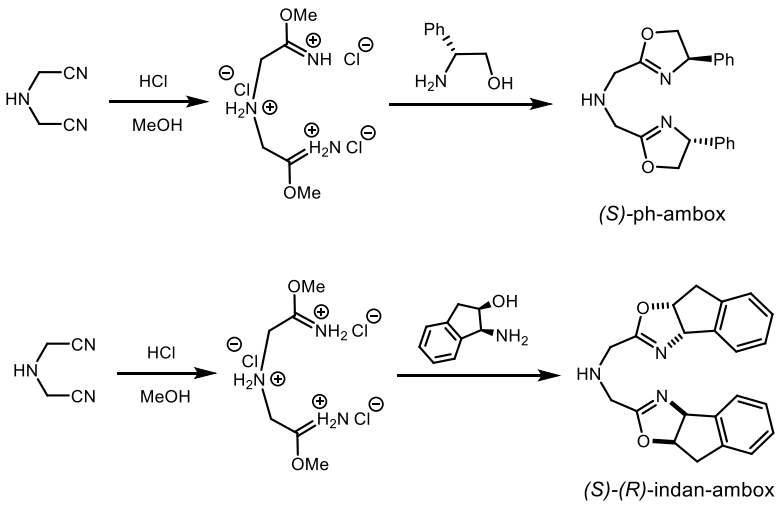

Figure 1.11. Synthesis of ambox.

1.2.4 Synthesis of novel chiral tridentate PNN ligands

Previous chiral tridentate ligands are almost all NNN ligands, weak lectron donating property leads to low reactivity. For example, ph-ambox could be used in transfer hydrogenation of ketone with only 100 TON (turnover number).

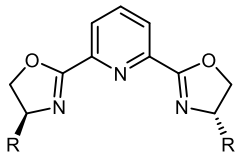

Pybox (42)

Absence of NH limits its application.

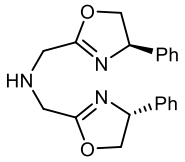

(R)-ph-ambox (43)

Weak electron donating property leads to low reactivity.

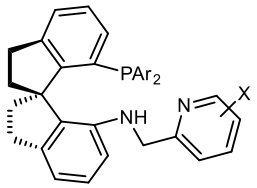

SpiroPAP (45)

Tedious systhetic route limits its application.

Figure 1.12. Drawbacks of current chiral tridentate ligands.

SpiroPAP could be a breakthrough due to the introducing of phosphine. The TON of Ir-SpiroPAP catalyzed hydrogenation of ketone could be 100,000. But tedious synthesis route limits its application.[23] Resolution with *N*-benzylcinchonidinium chloride is needed to obtain chiral Spinol.[24]

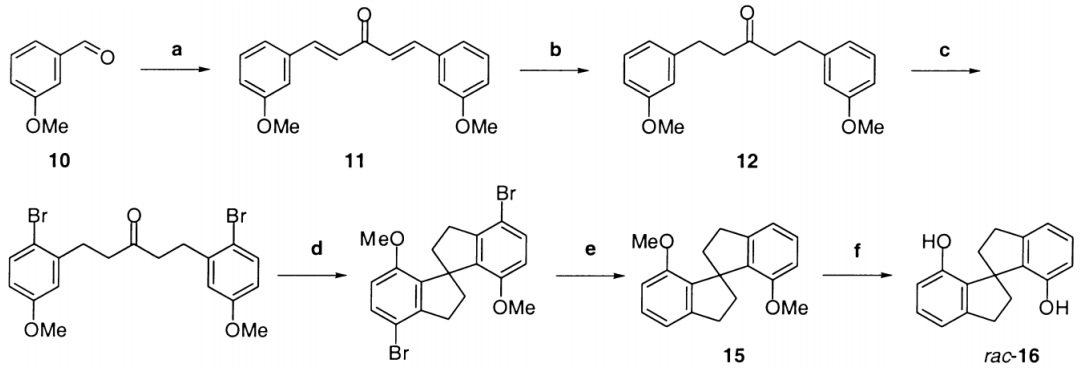

Reaction Conditions: (a) 0.5 eq Me_2CO, NaOH, 50% EtOH-H_2O, rt, 2h, 62%;[9] (b) Raney Ni, Me_2CO, rt, 1 atm. H_2, 1 day; (c) 2.5 eq Br_2, 3.5 eq pyridine, CH_2Cl_2; -10 °C to rt, 4h; (d) polyphosphoric acid, 105 °C, 5.5h, 57% for 3 steps;[7d] (e) *n*-BuLi (4 eq), THF, -78 °C, 1h; EtOH, 93%; (f) 2.3 eq BBr_3, CH_2Cl_2, -78 °C to rt overnight, 85%.

Figure 1.13. Synthesis of racemic Spinol.

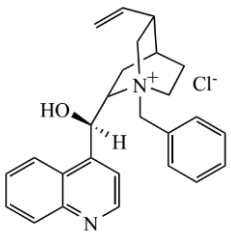

Figure 1.14. *N*-benzylcinchonidinium chloride used for the resolution of Spinol.

Inspired by previous work in Zhang's lab, I designed a class of new chiral tridentate PNN ligands. This class of ligand has the following advantages: 1) NH moiety will introduce a secondary interaction between catalyst and substrate, which will form a six-membered ring in the catalytic cycle; 2) replacing one nitrogen by a phosphine makes the ligand more electron donating, which may lead to higher reactivity; and 3) starting material, chiral Ugi-amine and chiral amino alcohols, are commercial available, which makes the synthesis much easier.

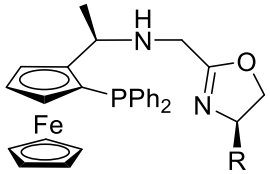

General Model of PNN

Figure 1.15. General Model of PNN

At first, based on the synthetic route of ambox, I proposed one synthetic route of new chiral tridentate PNN ligand as summarized:

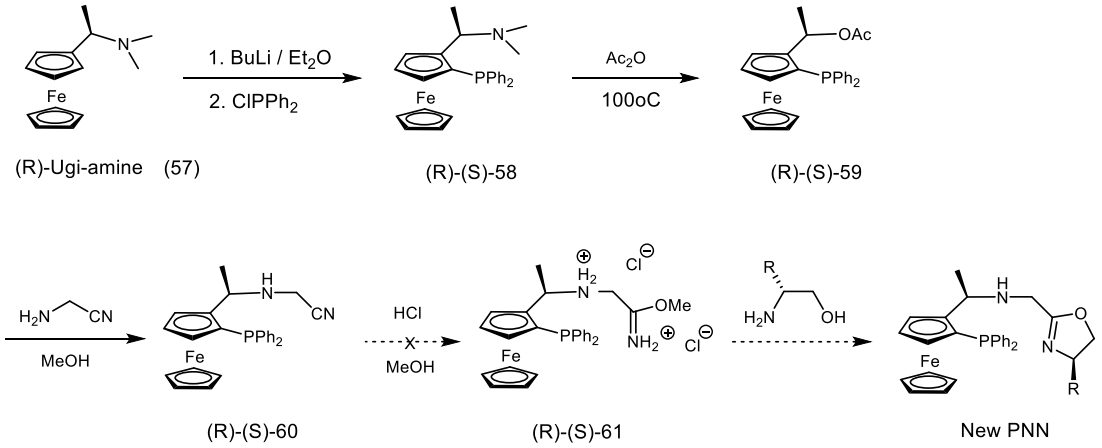

Figure 1.16. Proposed synthetic route of PNN based on the synthesis of ambox

(I) 12.4 ml of 1.4 M butyllithium in hexane was added to a solution of 3.60 g (14 mmol) of (R)-Ugi-amine (**57**) in 20 ml of dry ether at 0 ^{O}C over a period of 20 min. The mixture was stirred at room temperature for 1.5 h and then 6.2 g (28 mmol) of chlorodiphenylphosphine in 10 ml of ether was added with heating under gentle reflux in the course of 45 min. After 4 h reflux aqueous sodium bicarbonate was slowly added with cooling in an ice-bath. The resulting organic layer and ether extracts from the aqueous layer were combined, washed with water, dried over anhydrous sodium sulfate, and concentrated in vacuo to afford red oil. The oil was chromatographed to give a crud product. The product (**58**) was purified by recrystallization from ethanol to give 2.60 g (42% yield).

(II) In a degassed sealed glass tube, a mixture of 1 g (2.26 mmol) of (*R*)-(*S*)-**58** and 2.0 ml of acetic anhydride was heated at 100 ^{O}C for 2 h. It was then cooled to room temperature and aqueous ammonium chloride

was added to quench the reaction. The resulting organic layer and DCM extracts from the aqueous layer were combined, washed with water, dried over anhydrous sodium sulfate, and concentrated in vacuo to afford orange solid. This crude product (**59**) is directly used in the next step without purification.

(III) In a degassed sealed glass tube, a mixture of 1 g (2.26 mmol) of (*R*)-(*S*)-**59** and five equivalent of aminoacetonitrile were added. Seal the tube tightly. Purged by nitrogen twice. 10 ml of methanol was added. Then reflux the reaction overnight. Remove solvent under vacuum. Crude product was purified by column chromatography with DCM: MeOH=98:2 as eluent to give 0.82 g of pure product (83% yield).

However, the 4th step, generation of imidate, was unexpected failed. Under the same reaction condition as the condition in the synthesis of ambox, only starting material and some very polar things left. This may due to the instability of ferrocene ring under acidic condition.

An alternative route was proposed. Oxazoline was form before introducing to the ferrocene. The synthesis of (*S*)-(*R*)-f-amphox:

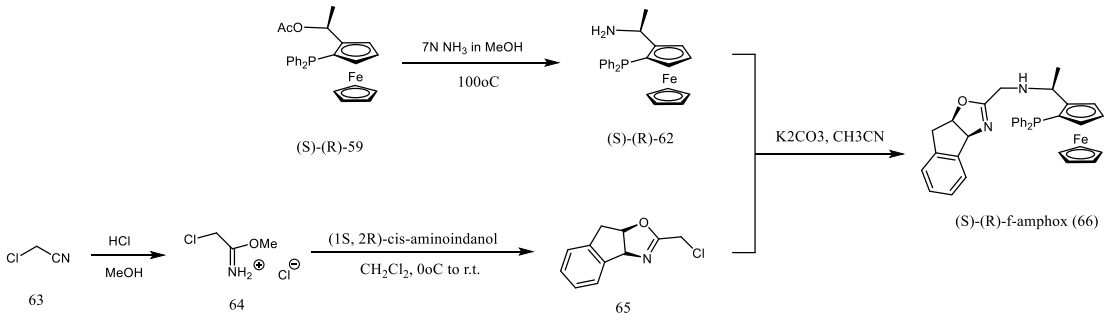

Figure 1.17. Alternative synthetic route of PNN

(1) 1g (2.19 mmol) of (*S*)-(*R*)-**59** was added in a sealed glass tube, purged by nitrogen twice. Then 10 ml of 7 M NH3 solution in MeOH was added from the sidearm. Seal the tube tightly. Then reflux the reaction overnight. Remove solvent under vacuum. Crude product was purified by column chromatography with DCM: MeOH=98:2 as eluent to give 0.78 g of pure product (86% yield).

(2) Under nitrogen atmosphere, 1ml (15.76 mmol) of 2-chloroacetonitrile (**63**) was added to a Schlenk flask with 30 ml of 2 M HCl in methanol at 0 ^{O}C. After 24 h, methanol was removed under vacuum. Crude product (**64**) was formed as white solid, and could be used without purification.

(3) Under nitrogen atmosphere, 3.5 g (23.64 mmol) of (1*S*, 2*R*)-*cis*-aminoindanol and 20 ml of DCM was added to (**64**) at 0 ^{O}C. Then let it went to room temperature. After 12 h, solvent was removed under vacuum to get crude product. Crude product was purified by column chromatography. 2.64 g pure product (**65**) was obtained (96% yield).

(4) Place 500 mg (1.2 mmol) of (*S*)-(*R*)-**62**, 10 eq K2CO3 and 1.1 eq oxazoline (**65**) in a round bottom flask, purged by nitrogen twice. 15 ml anhydrous acetonitrile was added by using syringe. Then reflux the reaction overnight. Remove solvent under vacuum. Crude product was purified by column chromatography with DCM:MeOH = 99:1 as eluent to give 230 mg of pure product (33% yield).

Other f-amphox families could be synthesized using the same strategy. The general synthesis strategy could be summarized:

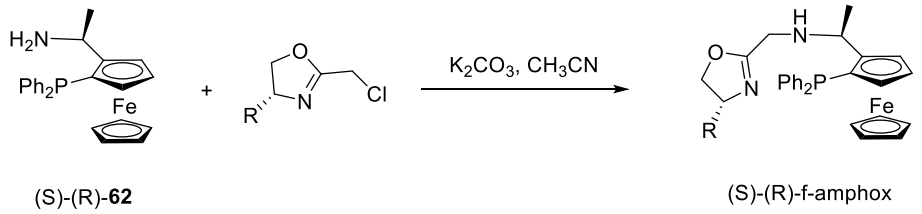

(S)-(R)-**62** (S)-(R)-f-amphox

Figure 1.18. General synthesis strategy of f-amphox

1.3 Application of novel tridentate PNN ligand in highly enantioselective iridium-catalyzed asymmetric hydrogenations of ketones

1.3.1 Asymmetric hydrogenation of β-aryl β-ketoesters Catalyzed by an Iridium-f-amphox Complex

In the Ru-NH catalyzed systems, hydrogenation of simple aryl alkyl ketones have been achieved in high ee's and high turnovers. Yet, no results have been reported for hydrogenation of β-aryl β-ketoesters due to negative impacts of chelating of substrates. For hydrogenation of β-alkyl β-ketoesters, $RuCl_2$(BINAP) system offer excellent ee's and turnovers under an acidic condition. However, for hydrogenation of β-aryl β-ketoesters, an important reaction for making key drug intermediates such as duloxetine and atomoxetine, much lower ee's and turnovers were observed.[25] Hydrogenation of β-aryl β-ketoesters remains as a significant problem in asymmetric hydrogenation area.

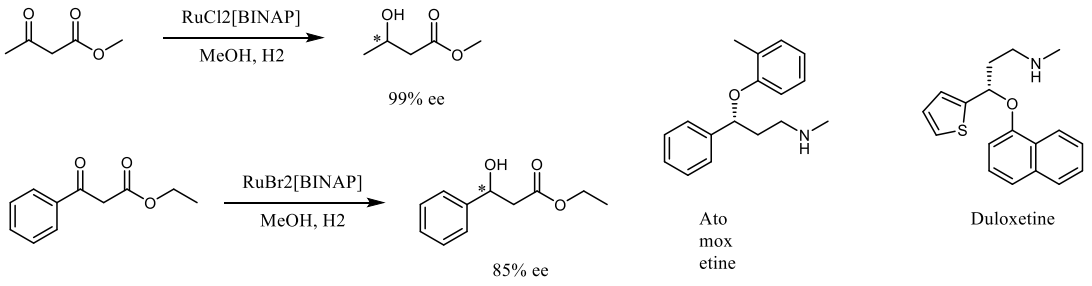

Figure 1.19. Ru catalyzed hydrogenation of β-ketoesters and applications of β-aryl β-hydroxylester in drug synthesis.

In 2012, Zhou has made a breakthrough using catalysts with Ir-NH species for hydrogenation of β-aryl β-ketoesters in an Ir-SpiroPAP system.[26] Excellent ee's and turnovers have been achieved. Slight drawback is that the ligand

synthesis is tedious. With f-amphox in hand, I applied Ir-f-amphox catalyst system to asymmetric hydrogenation of a variety of β-aryl β-ketoesters.

The general procedure to conduct the Ir-f-amphox catalyzed asymmetric hydrogenation is: in a nitrogen-filled glovebox, (S)-(R)-f-amphox (9.6 mg, 0.0165 mmol) and $[Ir(COD)Cl]_2$ (5.0 mg, 0.015 mmol) were placed into a vial and stirring for 30 min in methanol (1.5 ml). Ethyl 3-oxo-3-phenylpropanoate (0.2 mmol) were placed into 4 ml hydrogenation vials. 0.02 ml catalyst solution, remaining solvent and 1 mg of *t*BuOK were added. The vials were placed in an autoclave and following three H_2 purges, pressurized to 20 atm at room temperature for 20 h. After carefully releasing the hydrogen, solvent was removed under vacuum. Product was purified by column chromatography to give the corresponding hydrogenation products. Selectivities were determined by GC or HPLC.

Our initial study began with ethyl 3-oxo-3-phenylpropanoate (**68a**) as the model substrate and a brief screening of the performance of Iridium f-amphox in different solvent. Under 20 atm of hydrogen with 0.1 mol% Ir-(S)-(R)-f-amphox generated in situ, methanol could give 99% ee and 99% conversion (Table 1-1, entry 1). Our results showed that the smaller alcohol is, the better activity and enantioselectivity could be achieved and methanol provided the best enantioselectivity while in Ir-SpiroPAP system, ethanol provides the best result (entry 1 to 3). Non-polar solvents or polar aprotic solvents give low activities or low enantioselectivities (entry 2 to 6).

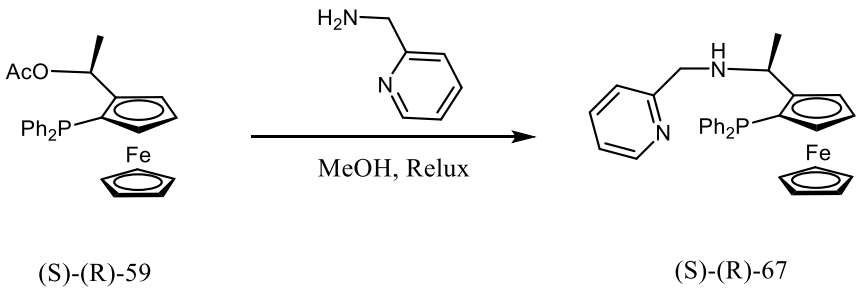

(S)-(R)-59 (S)-(R)-67

Figure 1.20. Synthesis of PNN with only one “chiral fence”

Unlike the orientation of N-H in Ir-SpiroPAP system is fixed, in Ir-f-amphox, the proton from NH could locate both sides of the PNN plane. To achieve high enantioselectivity, both “arms” of tridentate ligand should provide similar chiral atmosphere to make sure efficient chiral pocket established on the side, which six-membered ring transition state formed. If oxazoline-arm is replaced by pyridine (**67**) which is planar[27], ee value drops dramatically to 33% (entry 7). When the catalyst loading drops from 0.1 to 0.01 mol%, it also provided good conversion with 99% ee (entry 9).

Table 1.1. Asymmetric hydrogenation of ethyl 3-oxo-3-phyneylpropanoate. Optimizing reaction conditions.[a]

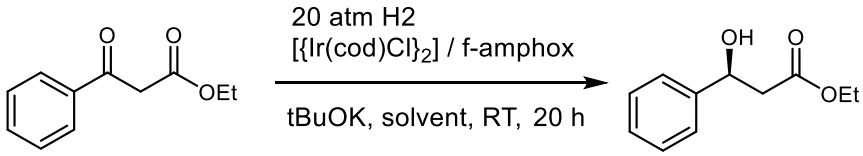

68a **69a**

Entry	Solvent	Conversion (%)[b]	ee (%)[b]
1	MeOH	99	99
2	EtOH	99	64
3	iPrOH	15	70
4	CH2Cl2	99	10
5	Toluene	0	-
6	THF	5	60
7[c]	EtOH	99	33
8[d]	MeOH	N.R.	-
9[e]	MeOH	99	99

[a] Reaction conditions: **68a** 0.2 M, 0.05 mol % [{Ir(cod)Cl}2], 0.1 mol % ligand, 1 mg *t*BuOK, solvent volumn=2.0 ml, 20 h. [b] Conversions were determined by NMR and enantiomeric excesses were determined by chiral HPLC or GC. [c] ligand = L2. [d] No tBuOK. [e] S/C=10000.

With the optimized condition, a variety of 3-oxo-3-arylpropionic acid ethyl esters (**68a-68m**) have been reduced to the corresponding secondary alcohols (Table 1-2) over Ir/(*S*)-(*R*)-f-amphox at S/C=1000. All of them provide high yield (91-99 %) and excellent enantioselectivities (92-99 %). Change of substituents on substrates has little effect on the enantioselectivities and activities.

Table 1.2. Iridium-catalysed asymmetric hydrogenation of β-aryl-β-ketoesters.[a]

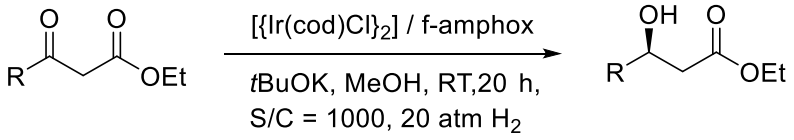

68 **69**

Entry	R	Product	Yield (%)[b]	*ee* (%)[c]
1	C_6H_5 (**68a**)	**69a**	99	99
2	2-MeC_6H_4 (**68b**)	**69b**	98	96
3	3-MeC_6H_4 (**68c**)	**69c**	96	99
4	4-MeC_6H_4 (**68d**)	**69d**	91	99
5	3-$MeOC_6H_4$ (**68e**)	**69e**	95	93
6	4-$MeOC_6H_4$ (**68f**)	**69f**	99	95
7	2-ClC_6H_4 (**68g**)	**69g**	99	92
8	3-ClC_6H_4 (**68h**)	**69h**	99	93
9	4-ClC_6H_4 (**68i**)	**69i**	93	95
10	4-BrC_6H_3 (**68k**)	**69k**	97	94
11	4-FC_6H_3 (**68l**)	**69l**	90	92
12	4-EtC_6H_3 (**68m**)	**69m**	95	98

[a] Reaction conditions: **68** 0.2 M, 0.05 mol % [{Ir(cod)Cl}$_2$], 0.1 mol % ligand, 1 mg *t*BuOK, solvent volumn=2.0 ml, 20 h. [b] Yields are isolated yields. [c] Enantiomeric excesses were determined by chiral GC or chiral HPLC.

In conclusion, a new chiral tridentate f-amphox ligand was synthesized and has formed a highly enantioselective iridium catalyst for direct hydrogenation of β-aryl β-ketoesters (up to 99% ee).

1.3.2 Asymmetric hydrogenation of 2-hydroxy-1-phenylethan-1-one Catalyzed by an Iridium-f-amphox Complex

After the successful hydrogenation of β-aryl β-ketoesters, the hydrogenation of 2-hydroxy-1-phenylethan-1-one draws our attention. The products, chiral diol, are ubiquitous structural motifs in natural products as well as key pharmacophores in many active pharmaceutical ingredients, such as Eluglustat, Levosalbutamol and Nebivolol.

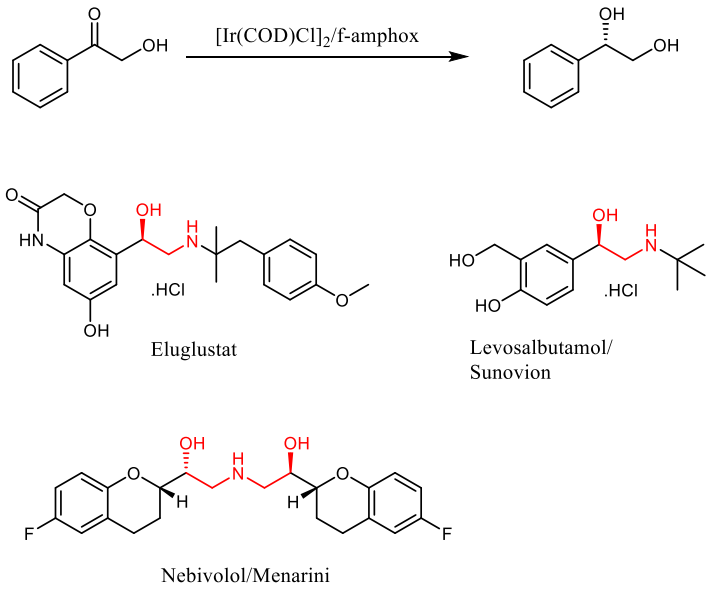

Figure 1.21. Synthesis of PNN with only one “chiral fence”

The optimized condition for this hydrogenation is similar to the condition applied to the hydrogenation of β-aryl β-ketoesters. This only difference is the solvent combination changed from methanol to CH_2Cl_2/*i*PrOH. With this optimized condition, a variety of 3-oxo-3-arylpropionic acid ethyl esters

(**68a-68m**) have been reduced to the corresponding secondary alcohols (Table 1-2) over Ir/(*S*)-(*R*)-f-amphox at S/C=1000. All of them provide high yield (91-99 %) and excellent enantioselectivities (92-99 %). Change of substituents on substrates has little effect on the enantioselectivities and activities.

Table 1.3. Iridium-catalysed asymmetric hydrogenation of 2-hydroxy-1-phenylethan-1-one.[a]

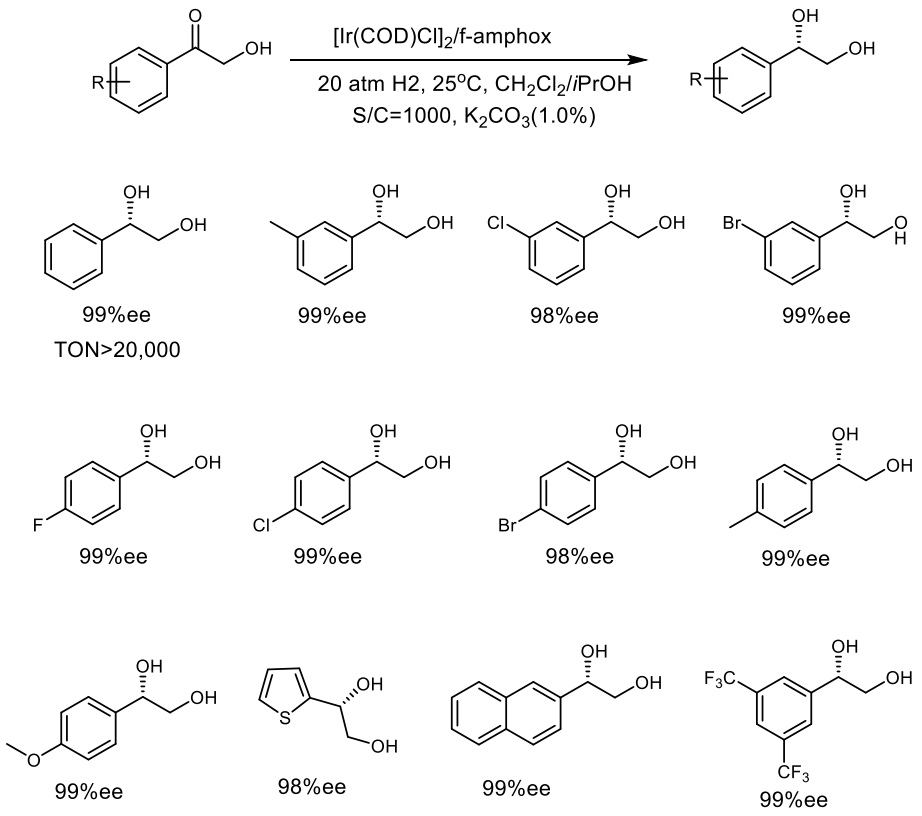

[a] Reaction conditions: **68** 0.2 M, 0.05 mol % [{Ir(cod)Cl}$_2$], 0.1 mol % ligand, 1 mg *t*BuOK, solvent volumn=2.0 ml, 20 h. Yields are isolated yields. Enantiomeric excesses were determined by chiral GC or chiral HPLC

In conclusion, tridentate f-amphox ligand has formed a highly enantioselective iridium catalyst for direct hydrogenation of 3-oxo-3-arylpropionic acid ethyl esters (up to 99% ee) with high turnover number.

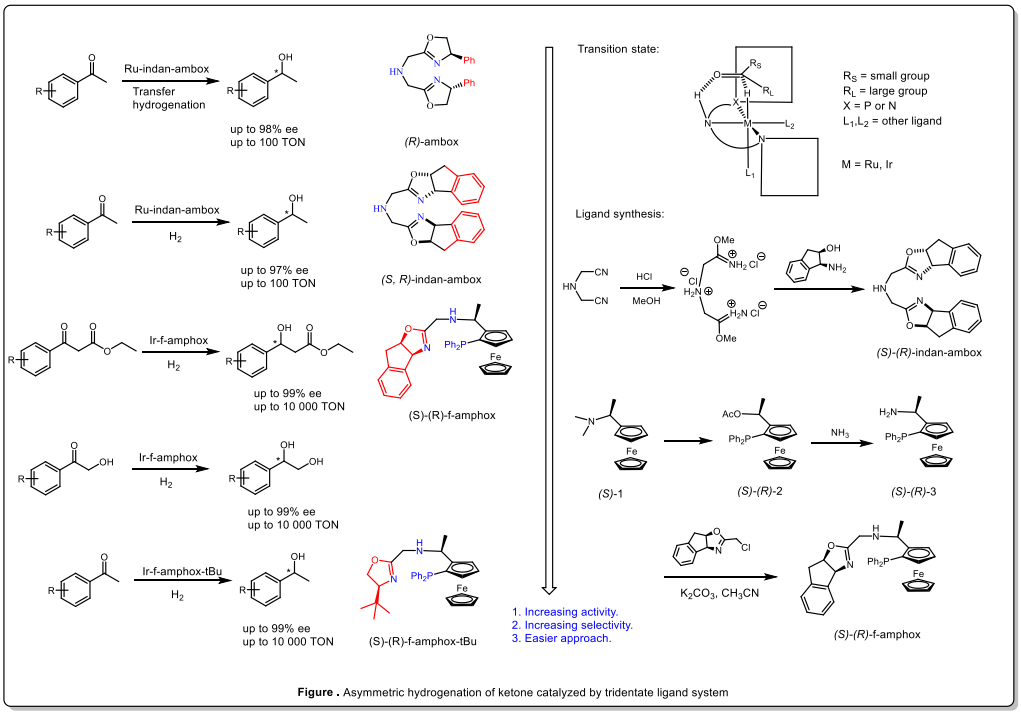

Figure . Asymmetric hydrogenation of ketone catalyzed by tridentate ligand system

Figure 1.22 Summary of tridentate ligands and their applications in asymmetric hydrogenation

1.3.3 Calculations

Density functional theory calculations as implemented in the Gaussian 09 series of programs21 have been applied to gain further insights into mechanism and the origins of enantioselectivity for reactants 5H-thiazol-4-ones 5a, allenoate 6c and 2c. All the stationary points are optimized at B3LYP/6-31G(d)22-23 level of theory (LANL08(f) basis set for Ir atom24-26). The harmonic vibrational frequencies were computed at the same level of theory to check whether the optimized structure is at an energy minimum or a transition state and to evaluate the corrections of enthalpy and Gibbs free energy. Solvent effects were computed by the PCM salvation model27 at the M05-2X/6-311+G(d,p)28 level of theory (LANL08(f) basis set for Ir atom) using the gas phase optimized structures. The values given by kcal/mol are the M05-2X calculated relative free energies in DCM solvent.

As shown in Figure 4, there are two possible conformational 7 isomers of the active catalyst hydrideiridium(III) species, which is endo-CP1 and exo-CP4. The isomerization barrier from CP1 to CP4 is only 10.9 kcal/mol via transition state TS4. The conformation of iridium-contained six-membered ring for both of CP1 and CP4 is boat type, although the six atoms of that ring are almost on the same plane. In conformational isomer CP4, the methyl group on C4 is equatorial, which leads to a strong static repulsion toward neighbored C2 and C6 moieties. Therefore, the relative free energy of CP4 is 8.4 kcal/mol higher than that of its conformational isomer CP1. The coordination of one molecule

hydrogen on complex CP1 generates an octahedral intermediate CP2 with 14.0 kcal/mol endothermic. The hydrogenation on the Re-face of N5 takes place via a concerted four-membered ring type transition state TS1, which a hydrideiridium intermediate CP3. The overall activation free energy of this step is 24.1 kcal/mol. In another case, the corresponding hydrogenation on the Si-face of N5 could occur from intermediate CP4 to afford intermediate CP6 with an activation free energy of 28.4 kcal/mol via transition state TS6. The computational results indicate that the formation of intermediate CP3 is kinetically and thermodynamically favorable.

Figure 1.23 Calculations

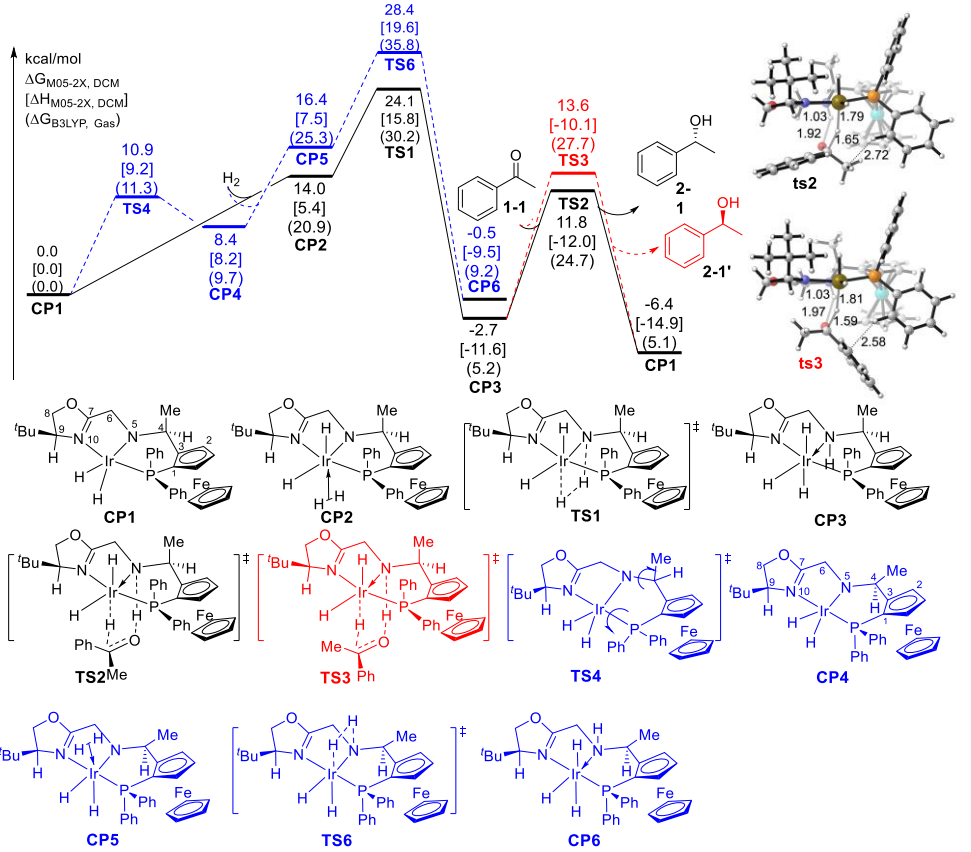

Figure 4 | The DFT computed energy surfaces of the iridium-catalyzed asymmetric hydrogenation of acetophenone. The values given by kcal/mol are the M05-2X calculated relative free energies in DCM solvent. The values in brackets are the M05-2X calculated relative Enthalpy in DCM solvent. The values in parentheses are the B3LYP calculated relative free energies in gas phase. Distances in geometry information are valued in Å.

The hydrogenation of acetophenone 1-1 with intermediate CP3 could take place via transition state TS2 or TS3, which forms the major product b-R or its enantioisomer 2-1', respectively. The relative enthalpy of TS2 is 1.8 kcal/mol lower than that of TS3. Therefore, 2-1 is the major product, and the theoretical predicated ee% is 90.1%, which is a little lower than that of experimental observation (92.8%). Moreover, the calculated free energy difference in gas phase is 3.0 kcal/mol,

which indicates an ee% value of 99%. Therefore, the computational deviation of enatioselectivity would be attributed to the solvent effect calculation. The geometry information of TS2 and TS3 are shown in Figure 4. In transition state TS2, the lengths of forming C-H bond and breaking Ir-H bond are 1.65Å and 1.79 Å, which are significantly longer and shorter than the corresponding typical single bonds, respectively. However, the lengths of the forming O-H bond and breaking N-H bond are 1.92 and 1.03, respectively, which are closed to a corresponding typical N-H…O hydrogen bond. Moreover, intrinsic reaction coordinate

Figure 1.24 2D contour maps of the Van der Waals surface of

intermediate CP3

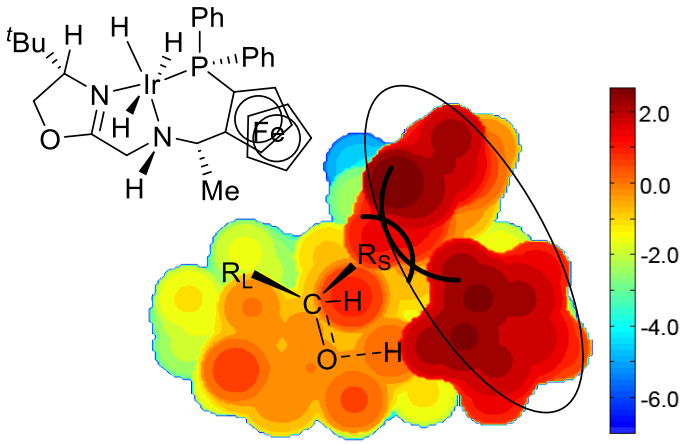

Figure 5 I Bottom-view 2D contour maps of the van der Waals surface of intermediate CP3. Distances are valued in Å. Negative distance (blue) indicates the atoms on complex is farther away from substrate; positive distance (red) indicates the atoms on complex is closer to substrate.

calculations indicate that transition state TS2 linked the reactant acetophenone with hydrogenated intermediate CP3 and phenylethanol with dehydrogenated intermediate CP1. Therefore, the hydrogenation step could be descripted as a polarized concerted hydride transfer followed by proton transfer. In geometry information of transition state TS3, the distance between the phenyl group of reacting acetophenone and the equatorial phenyl of ligand is only 2.58 Å, which indicates a significant repulsion. Therefore, the relative energy of transition state TS3 is higher than that of TS2.

To better illustrate the steric repulsions at different regions of hydrogenation step, a bottom-view 2D contour map along the z axis of the van

der Waals surface of intermediate CP3 is plotted in Figure 5. In this map, the z-axis is defined as the reacting Rh-H bond. The 2D contour map clearly indicates that the right part is occupied by the cyclopentadinene moiety and equatorial phenyl group in ligand, which block the right part when the hydrogenation takes place. Therefore, when acetophenone reacting with intermediate CP3, the larger group should be arranged at left.

1.4 Experiment Section

1.4.1 General remarks

All reactions were performed in the nitrogen-filled glovebox or under nitrogen using standard Schlenk techniques unless otherwise noted. Column chromatography was performed using Sorbent silica gel 60 (230 – 450 mesh). 1H NMR, and 13C NMR spectral data were obtained from Bruker 400 MHz spectrometers. Chemical shifts are reported in ppm. Enantiomeric ratios were determined by chiral GC or HPLC analysis. All new products were further characterized by HRMS. A positive ion mass spectrum of sample was acquired on a Micromass 70-VSE mass spectrometer with an electron ionization source.

1.4.2 General Procedures

Synthesis of (*S*)-*N,N*-Dimethyl-1-[(*R*)-2-(diphenylphosphin)ferrocenyl] ethylamine, (*S*)-(*R*)-58[28].

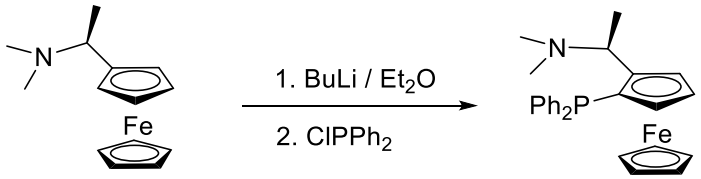

(*S*)-57 (*S*)-(*R*)-58

12.4 ml of 1.4 M butyllithium in hexane was added to a solution of 3.60 g (14 mmol) of (S)-1 in 20 ml of dry ether at 0 ^{O}C over a period of 20 min. The mixture was stirred at room temperature for 1.5 h and then 6.2 g (28 mmol) of chlorodiphenylphosphine in 10 ml of ether was added with heating under gentle reflux in the course of 45 min. After 4 h reflux aqueous sodium bicarbonate was slowly added with cooling in an ice-bath. The resulting organic layer and ether extracts from the aqueous layer were combined, washed with water, dried over anhydrous sodium sulfate, and concentrated in vacuo to afford red oil. The oil was chromatographed to give a crud product. The product was purified by recrystallization from ethanol to give 2.60 g (42% yield). ^{1}H-NMR (400 MHz, CDCl3): δ 1.25 (d, J = 6.8 Hz, 3H), 1.76 (s, 6H), 3.85 (d, J = 0.8 Hz, 1H), 3.94 (m, 5H), 4.17 – 4.10 (m, 1H), 4.24 (t, J = 2.3 Hz, 1H), 4.36 (d, J = 0.6 Hz, 1H), 7.27 – 7.13 (m, 5H), 7.39 – 7.31 (m, 3H), 7.64 – 7.54 (m, 2H). ^{13}C-NMR (400 MHz, CDCl3): δ 9.34, 39.01, 57.05, 57.12, 68.14, 69.23, 69.27, 69.62, 71.70, 71.75, 97.04, 97.27, 127.06, 127.24, 127.31,

127.82, 127.89, 128.63, 132.26, 132.45, 135.07, 135.28, 138.98, 139.08, 140.90, 140.97. ^{31}P-NMR (400 MHz, CDCl3): δ -22.86.

Synthesis of (*S*)-1-[(*R*)-2-(diphenylphosphin)ferrocenyl]ethyl acetate, (*S*)-(*R*)-59[28].

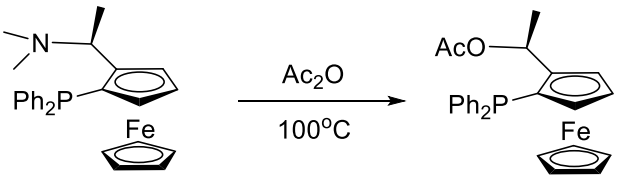

(*S*)-(*R*)-58 (*S*)-(*R*)-59

In a degassed sealed glass tube, a mixture of 1 g (2.26 mmol) of (S)-(R)-1* and 2.0 ml of acetic anhydride was heated at 100 ^{O}C for 2 h. It was then cooled to room temperature and aqueous ammonium chloride was added to quench the reaction. The resulting organic layer and DCM extracts from the aqueous layer were combined, washed with water, dried over anhydrous sodium sulfate, and concentrated in vacuo to afford orange solid. This crude product is directly used in the next step without purification. ^{1}H-NMR (400 MHz, CDCl3): δ 1.17 (s, 3H), 1.63 (d, J = 6.4 Hz, 3H), 3.83 – 3.77 (m, 1H), 4.08 – 4.03 (m, 2H), 4.35 (t, J = 2.5 Hz, 1H), 4.57 (dt, J = 2.5, 1.4 Hz, 1H), 6.21 (qd, J = 6.4, 2.8 Hz, 1H), 7.27 – 7.13 (m, 5H), 7.37 – 7.33 (m, 3H), 7.57 – 7.48 (m, 2H). ^{13}C-NMR (400 MHz, CDCl3): δ 18.45, 20.03, 68.37, 68.46, 69.17, 69.21, 69.57, 69.84, 70.38, 72.32, 72.36, 91.58, 91.82, 127.85, 127.93, 128.00, 128.07, 128.15, 129.13,

132.64, 132.83, 134.98, 135.19, 136.96, 137.05, 139.59, 139.69, 169.82. ^{31}P-NMR (400 MHz, CDCl3): δ -24.88

Synthesis of (*S*)-1-[(*R*)-2-(diphenylphosphin)ferrocenyl]ethyl amine, (*S*)-(*R*)-62.

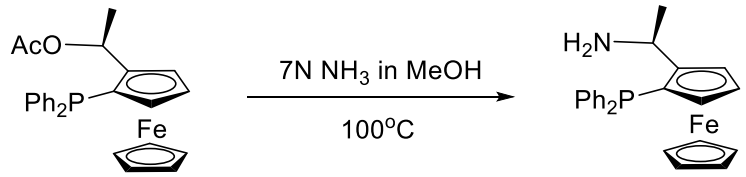

(*S*)-(*R*)-59 (*S*)-(*R*)-62

1g (2.19 mmol) of (S)-(R)-2 was added in a sealed glass tube, purged by nitrogen twice. Then 10 ml of 7 M NH3 solution in MeOH was added from the sidearm. Seal the tube tightly. Then reflux the reaction overnight. Remove solvent under vacuum. Crude product was purified by column chromatography with DCM: MeOH=98:2 as eluent to give 0.78 g of pure product (86% yield). ^{1}H-NMR (400 MHz, CDCl3): δ 1.57 (d, J = 6.7 Hz, 3H), 3.89 – 3.84 (m, 1H), 4.07 (d, J = 4.5 Hz, 5H), 4.38 – 4.30 (m, 2H), 4.54 (s, 1H), 5.83 (s, -NH2), 7.28 (m, 5H), 7.45 – 7.38 (m, 3H), 7.55 (ddd, J = 9.3, 6.7, 3.0 Hz, 2H). ^{13}C-NMR (400 MHz, CDCl3): δ 21.50, 21.75, 46.08, 69.38, 69.66, 69.77, 70.76, 71.67, 74.83, 96.36, 96.66, 128.22, 128.29, 128.60, 128.67, 129.33, 132.64, 132.83, 134.69, 134.90, 136.45, 139.33, 175.78. ^{31}P-NMR (400 MHz, CDCl3): δ -25.18

Synthesis of (*S*)-(*R*)-67.

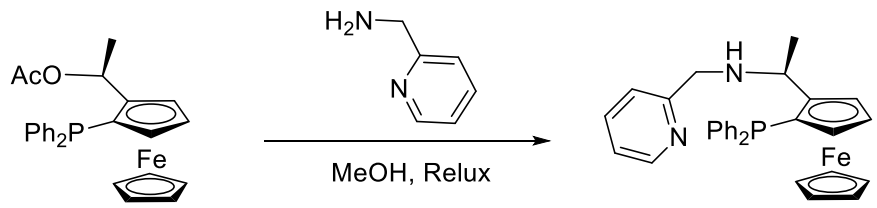

(*S*)-(*R*)-59 (*S*)-(*R*)-67

Place 1 g (2.19 mmol) of (S)-(R)-2 , 5 mmol of pyridin-2-ylmethanamine in a sealed glass tube, purged by nitrogen twice. 10 ml anhydrous methanol was added by using syringe. Then reflux the reaction overnight. Remove solvent under vacuum. Crude product was purified by column chromatography with DCM:MeOH=99:1 as eluent to give 0.85 g of pure product (77% yield). ^{1}H-NMR (400 MHz, CDCl3): δ 1.56 (d, J = 6.6 Hz, 3H), 3.63 (d, J = 3.1 Hz, 2H), 3.86 – 3.79 (m, 1H), 4.02 (s, 5H), 4.21 (d, J = 2.9 Hz, 1H), 4.31 (t, J = 2.4 Hz, 1H), 4.54 (s, 1H), 6.55 (d, J = 7.8 Hz, 1H), 6.98 (dd, J = 6.9, 5.1 Hz, 1H), 7.17 (dd, J = 4.9, 3.2 Hz, 3H), 7.42 – 7.31 (m, 7H), 7.61 – 7.54 (m, 1H), 8.33 (d, J = 4.6 Hz, 1H). ^{13}C-NMR (400 MHz, CDCl3): δ 19.50, 51.22, 51.31, 52.23, 69.12, 69.45, 69.49, 69.65, 71.27, 71.31, 75.05, 75.13, 97.60, 97.84, 121.34, 121.56, 128.05, 128.13, 128.23, 128.29, 132.72, 134.90, 135.11, 148.67, 159.88. ^{31}P-NMR (400 MHz, CDCl3): δ -25.02

Synthesis of

(3a*R*,8a*S*)-2-(chloromethyl)-3a,8a-dihydro-8H-indeno[1,2-d]oxazole 65.

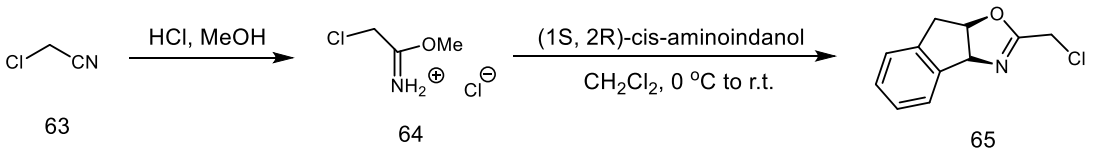

63 64 65

Under nitrogen atmosphere, 1ml (15.76 mmol) of 2-chloroacetonitrile was added to a Schlenk flask with 30 ml of 2 M HCl in methanol at 0 ^{O}C. After 24 h, methanol was removed under vacuum. 3.5 g (23.64 mmol) of (1S, 2R)-cis-aminoindanol and 20 ml of DCM was added at 0 OC. Then let it went to room temperature. After 12 h, solvent was removed under vacuum to get crude product. Crude product was purified by column chromatography. 2.64 g pure product was obtained (96% yield). ^{1}H-NMR (400 MHz, CDCl3): δ 3.28 (d, J = 18.1, 1H), 3.46 (dd, J = 18.0, 6.9 Hz, 1H), 4.15 – 3.98 (m, 2H), 5.51 – 5.36 (m, 1H), 5.60 (d, J = 7.9 Hz, 1H), 7.34 – 7.21 (m, 3H), 7.54 – 7.44 (m, 1H). ^{13}C-NMR (400 MHz, CDCl3): δ 36.53, 39.63, 84.37, 125.35, 125.49, 127.61, 128.76, 139.57, 141.09, 162.94.

Synthesis of (*S*)-(*R*)-f-amphox (66).

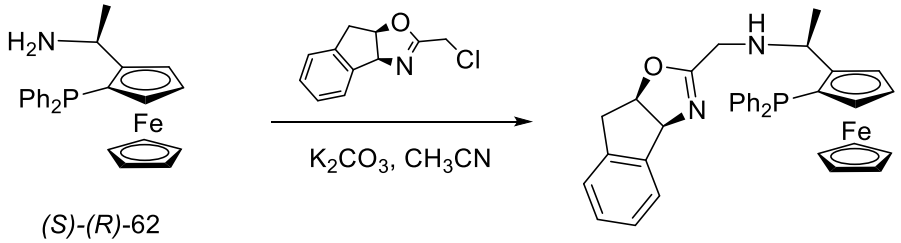

(S)-(R)-62 *(S)-(R)*-f-amphox (66)

Place 500 mg (1.2 mmol) of (*S*)-(*R*)-3 , 10 eq K2CO3 and 1.1 eq oxazoline in a round bottom flask, purged by nitrogen twice. 15 ml anhydrous acetonitrile

was added by using syringe. Then reflux the reaction overnight. Remove solvent under vacuum. Crude product was purified by column chromatography with DCM:MeOH=99:1 as eluent to give 230 mg of pure product (33% yield). ^{1}H-NMR (400 MHz, CDCl3): δ 1.40 (d, J = 6.6 Hz, 3H), 3.07 – 2.97 (m, 2H), 3.18 (d, J = 17.9 Hz, 1H), 3.32 (dd, J = 17.9, 6.9 Hz, 1H), 3.74 (d, J = 10.0 Hz, 1H), 4.02 – 3.90 (m, 7H), 4.26 (t, J = 2.4 Hz, 1H), 4.43 (s, 1H), 5.13 – 5.03 (m, 1H), 5.36 (d, J = 7.9 Hz, 1H), 7.58 – 7.05 (m, 14H). ^{13}C-NMR (400 MHz, CDCl3): δ 19.15, 39.62, 43.17, 50.65, 50.74, 69.02, 69.66, 69.72, 71.24 75.20, 75.28, 76.22, 83.00, 96.87, 97.11, 125.18, 125.50, 127.31, 128.07, 128.15, 128.20, 128.28, 128.37, 129.04, 132.58, 132.77, 134.76, 134.97, 137.10, 139.77, 142.07, 166.02.^{31}P-NMR (400 MHz, CDCl3): δ -25.07. HRMS calcd for C35H34FeN2OP+: 585.1753, found: 585.1750.

General Procedure for asymmetric hydrogenation

In a nitrogen-filled glovebox, (S)-(R)-f-amphox (9.6 mg, 0.0165 mmol) and [Ir(COD)Cl]2 (5.0 mg, 0.015 mmol) were placed into a vial and stirring for 30 min in methanol (1.5 ml). Ethyl 3-oxo-3-phenylpropanoate (0.2 mmol) were placed into 4 ml hydrogenation vials. 0.02 ml catalyst solution, remaining solvent and 1 mg of tBuOK were added. The vials were placed in an autoclave and following three H2 purges, pressurized to 20 atm at room temperature for 20 h. After carefully releasing the hydrogen, solvent was removed under

vacuum. Product was purified by column chromatography to give the corresponding hydrogenation products. Selectivities were determined by GC or HPLC.

ethyl 3-hydroxy-3-phenylpropanoate[29] (69a):

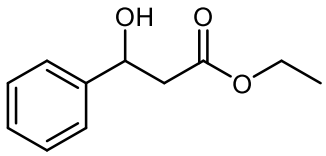

^{1}H NMR (400 MHz, CDCl3): δ 7.39-7.27 (m, 5H), 5.13 (dd, J = 4.0, 8.8 Hz, 1H), 4.18 (q, J = 7.2 Hz, 2H), 3.30 (brs, 1H), 2.79-2.67 (m, 2H), 1.26 (t, J = 7.2 Hz, 3H).

Enantiomeric excess was determined by Chiral HPLC, Chiralpak AD-H, hexane: i-PrOH = 95:5, flow rate: 1 mL/min, UV detector: 254 nm, t1 = 14.37 min, t2 = 15.15 min.

ethyl 3-hydroxy-3-(o-tolyl)propanoate[29] (69b):

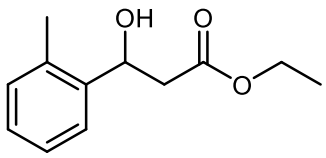

^{1}H NMR (400 MHz, CDCl3): δ 7.52–7.50 (m, 1H), 7.24–7.13 (m, 3H), 5.37–5.35 (m, 1H), 4.21 (q, J = 7.2 Hz, 2H), 3.21 (brs, 1H), 2.73–2.62 (m, 2H), 2.35 (s, 3H), 1.29 (t, J = 7.2 Hz, 3H).

Enantiomeric excess was determined by GC: Beta-390 column, 120 ^{o}C, 1 ml/min, t1 = 33.23 min, t2 = 38.79 min.

ethyl 3-hydroxy-3-(m-tolyl)propanoate[30] (69c):

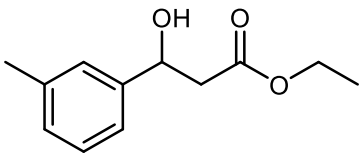

^{1}H NMR (400 MHz, CDCl3): δ 7.25–7.09 (m, 4H), 5.12–5.08 (m, 1H), 4.19 (q, J = 7.2 Hz, 2H), 3.24 (d, J = 3.2 Hz, 1H), 2.76 (dd, J = 8.8, 16.4 Hz, 1H), 2.69 (dd, J = 4.0, 16.4 Hz, 1H), 2.36 (s, 3H), 1.27 (t, J = 7.2 Hz, 3H).

Enantiomeric excess was determined by GC: Beta-390 column, 120 ^{o}C, 1 ml/min, t1 = 24.60 min, t2 = 26.40 min.

ethyl 3-hydroxy-3-(p-tolyl)propanoate[29] (69d):

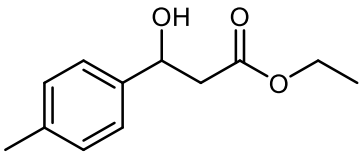

^{1}H NMR (400 MHz, CDCl3): δ 7.28–7.26 (m, 2H), 7.18–7.16 (m, 2H) , 5.10 (dd, J = 3.6, 8.8 Hz, 1H), 4.18 (q, J = 7.2 Hz, 2H), 3.20 (brs, 1H), 2.76 (dd, J = 4.4, 16 Hz, 1H), 2.68 (dd, J = 4, 16.4 Hz, 1H), 2.34 (s, 3H), 1.26 (t, J = 7.2 Hz, 3H).

Enantiomeric excess was determined by GC: Beta-390 column, 120 ^{o}C, 1 ml/min, t1 = 22.40 min, t2 = 23.99 min.

ethyl 3-hydroxy-3-(3-methoxyphenyl)propanoate[30] (69e):

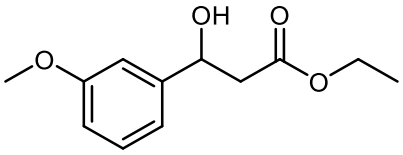

^{1}H NMR (400 MHz, CDCl3): δ 7.28–7.24 (m, 1H), 6.94–6.93 (m, 2H), 6.84–6.81 (m, 1H), 5.11 (dd, J = 4.4, 8.8 Hz, 1H), 4.19 (q, J = 7.2 Hz, 2H), 3.81 (s, 3H), 3.30 (brs, 1H), 2.78–2.67 (m, 2H), 1.27 (t, J = 7.2 Hz, 3H).

Enantiomeric excess was determined by GC: Beta-390 column, 135 ^{o}C, 1 ml/min, t1 = 28.6 min, t2 = 30.2 min.

ethyl 3-hydroxy-3-(4-methoxyphenyl)propanoate[29] (69f):

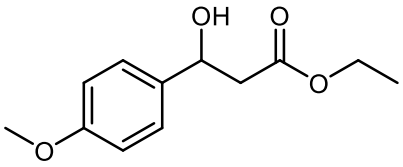

^{1}H NMR (400 MHz, CDCl3): δ 7.31–7.26 (m, 2H), 6.89–6.87 (m, 2H), 5.09 (dd, J = 3.6, 9.2 Hz, 1H), 4.18 (q, J = 7.2 Hz, 2H), 3.80 (s, 3H), 3.19 (brs, 1H), 2.76 (dd, J = 9.2, 16.4 Hz, 1H), 2.67 (dd, J = 3.6, 16.4 Hz, 1H), 1.26 (t, J = 7.2 Hz, 3H).

Enantiomeric excess was determined by GC: Beta-390 column, 135 ^{o}C, 1 ml/min, t1 = 28.5 min, t2 = 29.5 min.

ethyl 3-(2-chlorophenyl)-3-hydroxypropanoate[29] (69g):

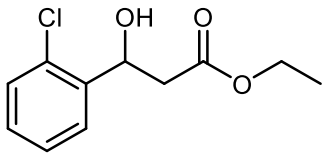

^{1}H NMR (400 MHz, CDCl3): δ 7.63 (d, J = 8 Hz, 1H), 7.34–7.29 (m, 2H), 7.24–7.20 (m, 1H), 5.49 (dd, J = 2.0, 9.6 Hz, 1H), 4.21 (q, J = 7.2 Hz, 2H), 3.59 (brs, 1H), 2.86 (dd, J = 2.8, 16.8 Hz, 1H), 2.58 (dd, J = 9.6, 16.8 Hz, 1H), 1.27 (t, J = 7.2 Hz, 3H).

Enantiomeric excess was determined by GC: Beta-390 column, 135 ^{o}C, 1 ml/min, t1 = 23.70 min, t2 = 33.30 min.

ethyl 3-(3-chlorophenyl)-3-hydroxypropanoate[31] (69h):

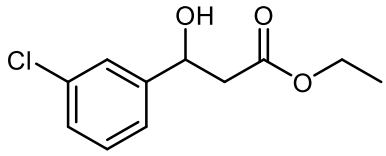

^{1}HNMR (400MHz, CDCl3) δ7.38 (s, 1H), 7.22-7.28 (m, 3H), 5.09(m, 1H), 4.18 (q, J=7.2H, 2H), 3.46 (br, 1H), 2.68-2.70 (m, 2H), 1.26 (t, J=7.2Hz, 3H).

Enantiomeric excess was determined by GC: Beta-390 column, 135 ^{o}C, 1 ml/min, t1 = 27.97 min, t2 = 28.94 min.

ethyl 3-(4-chlorophenyl)-3-hydroxypropanoate[29] (69i):

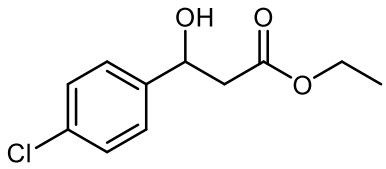

^{1}H NMR (400 MHz, CDCl3): δ 7.32 (m, 4H), 5.12–5.09 (m, 1H), 4.18 (q, J = 7.2 Hz, 2H), 3.40 (brs, 1H), 2.71–2.69 (m, 2H), 1.27 (t, J = 7.2 Hz, 3H).

Enantiomeric excess was determined by GC: Beta-390 column, 135 ^{o}C, 1 ml/min, t1 = 27.91 min, t2 = 29.12 min.

ethyl 3-(4-bromophenyl)-3-hydroxypropanoate[29] (69k):

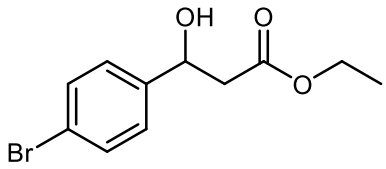

^{1}H NMR (400 MHz, CDCl3): δ 7.49–7.47 (m, 2H), 7.26–7.24 (m, 2H), 5.10–5.09 (m, 1H), 4.18 (q, J = 7.2 Hz, 2H), 3.41 (brs, 1H), 2.74–2.65 (m, 2H), 1.26 (t, J = 7.2 Hz, 3H).

Enantiomeric excess was determined by GC: Beta-390 column, 135 ^{o}C, 1 ml/min, t1 = 48.2 min, t2 = 50.2 min.

ethyl 3-(4-fluorophenyl)-3-hydroxypropanoate[29] (69l):

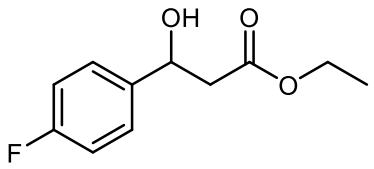

^{1}H NMR (400 MHz, CDCl3): δ 7.32 (m, 2H), 7.02 (m, 2H), 5.08 (dd, J=4.3, 8.6 Hz, 1H), 4.15 (q, J=7.1 Hz, 2H), 3.20 (br, 1H), 2.67 (m, 2H), 1.24 (t, J=7.0 Hz, 3H).

Enantiomeric excess was determined by GC: Beta-390 column, 115 ^{o}C, 1 ml/min, t1 = 23.4 min, t2 = 24.6 min.a

ethyl 3-(4-ethylphenyl)-3-hydroxypropanoate[32] (69m):

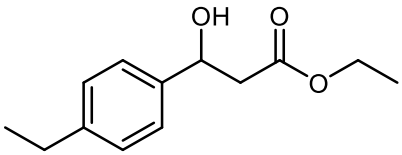

^{1}H NMR (400 MHz, CDCl3): δ 7.27 (d, J=8.0 Hz, 2H), 7.17 (d, J=8.0 Hz, 2H), 5.09 (dd, J=9.1, 3. Hz, 1H), 4.16 (q, J=7.1 Hz, 2H), 3.3 (s, 1H), 2.7 (ddd, J=16.2, 9.1, 3.8 Hz, 2H), 2.63 (q, J=7.5 Hz, 2H), 1.24 (t, J=7.1 Hz, 3H), 1.21 (t, J=7.6 Hz, 3H).

Enantiomeric excess was determined by GC: Beta-390 column, 120 ^{o}C, 1 ml/min, t1 = 37.9 min, t2 = 39.7 min.

1.5. Reference:

1. (a) Izumi, Y.; Tai, A. *Stereo-Differentiating Reactions: The Nature of Asymmetric Reactions*; Academic Press: New York, **1977**. (b) Bosnich, B., Ed. In *Asymmetric Catalysis*; Martinus Nijhoff: New York, **1986**. (c) Ojima, I., Ed. In *Catalytic Asymmetric Synthesis*; VCH: New York, **1993**. (d) Noyori, R. *Asymmetric Catalysis in OrganicSynthesis*; Wiley: New York, **1994**. (e) Jannes, G., Dubois, V., Eds. In *Chiral Reactions in Heterogeneous Catalysis*; Plenum: New York, **1995**. (f) Cornils, B., Herrmann, W. A., Eds. In *Applied Homogeneous Catalysis with Organometallic Compounds*; VCH: Weinheim, **199**6; Vols. 1 and 2. (g) Ojima, I., Ed. In *catalytic Asymmetric Synthesis*; Wiley-VCH; New York, 2010.

2. (a) Noyori, R.; Kitamura, M. In *Modern Synthetic Methods*; Scheffold, R., Ed.; Springer: Berlin, **1989**; Vol. 5, p 115. (b) Takaya, H.; Ohta, T.; Noyori, R. In *Catalytic Asymmetric Synthesis*; Ojima, I., Ed.; VCH: New York, **1993**; p 1. (c) Tang, W.; Zhang, X. *Chem. Rev*. **2003**, *103*, 3029.

3. (a) Knowles, W. S.; Sabacky, M. J. *Chem. Commun.* **1968**, 1445. (b) Horner, L.; Siegel, H.; Buthe, H. *Angew. Chem. Int. Ed.* **1968**, *7*, 942.
4. (a) Vineyard, B. D.; Knowles, W. S.; Sabacky, M. J.; Bachman, G. L.; Weinkauff, O. J. *J. Am. Chem. Soc.* **1977**, *99*, 5946. (b) Knowles, W. S. *Acc. Chem. Res.* **1983**, *16*, 106.

5. Miyashita, A.; Yasuda, A.; Takaya, H.; Toriumi, K.; Ito, T.; Souchi, T.; Noyori, R. *J. Am. Chem. Soc.* **1980**, *102*, 7932.
6. (a) Noyori, R.; Ohkuma, T. *Angew. Chem. Int. Ed.* **2001**, *40*, 40. (b) Noyori, R. *Angew. Chem. Int. Ed.* **2002**, *41*, 2008.
7. (a) Burk, M. J. *J. Am. Chem. Soc.* **1991**, *113*, 8518. (b) Burk, M. J.; Feaster, J. E.; Nugent, W. A.; Harlow, R. L. *J. Am. Chem. Soc.* **1993**, *115*, 10125. (c) Burk, M. J. *Acc. Chem. Res.* **2000**, *33*, 363.
8. (a) Togni, A.; Breutel, C.; Schnyder, A.; Spindler, F.; Landert, H.; Tijani, A. *J. Am. Chem. Soc.* **1994**, *116*, 4062. (b) Blaser, H.-U.; Brieden, W.; Pugin, B.; Spindler, F.; Studer, M.; Togni, A. *Top. Catal.* **2002**, *19*, 3.
9. (a) Imamoto, T.; Watanabe, J.; Wada, Y.; Masuda, H.; Yamada, H.; Tsuruta, H.; Matsukawa, S.; Yamaguchi, K. *J. Am. Chem. Soc.* **1998**, *120*, 1635.
10. (a) Halpern, J.; Riley, D. P.; Chan, A. S. C.; Pluth, J. J. *J. Am. Chem. Soc*. **1977**, *99*, 8055. (b) Chan, A. S. C.; Halpern, J. *J. Am. Chem. Soc.* **1980**, *102*, 838. (c) Chan, A. S. C.; Pluth, J. J.; Halpern, J. *J. Am. Chem. Soc.* **1980**, *102*, 5952. (d) Halpern, J. *Science* **1982**, *217*, 401. (e) Landis, C. R.; Halpern, J. *J. Am. Chem. Soc.* **1987**, *109*, 1746. (f) Landis, C. R.; Hilfenhaus, P.; Feldgus, S.; *J. Am. Chem. Soc.* **1999**, *121*, 8741. (g) Feldgus, S.; Landis, C. R. *J. Am. Chem. Soc.* **2000**, *122*, 12714.
11. (a) Halpern, J.; Riley, D. P.; Chan, A. S. C.; Pluth, J. J. *J. Am. Chem. Soc*. **1977**, *99*, 8055. (b) Chan, A. S. C.; Halpern, J. *J. Am. Chem. Soc.* **1980**, *102*, 838. (c) Chan, A. S. C.; Pluth, J. J.; Halpern, J. *J. Am. Chem. Soc.* **1980**, *102*, 5952. (d) Halpern, J. *Science* **1982**, *217*, 401. (e) Landis, C. R.; Halpern, J. *J. Am. Chem. Soc.* **1987**, *109*, 1746. (f) Landis, C. R.; Hilfenhaus, P.; Feldgus, S.; *J. Am. Chem. Soc.* **1999**, *121*, 8741. (g) Feldgus, S.; Landis, C. R. *J. Am. Chem. Soc.* **2000**, *122*, 12714.

12. (a) Brown, J. M.; Chaloner, P. A. *J. Chem. Soc., Chem. Commun.* **1978**, 321. (b) Brown, J. M.; Chaloner, P. A. *Tetrahedron Lett.* **1978**, *19*, 1877 (c) Brown, J. M.; Chaloner, P. A. *J. Chem. Soc., Chem. Commun.* **1979**, 613. (d) Brown, J. M.; Chaloner, P. A. *J. Chem. Soc., Chem. Commun.* **1980**, 344. (e) Brown, J. M.; Chaloner, P. A.; Glaser, R.; Geresh, S. *Tetrahedron* **1980**, *36*, 815. (f) Alcock, N. W.; Brown, J. M.; Derome, A.; Lucy, A. R. *J. Chem. Soc., Chem. Commun.* **1985**, 575. (g) Brown, J. M.; Chaloner, P. A.; Morris, G. A. *J. Chem. Soc., Chem. Commun.* **1983**, 664. (h) Brown, J. M.; Chaloner, P. A.; Morris, G. A. *J. Chem. Soc., Perkin Trans. 2*, **1987**, 1583. (i) Brown, J. M. *Chem. Soc. Rev.* **1993**, *22*, 25. (j) Giernoth, R.; Heinrich, H.; Adams, N. J.; Deeth, R. J.; Bargon, J.; Brown, J. M. *J. Am. Chem. Soc.* **2000**, *122*, 12381.
13. (a) Hashigushi, S.; Fujii, A.; Takehara, J.; Ikariya, T.; Noyori, R. *J. Am. Chem. Soc.* **1995**, 117, 7562. (b) Gao, J.; Ikariya, T.; Noyori, R. *Organometallics* **1996**, 15, 1087. (c) Gamez, P.; Fache, F.; Lemaire, M. *Tetrahedron Asymmetry* **1995**, 6, 705.
14. (a) Nishiyama, H.; Sakaguchi, H.; Nakamura, T.; Horihata, M.; Kondo, M.; Itoh, K. *Organometallics* **1989**, 8, 846. (b) Desimoni, G.; Faita, G.; Quadreil, P. *Chem. Rev.* **2003**, 103, 3119. (c) McManus, H. A.; Guiry, P. *J. Chem. Rev.* **2004**, 106, 3561.
15. Jiang, Y.; Jiang, Q.; Zhang, X. *J. Am. Chem. Soc.* **1998**, 120, 3817.
16. Li, W.; Hou, G.; Wang, C.; Jiang, Y.; Zhang, X. *Chem. Commun.* **2010**, 46, 3979.
17. Xie, J.; Liu, X.; Xie, J.; Wang, L.; Zhou, Q. *Angew. Chem. Int. Ed.* **2011**, 50, 7329.
18. Xie, J.; Liu, X.; Yang, X.; Xie, J.; Wang, L.; Zhou, Q. *Angew. Chem. Int. Ed.* **2012**, 51, 201.
19. Marquarding, D.; Klusacek, H.; Gokel, G.; Hoffmann, P.; and Ugi, I. *J. Am. Chem. Soc.* **1970**, 5389.
20. a) Hayashi, T.; Mise, T.; Mitachi, S.; Yamamoto, K.; and Kumada, M. *Tetrahedron Lett.*, **1976**, 1133. b) Cullen, W. and Yeh, E-S. *J. Organomet. Chem.*, **1977**, 13. c) Hayashi, T.; Mise, T. and Kumada, M. *Tetrahedron Lett.*, **1976**, 4351.
21. Lindsay, J. K. and Hauser, C. R. *J. Org. Chem.* **1957**, 355.
22. Lindsay, J. K. and Hauser, C. R. *J. Org. Chem.* **1957**, 906.
23. Birman, V.; Rheingold, A. and Lam K.C. *Tetrahedron: Asymmetric*, **1999**, 125.
24. Zhang, J.; Liao, J.; Cui, X.; Yu, K.; Zhu, J.; Deng, J.; Zhu, S.; Wang, L.; Zhou, Q.; Chung, L. and Ye, T. *Tetrahedron: Asymmetric*, **2002**, 1363-1366.
25. a) Tang, W.; Zhang, X. *Chem. Rev.* **2003**, 103, 3029; b) Noyori, R. *Angew. Chem.* **2002**, 114, 2108; *Angew. Chem. Int. Ed.* **2002**, 41, 2008.
26. Xie, J.; Liu, X.; Yang, X.; Xie, J.; Wang, L.; Zhou, Q. *Angew. Chem. Int. Ed.* **2012**, 51, 201.
27. Nie, H.; Zhou, G.; Wang, Q.; Chen, W.; Zhang S. *Tetrahedron: Asymmetry* **2013**, 24, 1567.
28. Hayashi, T.; Mise, T.; Fukushima, M.; Kagotani, M.; Nagashima, N.; Hamada, Y.; Matsumoto, A.; Kawakami, S.; Konishi, M.; Yamamoto, K. *Bull. Chem. Soc. Jpn.* **1980**, 53, 1138.
29. Zhou, Y.; Tang, W.; Wang, W.; Li, W.; and Zhang, X. *J. Am. Chem. Soc.* **2002**, 124, 4953.
30. Xie, J.; Liu, X.; Yang, X.; Xie, J.; Wang, L.; Zhou, Q. *Angew. Chem. Int. Ed.* **2012**, 51, 201.
31. Wan, X.; Sun, Y.; Luo, Y.; Li, D.; Zhang, Z. *J. Org. Chem.* **2005**, 70, 1070.
32. Padhi, S.; Titu, D.; Pandian, N.; Chadha, A. *Tetrahedron*, **2006**, 62, 5133.

Chapter 2

Direct Catalytic Asymmetric Reductive Amination of Simple Aromatic Ketones

2.1 Introduction

The paramount significance of chiral amines in pharmaceutical and agrochemical substances drives the development of efficient catalytic asymmetric methods for their formation.[1] Reductive amination with ammonia could be an efficient, tandem process for the synthesis of chiral amines. In this process, aldehydes or ketones react with ammonia to form an imine, and the imine undergoes metal-catalyzed hydrogenation to form an amine.

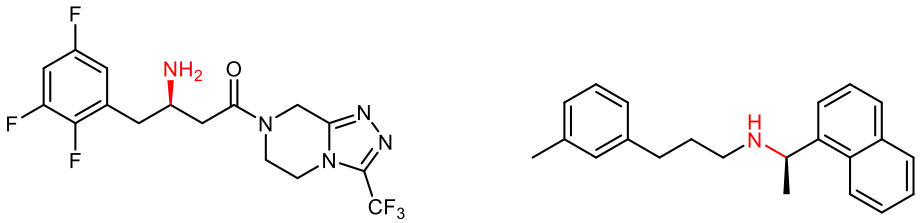

Januvia
By Merck

Cinacalcet
By Amgen

Figure 2.1. Examples of chiral amine moiety in drugs

The first example of asymmetric reductive amination was reported by Blaser et al. Using the Ir-Xyliphos complex, they found that methoxyacetone reacted

with 2-methyl-5-ethylaniline to yield an enriched chiral amine as a precursor of an important grass herbicide, with complete conversion and 78% ee.[2]

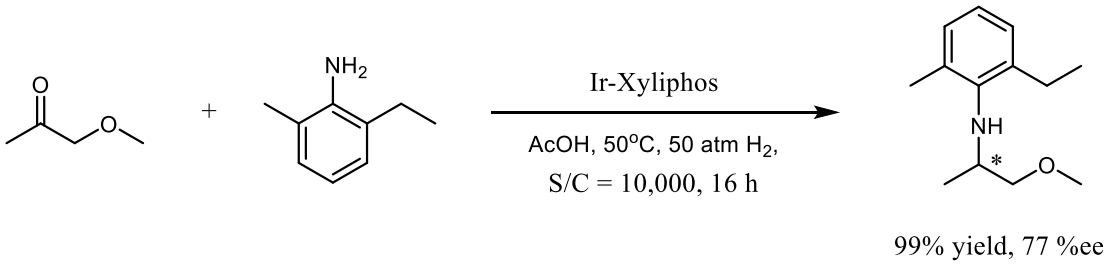

Figure 2.2. First reductive amination reported by Blaser *et al.*

In 2000, Borner et al. reported the first general homogeneous catalytic reductive amination of aldehydes with secondary amines as nucleophiles and hydrogen gas as the reductant.[3] Beller et al. then reported a rhodium-catalyzed reductive amination of aldehydes with ammonia.

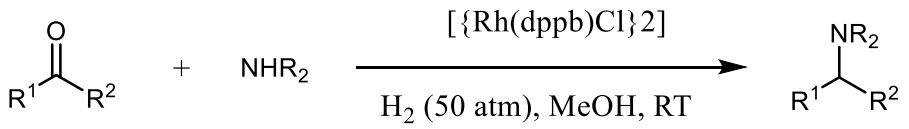

R1= alkyl, aryl
R2=H, alkyl
NHR_2=pyrrolidine, piperidine, dimethylamine, diethylamine

Figure 2.3. First general homogeneous catalytic reductive amination reported by Borner *et al.*

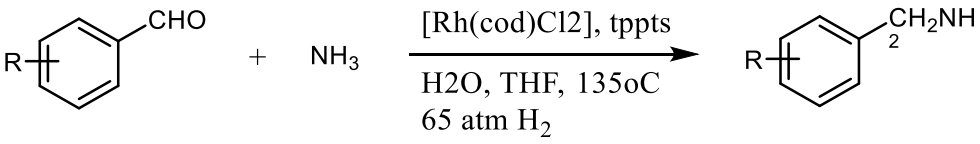

Figure 2.4. First reductive amination with ammonia reported by Beller *et al.*

A biphasic system was used to segregate the amine product from the water-soluble rhodium catalyst and ammonia nucleophile.[4] The asymmetric hydrogenation of *N*-(1-phenylethylidene) aniline with Ir-f-Binaphane complex was reported Zhang.[1] The presence of Ti(O-*i*-Pr)$_4$ and I_2 during asymmetric reductive amination of aryl ketones with Ir-f-Binaphane catalyst offered high enantioselectivity with high order of catalytic. Reductive amination with ammonia was first shown by Fukuzumi and coworkers to form α-amino acids from α-keto acids in aqueous solvent.[5] Careful control of the reaction conditions was necessary, and the highest yields of α-amino acids were achieved with ammonium formate and a pH between 5 and 6.5.

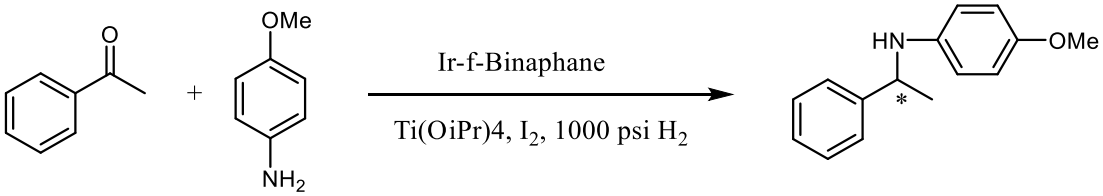

Figure 2.5. First general homogeneous catalytic asymmetric reductive amination reported by Zhang *et al.*

The first asymmetric reductive amination involving an ammonium salt was discovered by workers at Merck and applied to the synthesis of the Type II Diabetes drug, Januvia.[6] Reaction of a 1,3-diketone with ammonium acetate formed the unprotected enamine. Asymmetric hydrogenation of the enamine with [{Rh(cod)Cl}$_2$] and the Josiphos ligand PPF-tBu formed Januvia with greater than 99% conversion and 95% ee.

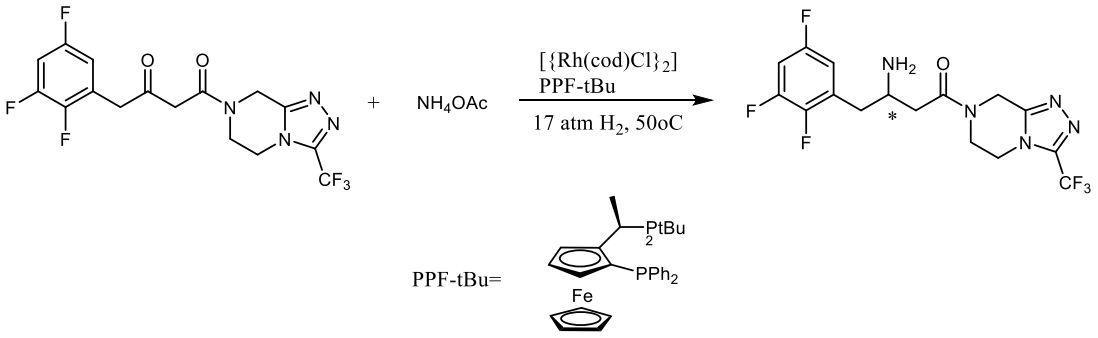

Figure 2.6. Reductive amination as the key step in the synthesis of Januvia by Merck.

The challenges stands as obstacle to the advance on reductive amination are: 1) The starting ketones can be reduced before the reductive amination takes place; 2) The E/Z isomers resulting from the acyclic imine intermediate make stereoselective reduction difficult; 3) The amine used as nitrogen source inhibits the reactivity of the transition metal.

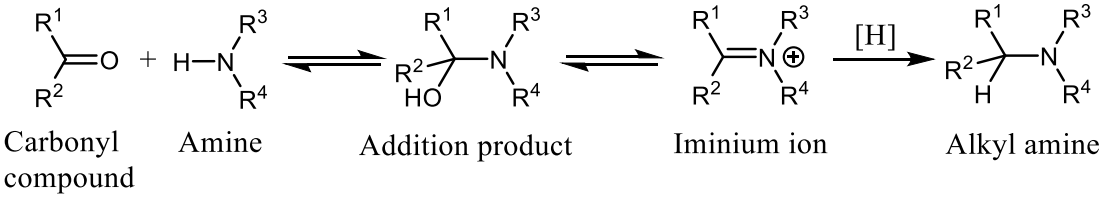

Figure 2.7. General steps in reductive amination.

The pH is a critical factor in reductive amination.[5] The reaction is started by acid-catalyzed nucleophilic attack of amine to the carbonyl carbon to produce intermediate, followed by subsequent reduction of the C=N bond. Protonation of the carbonyl oxygen makes carbonyl carbon more susceptible to the nucleophilic addition. Under acidic conditions, amine also undergoes protonation to form aminium that cannot act as the amine donor, when only hydrogenation takes place. Thus, a suitable pH condition is important.

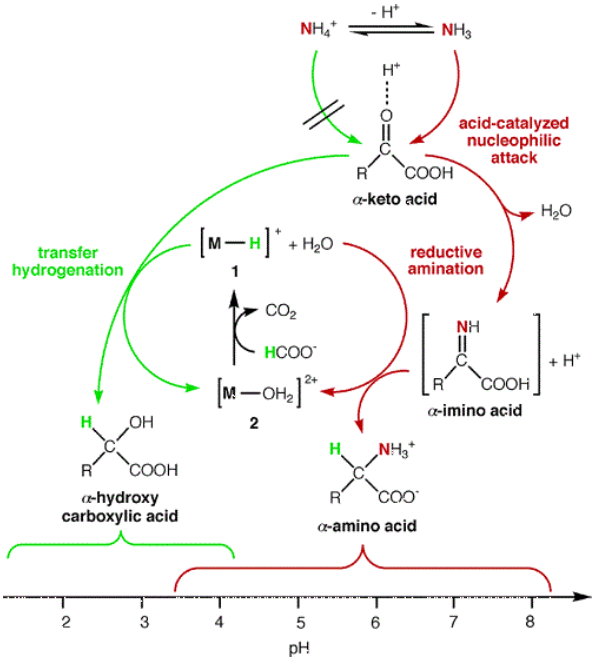

Figure 2.8. The pH-dependent reductive amination.

2.2 Reductive amination of simple ketones using phenylhydrazide

The chiral hydrazide products were made in high enantioselectivity by Burk and Feaster in 1992 from the asymmetric hydrogenation of *N*-benzoylhydrazone of aromatic and aliphatic ketones.[7] However, the direct reductive amination was not realized in this system.[8]

Phenylhydrazide is a suitable nitrogen source due to its strong nucleophilicity and potential possibility of secondary chelating effect. Its product benzohydrazide can be easily converted to primary amine by being treated with SmI2 (Scheme 2) or hydrazine by using HCl.

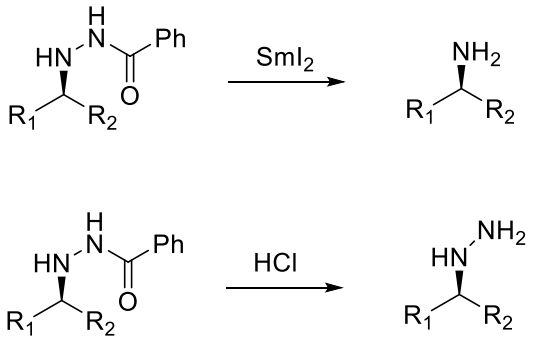

Figure 2.9. Deprotection of benzohydrazide.

In our experiment, we explored phenylhydrazide as nitrogen source for reductive amination using acetophenone as a standard ketone, and results are summarized in table 3-1. We selected an iridiumf-Binaphane complex as the catalyst because it does not promote ketone reduction, and it exhibited

excellent performance in the asymmetric hydrogenation of imines and reductive amination.[9]

Additives are key to the success of this reaction. Without any additive, there was no reaction (Table1, entry1). With the addition of 10 mol% p-toluenesulfonic acid, the major product was *N*-benzoylhydrazone intermediate 4 and some alcohol product 5. After using iodine along with p-toluenesulfonic acid, some product 3a started to appear. And when molecular sieves (4 A˚), p-toluenesulfonic acid, and iodine were added at the same time, the desired product 3a was obtained as the major product with 88% ee, and the alcohol side product **5** disappeared (Table 1, entries 25). From the data in Table 1 the addition of molecular sieves and p-toluenesulfonic acid facilitated the formation of intermediate imine 4, and I_2 benefited the yield of the desired product 3a. From solvent screening, the highest enantioselectivity and reactivity were achieved from the combination of methanol and dichloromethane (Table 1, entry 8). When the catalyst loading was 0.1 mol %, full conversion was still achieved (Table 1, entry 10). Under the same reaction conditions, other chiral diphosphines ligands were tested (Figure 2-2). DuanPhos, JosiPhos, Et-DuPhos, and BINAP yielded predominately hydrozone intermediate **4**.

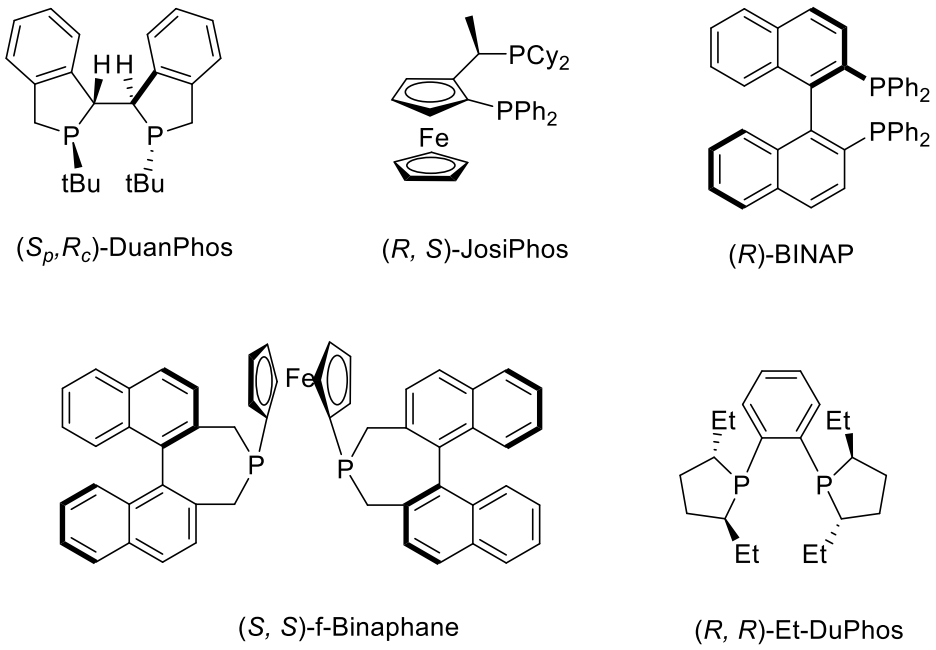

Figure 2.10. chiral phosphine ligands.

Table 2.1. Direct asymmetric reductive amination of acetophenone with phenylhydrazide using iridium-f-Binaphane.[a]

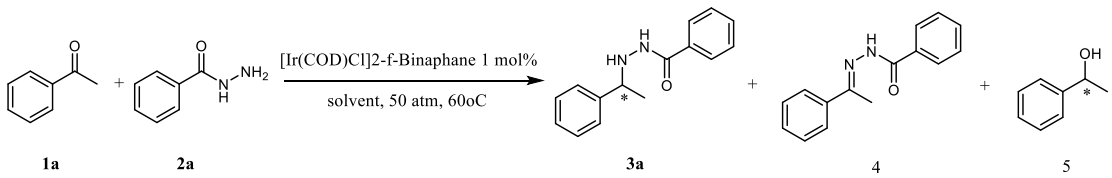

Entry	Solvent	Additives[b]	Conversion (%)[c]	Ratio (3:4:5)[c]	ee (%)[b]
1	CH_2Cl_2	None	N. R.	-	-
2	CH_2Cl_2	TsOH	>95%	0:75:25	-
3	CH_2Cl_2	TsOH, I_2	>95%	14:81:5	-
4	CH_2Cl_2	MS, I_2	65	9:48:43	-
5	CH_2Cl_2	TsOH, MS, I_2	>99%	85:15:0	88
6	EtOAc	TsOH, MS, I_2	<5	-	-
7	MeOH	TsOH, MS, I_2	>99%	3:97:0	-
8	MeOH/ CH_2Cl_2=1:1	TsOH, MS, I_2	>99%	100:0:0	92
9[d]	MeOH/ CH_2Cl_2=1:1	TsOH, MS, I_2	>99%	100:0:0	94
10[d,e]	MeOH/ CH_2Cl_2=1:1	TsOH, MS, I_2	>99%	100:0:0	94

[a] Reaction conditions: [Ir]/ligand/ketone/phenylhydrazide = 1:1:110:100, ligand/metal 1:1, 50 atm of H_2, 60 ^oC, 24 h. [b] TsOH = p-toluene-sulfonic acid, 10 mol %; MS = 4 A˚ molecular sieves, 0.2 g; I_2 = iodine, 10 mol %. [c] Conversions, product ratios, and enantiomeric excesses were determined by chiral HPLC. [d] Reaction temperature was room temperature. [e] Catalyst loading was 0.1 mol %.

To gain a better understanding of the functions of additives, asymmetric hydrogenation of corresponding imine 4 was carried out (**Table 2-1**). Surprisingly, 4 A˚ molecular sieves facilitated this reaction. This result is interesting since molecular sieves were commonly believed to only promote imine formation in reductive amination.[10]

After establishing the optimized reaction conditions, a range of commercial available aromatic ketones were reductively animated using this Irf-Binaphane catalyst.

Table 2.2. Asymmetric Hydrogenation of N-Benzoylhydrazone 4. [a]

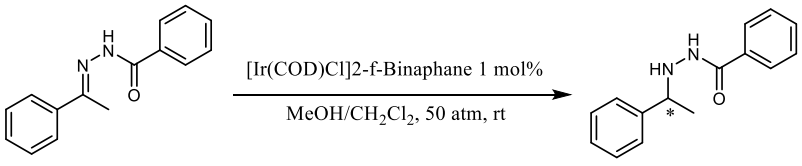

4 3a

Entry	Additives[b]	Yield (%)[c]	ee (%)[c]
1	I_2	18	92
2	I_2, TsOH	12	92
3	I_2, MS	>99	94
4	I_2, MS, TsOH	>99	94

[a] Reaction conditions: [Ir]/ligand/ketone/phenylhydrazide = 1:1:110:100, ligand/metal 1:1, 50 atm of H_2, room temperature, 24 h. [b] TsOH = p-toluene-sulfonic acid, 10 mol %; MS = 4 A˚ molecular sieves, 0.2 g; I_2 = iodine, 10 mol %. [c] Conversions, product ratios, and enantiomeric excesses were determined by chiral HPLC.

For all chosen *para*- (**1a-1f**) and meta-substituted (**1g-1i**) aromatic ketones, the chiral hydrazide products 3 were obtained in excellent yields and ee's (ee ranged from 94% to 99%, **Table 2-2**), regardless of their electronic properties. For ortho-substituted aromatic ketone (**1j**), the reactivity and enantioselectivity decreased slightly, maybe due to its sterical hindrance. This catalytic system also worked quite well for heteroaromatic ketone (**1l**) and 2-naphthalene ketone (**1k**). To evaluate the practical utility of our method, acetophenone and 4-methoxylacetophenone were reductively aminated on half-gram scale, and excellent ee's and yields were obtained for both ketones (**Table 2-3**).

Table 2.3. Direct Asymmetric Reductive Amination of Simple Aromatic Ketones Using Iridiumf-Binaphane. [a]

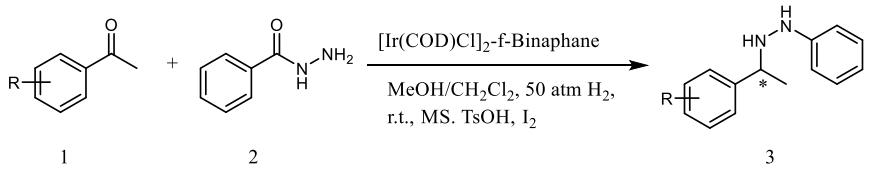

1 2 3

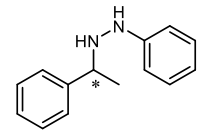

3a (*R*)
95% yield, 94% ee

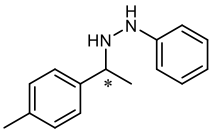

3b (+)
94% yield, 96% ee

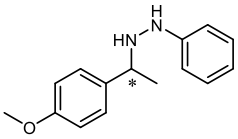

3c (+)
98% yield, 92% ee

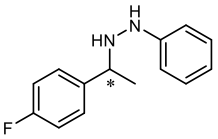

3d (+)
96% yield, 86% ee

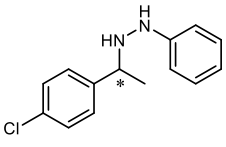

3e (+)
97% yield, 92% ee

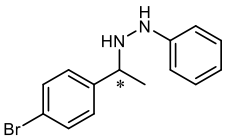

3f (R)
97% yield, 95% ee

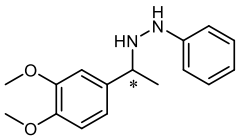

3g (+)
99% yield, 90% ee

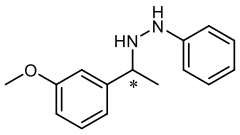

3h (+)
94% yield, 92% ee

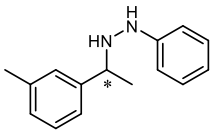

3i (+)
97% yield, 93% ee

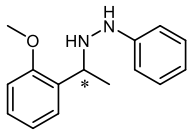

3j (+)
89% yield, 86% ee

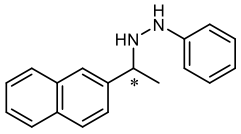

3k[b] (+)
90% yield, 91% ee

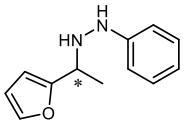

3l[b] (+)
89% yield, 91% ee

[a] Reaction conditions: [Ir]/ligand/ketone/phenylhydrazide = 1:1:110:100, ligand/metal 1:1, 50 atm of H2, room temperature, 24 h. TsOH = p-toluene-sulfonic acid, 10 mol %; MS = 4 A^{o} molecular sieves, 0.2 g; I2 = iodine, 10 mol %. Yields are isolated yields. Enantiomeric excesses were determined by chiral HPLC. The absolute configuration of product is assigned by comparison of rotation sign with literature data. Reaction temperature was 60 ^{o}C.

In summary, we have demonstrated the highly enantioselective direct reductive amination of aromatic ketones. With phenylhydrazide as the nitrogen

source, various chiral hydrazides were synthesized in excellent enantioselectivities and yields. The success of this reaction results from several factors: (a) H^+ facilitated the formation of imine intermediates; (b) 4 A° molecular sieves not only helped to remove H_2O to form imines but also promoted the reduction of imines; (c) with the addition of I_2, Ir(III)-I_2Cl(f-Binaphane) was formed,[11] which is an effective catalytic precursor for the hydrogenation of imines; (d) phenylhydrazide and the amine products have weak coordination ability to Ir, so the catalytic reaction can proceed smoothly; (e) f-Binaphane is a unique electrondonating ligand with a big bite angle (P*-Ir-P*).[12] f-Binaphane minimizes the inhibition effect from amines and helps iridium to accommodate sterically demanding imines, thus leading to a smooth reaction. The superb performance of the methodology offers an attractive route for chiral amine and chiral hydrazine derived heterocyclic compounds synthesis. We are currently examining the extension of this methodology to other substrates.

2.3 Experiment Section

2.3.1 General remarks

All reactions were performed in the nitrogen-filled glovebox or under nitrogen using standard Schlenk techniques unless otherwise noted. Column chromatography was performed using Sorbent silica gel 60 (230 – 450 mesh). 1H NMR, and 13C NMR spectral data were obtained from Bruker 400 MHz spectrometers. Chemical shifts are reported in ppm. Enantiomeric ratios were determined by chiral GC or HPLC analysis. All new products were further characterized by HRMS. A positive ion mass spectrum of sample was acquired on a Micromass 70-VSE mass spectrometer with an electron ionization source.

2.3.2 General Procedure for Asymmetric Hydrogenation.

Typical reductive amination procedure: In a nitrogen-filled glovebox, ketone (0.22 mmol), 4Å molecular sieves (0.2 g), p-toluenesulfonic acid (0.02 mmol) and phenylhydrazide (0.20 mmol) were stirred in anhydrous CH2Cl2 (0.5 mL) and MeOH (0.5 mL) for 10 min in a vial. Then [Ir(COD)f-Binaphane]Cl (0.002 mmol) in situ generated (from [Ir(COD)Cl]2 and f-Binaphane stirred in CH2Cl2 for 15 min) was added to this vial, followed by I2 (5.1 mg, 0.02 mmol). The total solution was made to 2.0 mL at a MeOH / CH2Cl2 ratio of 1:1. The resulting vial was transferred to an autoclave, which was charged with 50 atm of H2,

and stirred at room temperature for 24 h. The hydrogen gas was released slowly and the solution was concentrated and passed through a short column of silica gel to remove the metal complex and molecular sieve. The product was then analyzed by chiral HPLC to determine the enantiomeric excesses.

(*R*)- *N*'-(1-phenylethyl)benzohydrazide (3a):

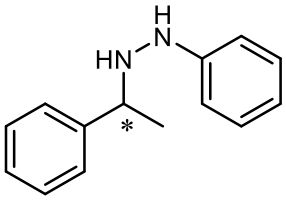

White solid (95% yield, 94 % ee). $[\alpha]^{20}D$ +167.2 (c = 1 in CHCl3); ^{1}H NMR (400 MHz, CDCl3) δ 7.22-7.76 (m, 11H), 4.22 (q, J=6.6 Hz, 1H), 1.41 (d, J=6.6 Hz, 2H). ^{13}C NMR (100 MHz, CDCl3) δ 167.3, 143.1, 133.0, 131.8, 128.6, 127.6, 127.3, 126.8, 60.1, 22.7. Enantiomeric excess was determined by HPL using Chiralcel OJ-H column, Hex/IPA=90:10, 1 mL/min.

(+)- *N*'-(1-(p-tolyl)ethyl)benzohydrazide (3b):

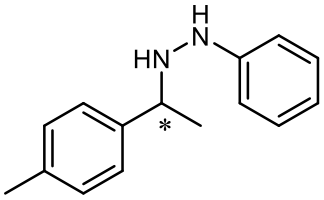

White solid (94% yield, 96 % ee). $[\alpha]^{20}D$ +164.6 (c = 0.25 in CHCl3); ^{1}H NMR (400 MHz, CDCl3) δ 7.61 (d, J=7.2 Hz, 2H), 7.38-7.53 (m, 4H), 7.28 (d, J=8 Hz,

2H), 7.10 (d, J=7.2 Hz, 2H), 4.18 (q, J=6.6 Hz, 1H), 2.33 (s, 3H), 1.41 (d, J=6.6 Hz, 2H). ^{13}C NMR (100 MHz, CDCl3) δ 167.2, 140.1, 137.2, 133.0, 131.7, 129.3, 128.6, 127.1, 126.8, 59.8, 21.2, 21.1. EI-HRMS: 255.1499 (Calculated for C16H19N2O+ ([M+H]$^{+}$): 255.1497). Enantiomer ratio was determine by HPLC using a Chiralcel OJ-H column, Hex/IPA=90:10, 1 mL/min.

(*R*)- *N*'-(1-(4-methoxyphenyl)ethyl)benzohydrazide (3c):

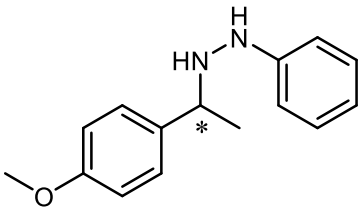

Light yellow oil (92% yield, 98 % ee). [α]^{20}D +148.3 (c = 1 in CHCl3); ^{1}H NMR (400 MHz, CDCl3)δ 7.61 (d, J=7.2 Hz, 2H), 7.40 (m, 1H), 7.32 (m, 2H), 7.28 (d, J=7.2 Hz, 2H), 6.82 (d, J=7.2 Hz, 2H), 4.18 (q, J=6.6 Hz, 1H), 3.79 (s, 3H), 1.40 (d, J=6.6 Hz, 2H). ^{13}C NMR (100 MHz, CDCl3) δ 166.2, 158.1, 134.0, 132.0, 130.7, 128.0, 127.8, 125.8, 113.0, 58.4, 54.3, 20.2. Enantiomer ratio was determine by HPLC using a Chiralcel OJ-H column, Hex/IPA=90:10, 1 mL/min.

(+)-*N*'-(1-(4-fluorophenyl)ethyl)benzohydrazide (3d):

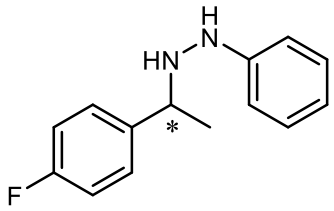

White solid (86% yield, 96 % ee). $[\alpha]^{20}D$ +177.6 (c = 0.5 in CHCl3); ^{1}H NMR (400 MHz, CDCl3)δ 7.72 (m, 2H), 7.54 (m, 2H), 7.32 (m, 4H), 6.98 (m, 2H), 5.02 (s, br,1H), 4.24 (q, J=6.6 Hz,1H), 1.30 (d, J=6.6 Hz, 3H). ^{13}C NMR (100 MHz, CDCl3) δ167.4, 163.5, 161.0, 138.9, 132.8, 131.9, 128.8, 128.7, 126.8, 115.5, 115.3, 59.3, 29.7, 21.3. EI-HRMS: 259.1253 (Calculated for C15H16N2OF+([M+H]+): 259.1247). Enantiomer ratio was determine by HPLC using a Chiralcel OJ-H column, Hex/IPA=94:6, 1 mL/min.

(+)-*N'*-(1-(4-chlorophenyl)ethyl)benzohydrazide (3e):

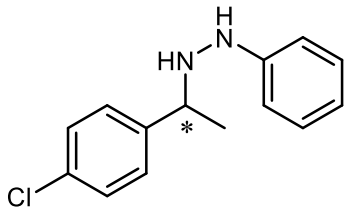

White solid (92% yield, 97 % ee). $[\alpha]^{20}D$ +159.3 (c = 0.5 in CHCl3); ^{1}H NMR (400 MHz, CDCl3)δ 7.62 (d, J=7.2 Hz, 2H), 7.48 (m, 1H), 7.28-7.44 (m, 7H), 4.24 (q, J=6.6 Hz, 1H), 1.42 (d, J=6.6 Hz, 1H). ^{13}C NMR (100 MHz, CDCl3) δ167.4, 141.8, 133.3, 132.7, 131.9, 128.8, 128.7, 128.6, 126.8, 59.4, 21.3. EI-HRMS: 275.0946 (Calculated for C15H16N2OCl+ ([M+H]+): 275.0951).

Enantiomer ratio was determine by HPLC using a Chiralcel OJ-H column, Hex/IPA=94:6, 1 mL/min.

(*R*)-*N*'-(1-(4-bromophenyl)ethyl)benzohydrazide (3f):

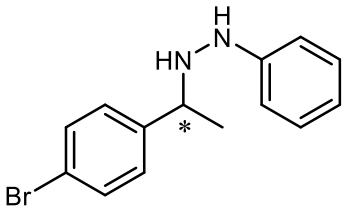

White solid (95% yield, 97 % ee). $[\alpha]^{20}D$ +144.3 (c = 1 in CHCl3); ^{1}H NMR (400 MHz, CDCl3)δ 7.68 (d, J=7.2 Hz, 2H), 7.20-7.50 (m, 8H), 4.24 (q, J=6.6 Hz, 1H), 1.42 (d, J=6.6 Hz, 1H). ^{13}C NMR (100 MHz, CDCl3) δ167.4, 142.3, 132.7, 131.9, 131.7, 129.0, 128.7, 126.8, 121.4, 59.5, 21.3. Enantiomer ratio was determine by HPLC using a Chiralcel OJ-H column, Hex/IPA=94:6, 1 mL/min.

(+)-*N*'-(1-(3,4-dimethoxyphenyl)ethyl)benzohydrazide (3g):

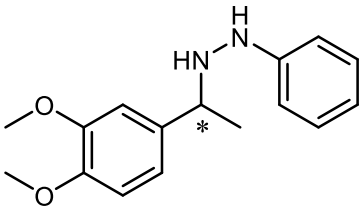

White solid (90% yield, >99 % ee). $[\alpha]^{20}D$ +143.9 (c = 1 in CHCl3); ^{1}H NMR (400 MHz, CDCl3)δ 7.64 (d, J=7.2 Hz, 2H), 7.50 (m, 1H), 7.40 (m, 2H), 7.04 (m, 1H), 6.88-7.00 (m, 2H), 6.84 (d, J=7.2 Hz,1H), 4.26 (q, J=6.6 Hz, 1H), 3.90 (m,

2H), 1.46 (d, J=6.6 Hz, 1H). ^{13}C NMR (100 MHz, CDCl3) δ167.2, 149.2, 148.6, 135.0, 132.7, 131.9, 128.7, 126.9, 119.6, 111.2, 110.2, 60.0, 55.9, 20.9. EI-HRMS: 301.1560 (Calculated for C17H21N2O3+([M+H]+): 301.1552). Enantiomer ratio was determine by HPLC using a Chiralcel OJ-H column, Hex/IPA=90:10, 1 mL/min.

(+)-*N*'-(1-(3-methoxyphenyl)ethyl)benzohydrazide (3h):

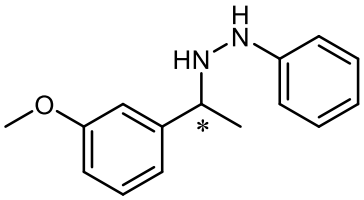

White solid (92% yield, 94 % ee). [α]^{20}D +176.5 (c = 0.25 in CHCl3); ^{1}H NMR (400 MHz, CDCl3) δ7.62 (d, J=7.2 Hz, 2H), 7.24-7.52 (m, 5H), 7.00 (m, 2H), 6.82 (m, 1H), 6.76 (d, J=6.6 Hz, 1H), 4.24 (q, J=6.6 Hz, 1H), 3.80 (s, 3H), 1.42 (d, J=6.6 Hz, 2H). ^{13}C NMR (100 MHz, CDCl3) δ167.3, 159.9, 144.9, 132.9, 131.8, 129.6, 128.7, 126.8, 119.6, 113.0, 112.6, 60.1, 55.2, 21.4. EI-HRMS: 271.1457 (Calculated for C16H19N2O2+([M+H]+): 271.1447). Enantiomeric excess was determined by HPLC using Chiralcel OJ-H column, Hex/IPA=90:10, 1 mL/min.

(+)-*N*'-(1-(m-tolyl)ethyl)benzohydrazide (3i):

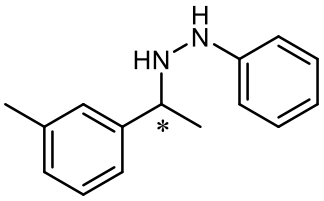

Colorless liquid (93% yield, 97 % ee). $[\alpha]^{20}D$ +156.6 (c = 1 in CHCl3); ^{1}H NMR (400 MHz, CDCl3)δ 7.60 (m, 3H), 7.40 (m, 1H), 7.30 (m, 2H), 7.16 (m, 3H), 7.00 (d, J=7.2 Hz,1H), 4.12 (q, J=6.6 Hz, 1H), 1.32 (q, J=6.6 Hz, 3H). ^{13}C NMR (100 MHz, CDCl3) δ 167.3, 143.0, 138.2, 133.0, 131.7, 131.5, 128.6, 128.5, 128.4, 128.0, 126.9, 124.3. EI-HRMS: 255.1503 (Calculated for C16H19N2O+([M+H]+): 255.1497). Enantiomeric excess was determined by HPLC using Chiralpak AD-H column, Hex/IPA=96:4, 1 mL/min.

(+)- *N*'-(1-(2-methoxyphenyl)ethyl)benzohydrazide (3j):

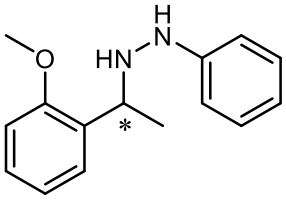

White solid (86% yield, 89 % ee). [α]20D +87.2 (c = 1 in CHCl3); 1H NMR (400 MHz, CDCl3)δ 7.62 (m, 2H), 7.32-7.48 (m, 5H), 7.22 (m, 1H), 6.94 (m, 1H), 6.82 (d, J=7.2 Hz,1H), 4.58 (q, J=6.6 Hz, 1H), 3.73 (s, 3H),1.36 (q, J=6.6 Hz, 3H). 13C NMR (100 MHz, CDCl3) δ 166.9, 157.4, 133.2, 131.6, 131.1, 128.6, 128.3, 126.9, 126.8, 120.7, 110.7, 55.4, 53.9, 19.6. EI-HRMS: 269.1292

(Calculated for C16H17N2O2+([M+H]+): 269.1290). Enantiomeric excess was determined by HPLC using Chiralpak AS-H column, Hex/IPA=75:25, 1 mL/min.

(R)- *N*'-(1-(naphthalen-2-yl)ethyl)benzohydrazide (3k):

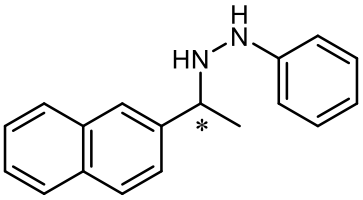

White solid (91% yield, 90 % ee). $[\alpha]^{20}D$ +195.9 (c = 1 in CHCl3); ^{1}H NMR (400 MHz, CDCl3)δ 7.76 (m, 4H), 7.54 (m, 4H), 7.40 (m, 3H), 7.30 (m, 2H), 6.70-6.78 (m, 3H), 4.40 (q, J=6.6 Hz, 1H), 1.42 (q, J=6.6 Hz, 3H). ^{13}C NMR (100 MHz, CDCl3) δ 167.4, 140.6, 133.5, 133.1, 132.9, 131.8, 128.6, 128.4, 127.9, 127.7, 127.2, 126.9, 126.1, 126.1, 125.8, 125.2, 60.2, 21.3. Enantiomeric excess was determined by HPLC using Chiralcel OJ-H column, Hex/IPA=85:15, 1 mL/min.

(+)-*N*'-(1-(furan-2-yl)ethyl)benzohydrazide (3l):

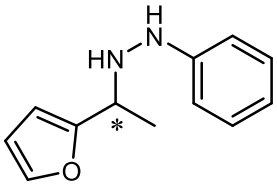

Yellow oil (91% yield, 89 % ee). $[\alpha]^{20}D$ +105.1 (c = 0.25 in CHCl3); ^{1}H NMR (400 MHz, CDCl3)δ 7.70 (m, 2H), 7.62 (s, 1H), 7.50 (m, 1H), 7.42 (m, 3H), 6.32 (m, 1H), 6.20 (m, 1H), 4.32 (q, J=6.6 Hz, 1H), 1.48 (q, J=6.6 Hz, 3H).. ^{13}C NMR (100 MHz, CDCl3) δ 167.3, 155.5, 142.1, 132.9, 131.9, 128.7, 126.9, 110.1, 106.7, 53.6, 17.6. EI-HRMS: 231.1138 (Calculated for C13H15N2O2+([M+H]+): 231.1134). Enantiomeric excess was determined by HPLC using Chiralcel OJ-H column, Hex/IPA=85:15, 1 mL/min.

2.4. Reference:

1. Yongxiang Chi, Yong-Gui Zhou, and Xumu Zhang *J. Org. Chem.* **2003**, 68, 4120 -4122.
2. Blaser, H.-U.; Buser, H.-P.; Jalett, H.-P.; Pugin, B.; Spindler, F. *Synlett* **1999**, 867-868.
3. Vitali I. Tararov, Renat Kadyrov, Thomas H. Riermeier and Armin Börner *Chem. Commun.* , **2000**, 1867–1868.
4. Thoralf Gross, Abdul Majeed Seayad, Moballigh Ahmad, and Matthias Beller *Org. Lett.*, **2002**, 2055
5. Seiji Ogo, Keiji Uehara, Tsutomu Abura, and Shunichi Fukuzumi. *J. AM. CHEM. SOC.* **2004** , *126* , 3020 -3021.
6. Dietrich Steinhuebel, Yongkui Sun, Kazuhiko Matsumura, Noboru Sayo, and Takao Saito *J. AM. CHEM. SOC.* **2009** , *131*, 11316–11317.
7. M. J. Burk, J. E Feaster, *J. AM. CHEM. SOC.* **1992** , *114* , 6267.
8. M. J. Burk, J. P. Martinez, J. E. Feaster, N. Cosforda, *Tetrahedron* **1994**, *50*, 4399.
9. (a) Xiao, D.; Zhang, X. *Angew. Chem., Int. Ed.* **2001**, *40*, 3425. (b)Hou,G.; Gosselin,F.; Li,W.; McWilliams,J.C.; Sun,Y.; Weisel,M.; O'Shea, P. D.; Chen, C.-Y.; Davies, I. W.; Zhang, X. *J. Am. Chem. Soc*. **2009**, *131*, 9882. (c) Hou, G.; Li, W.; Ma, M.; Zhang, X.; Zhang, X. *J. Am. Chem. Soc.* **2010**, *132*, 12844. (d) Chang, M.; Li, W.; Hou, G.; Zhang, X. *Adv. Synth. Catal.* **2010**, *352*, 3121. (e) Chang, M.; Li, W.; Zhang, X. *Angew. Chem., Int. Ed.* **2011**, *50*, 10679. (f) Chi, Y.; Zhou, Y.-G.; Zhang, X. *J. Org. Chem.* **2003**, *68*, 4120.

10. (a) Rueping, M.; Sugiono, E.; Azap, C.; Theissmann, T.; Bolte, M. *Org. Lett.* **2005**, *7*, 3781. (b) Hoffmann, S.; Seayad, A. M.; List, B. *Angew. Chem., Int. Ed*. **2005**, *44*, 7424. (c) Storer, R. I.; Carrera, D. E.; Ni, Y.; MacMillan, D. W. C. *J. Am. Chem. Soc*. **2006**, *128*, 84.
11. Xiao, D.; Zhang, X. *Angew. Chem., Int. Ed.* **2001**, *40*, 3425.
12. Yang, Q.; Shang, G.; Gao, W.; Deng, J.; Zhang, X. *Angew. Chem., Int. Ed*. **2006**, *45*, 3832.

Chapter 3

Iridium-Catalytic Asymmetric Hydrogenation of Pyridinium Salts

3.1 Introduction

Hydrogenation of readily available substituted pyridines is a straightforward and atom-economical approach for the preparation of substituted piperidines.[1] These piperidines are ubiquitous structural motifs in natural products as well as key pharmacophores in many active pharmaceutical ingredients (Figure 1).[2]

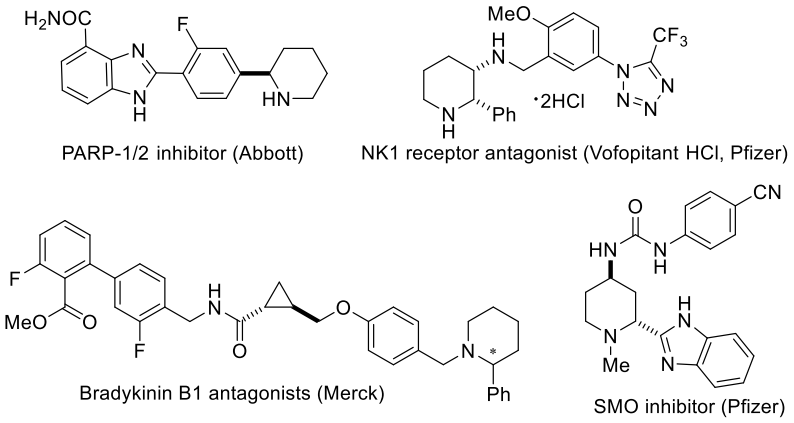

Figure 3.1. Selected pharmaceutical targets

Due to five potential substituted positions around a pyridine ring, up to five stereogenic centers could be formed in one single step, which provides great possibility in the synthesis.

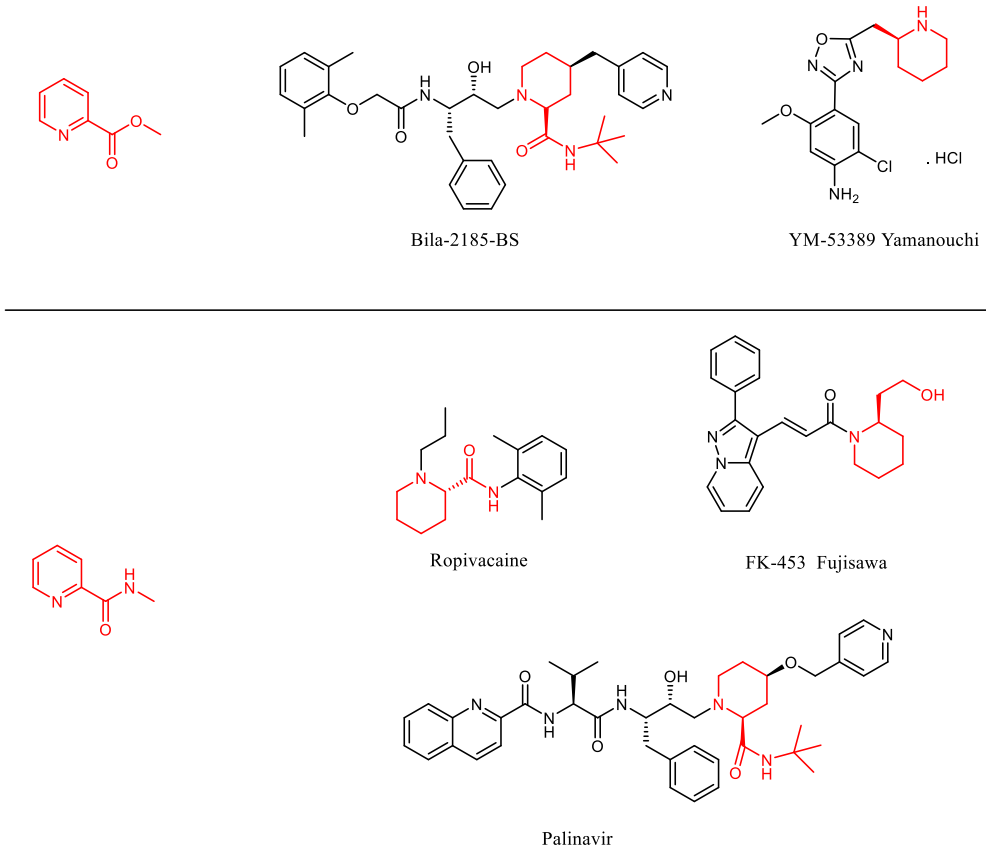

Figure 3.2. Drugs contain *ortho* substituted pyridine moiety

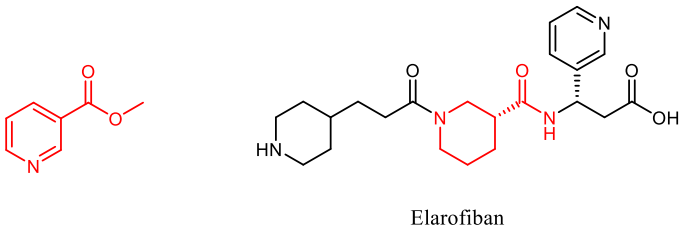

Elarofiban

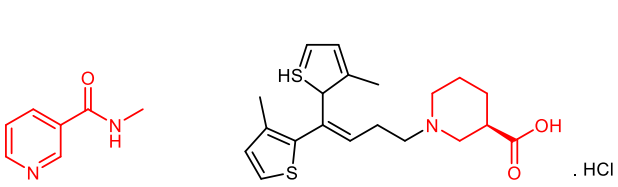

Tiagabine Hydrochloride

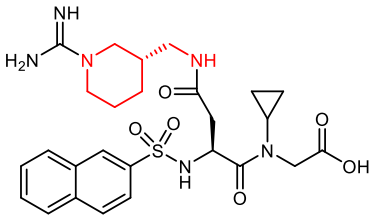

Napsagatran Roche

Figure 3.3. Drugs contain *meta* substituted pyridine moiety

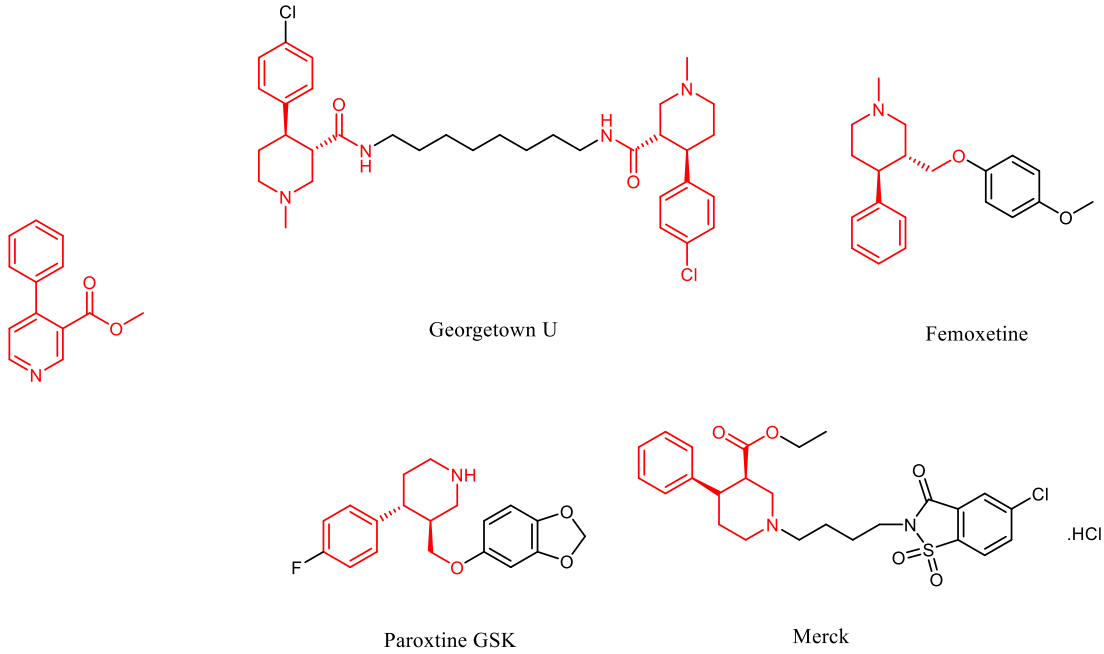

Georgetown U

Femoxetine

Paroxtine GSK

Merck

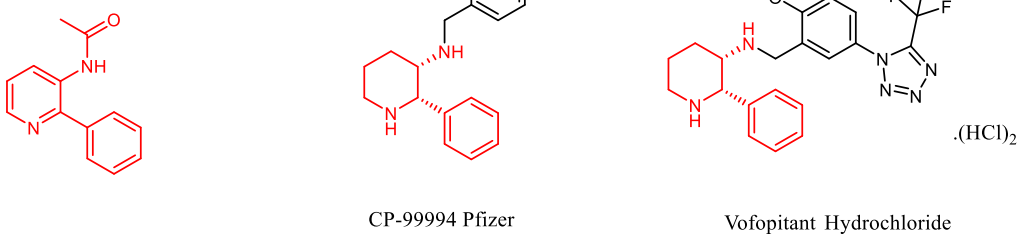

CP-99994 Pfizer

Vofopitant Hydrochloride

Figure 3.4. Drugs contain di-substituted pyridine moiety

Despite these advances, direct hydrogenation of simple pyridines is still a challenge. The inherent problems are apparent: First, substrates and corresponding products that possess strong coordination ability might cause the deactivation of catalysts. Second, pyridines have a stabilizing aromatic structure that might impede the reduction.[3]

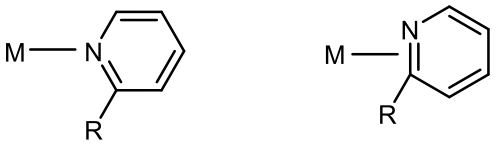

σ-Bond π-Bond

Figure 3.5. Two types of bonding between pyridine and metal catalyst

Substrate Inhibition Product Inhibition

Figure 3.6. Substrate and product inhibition

For indirect asymmetric hydrogenation of pyridines, several strategies were applied to address this problem: 1) Chiral auxiliary was introduced to the 2 position of pyridine to induce chirality, and then chopped off after

hydrogenation (**Scheme 3-1**);[4] 2) Step-wise reduction of the pyridine ring (Scheme 3-2).[5]

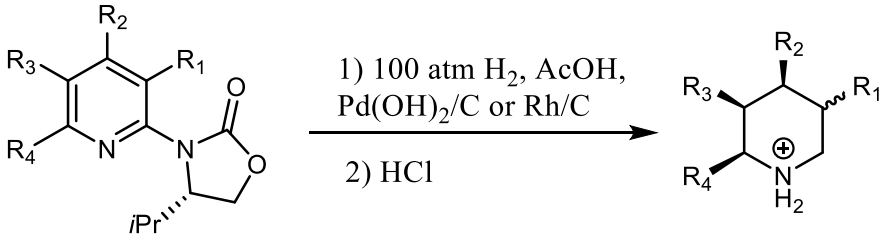

Figure 3.7. Utility of chiral auxiliary on the 2 position of pyridine to induce chirality

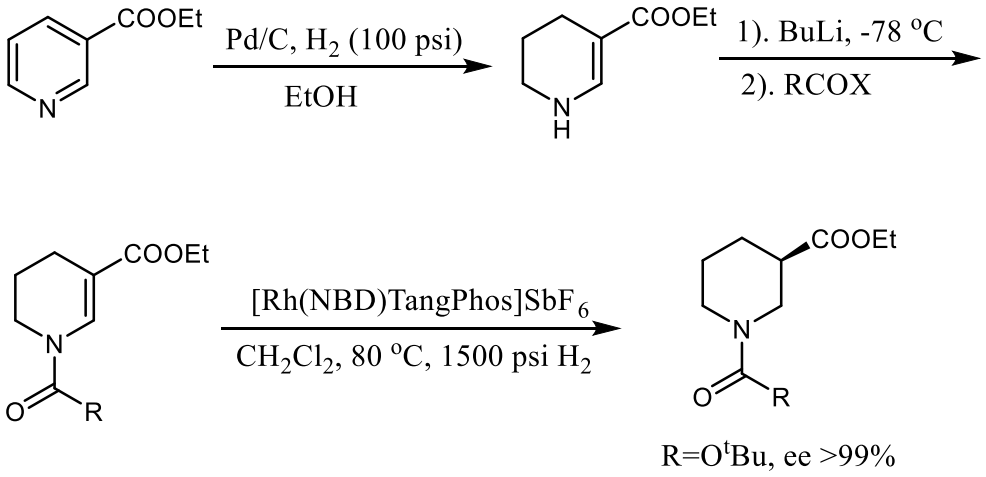

Figure 3.8. Step-wise hydrogenation of pyridine

Despite the increasing demand of making enantiomerically pure piperidines, only limited successful examples of direct asymmetric hydrogenations of pyridines have been reported. In 2000, Studer and co-workers reported the asymmetric reduction of pyridines in 27% ee using rhodium bis(phosphine) complexes.[6] Zhou's $[Ir(COD)Cl]_2$ / (S)-MeO-Biphep system reduced the related 7,8-dihydroquinolin-5(6H)-one substrates with

good enantioselectivities; however, the system was not general for pyridines (**Scheme 3-3**).[7]

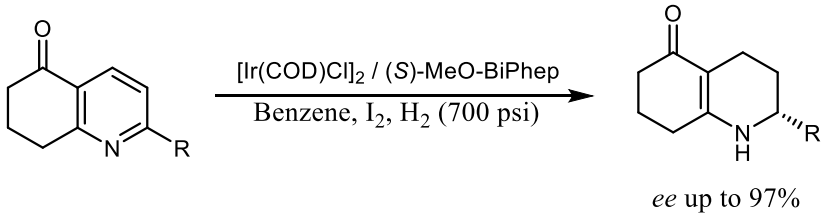

Figure 3.9. Reduction of 7,8-dihydroquinolin-5(6H)-one reported by Zhou

Recognizing that the major obstacle to achieving highly efficient asymmetric hydrogenations of pyridines is overcoming the thermodynamic stability associated with the aromaticity of the pyridine ring, a number of approaches have been explored to circumvent this issue. Charette and coworkers have employed *N*-iminopyridinium ylides to improve the reactivity of the pyridine ring and achieve efficient asymmetric hydrogenation (**Scheme 3-4**).[8]

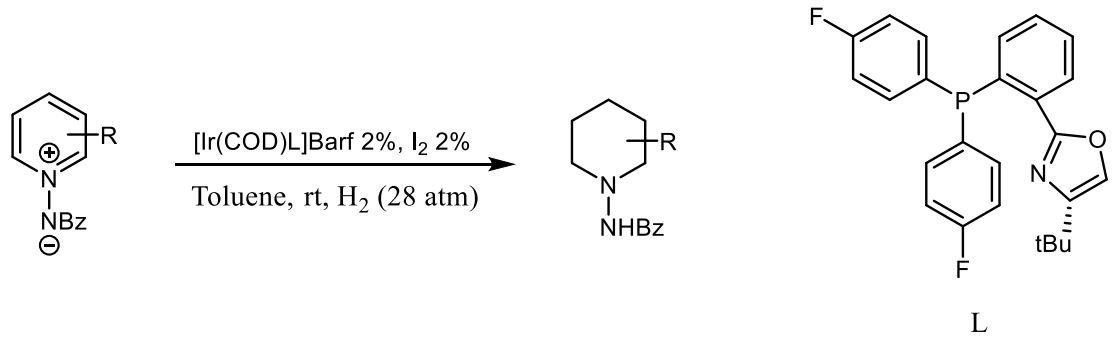

Figure 3.10. Reduction of *N*-iminopyridinium ylides reported by Charette

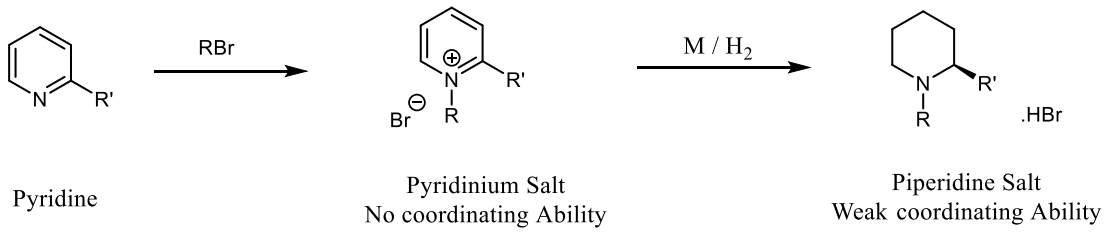

Figure 3.11. The strategy for hydrogenation of simple pyridines

Among all catalytic systems, iridium catalyst shows its efficiency in direct asymmetric hydrogenation of pyridinium salts. In 2012, Zhou and co-workers have reported the successful asymmetric hydrogenation of *N*-(2-CO_2*i*Pr)benzylpyridinium salts where the ester is believed to act as a directing group for the catalyst (**Scheme 3-6**).[3] In 2014, Zhang and co-workers reported the asymmetric hydrogenation of simple *N*-benzylpyridinium salts by using a unique iridium phosphole catalyst.[9] In 2014, Mashima and co-workers reported an iridium-catalyzed asymmetric hydrogenation of di-substituted pyridinium salts (**Scheme 3-7**).[10] In 2015, Zhou and co-workers applied the iridium phosphine catalyst in asymmetric hydrogenation of tri-substituted pyridinium salts (**Scheme 3-8**).[11]

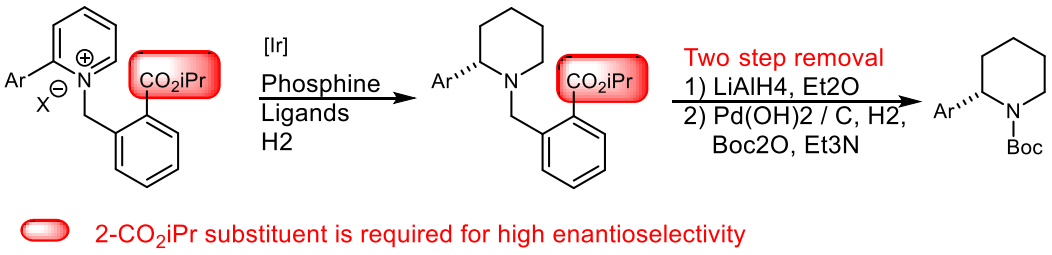

Figure 3.12. Hydrogenation of *N*-(2-CO_2*i*Pr)benzylpyridinium salts reported by Zhou

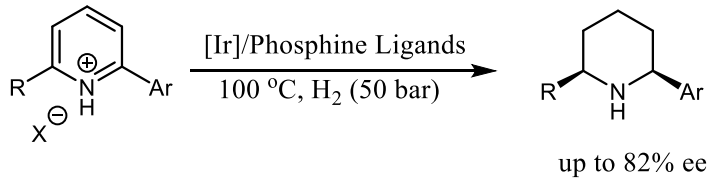

Figure 3.13. Hydrogenation of di-substituted pyridinium salts reported by Mashima

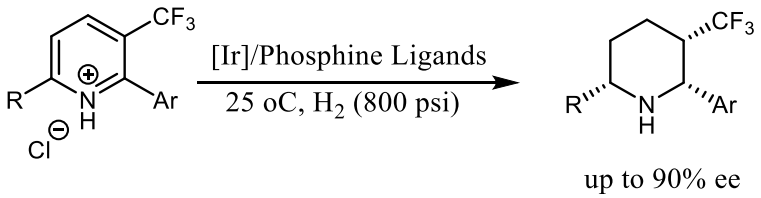

Figure 3.14. Hydrogenation of tri-substituted pyridinium salts reported by Zhou

3.2 High-throughput screening

One challenge that chemists need to face is reaction discover efficiency. Challenging reaction usually need to be conducted under a special or unexpected condition which is hard to discover. Due to limited time, finding out that condition seems impossible under traditional screening method. High-throughput screening (HTS) provides the solution.

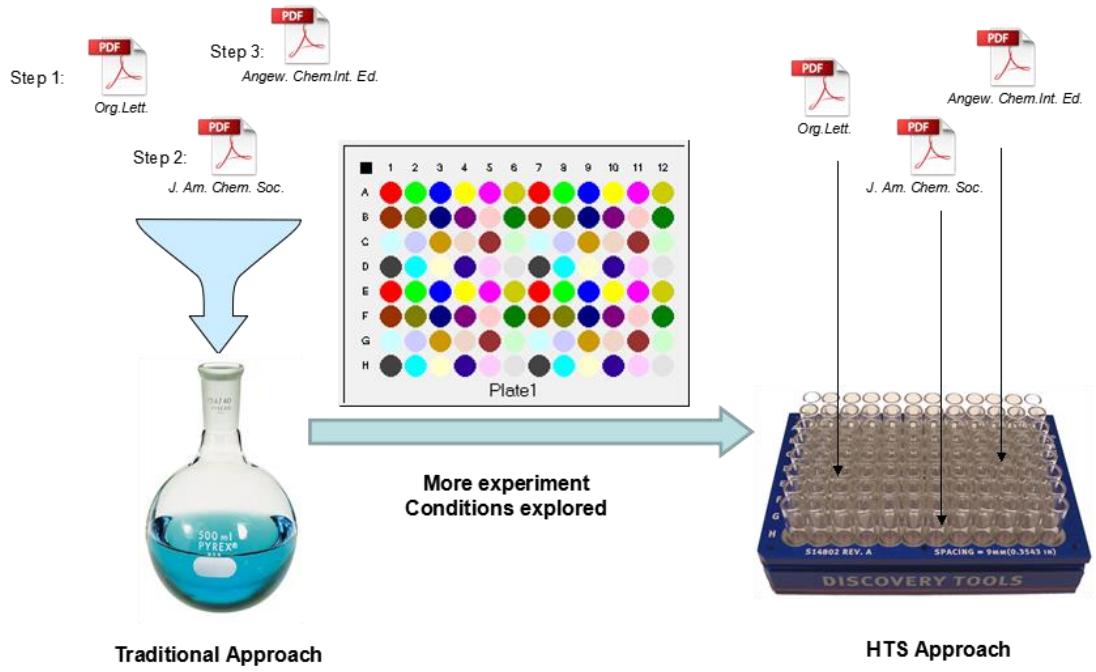

Figure 3.15. The power of high-throughput screening

High-throughput screening is a method for scientific experimentation especially used in drug discovery and relevant to the fields of biology and chemistry. Using robotics, data processing and control software, liquid handling devices, and sensitive detectors, high-throughput screening allows a researcher to quickly conduct millions of chemical, genetic, or pharmacological tests. Through this process one can rapidly identify active compounds, antibodies, or genes that modulate a particular biomolecular pathway. The results of these experiments provide starting points for drug design and for understanding the interaction or role of a particular biochemical process in biology.[12]

Some of its main advantages over other research techniques are: [13]

1. The use of very small amounts of chemicals necessary (reactions can be performed on as low as 2.5 μmol scale of substrate and 0.25 μmol of catalyst loading, which translates into microgram amounts of materials), thus minimizing waste and providing more sustainable development of new processes;
2. High screening capacity (more than 500 reactions/day can be performed);
3. Good analytical capacity (up to 4 blocks of 96 reactions can be simultaneously analyzed by using our 2 brand-new, state-of-the-art HPLC instruments and up to 120 reactions on our SFC instrument);

Until the 1980s, the number of compounds that could be screened by a single facility in a week was between 10 and 100. In 1986, Pfizer was involved in natural products screening by substituting fermentation broths with dimethyl sulfoxide solutions of synthetic compounds, using 96-well plates and reduced assay volumes of 50-100μl. A nominal 30mM source compound concentration provided high μM assay concentrations. Starting at 800 compounds each week, the process reached a steady state of 7200 compounds per week by 1989. By 1992, technology had advanced enough that thousands of compounds could now be screened by a single facility in a week. By this time, Pfizer was using HTS to produce approximately 40 percent of its ‘hits’ in its Discovery portfolio. By 1994, tens of thousands of compounds could be screened a week, but 384-well plates were still extremely rare. The 1994 International Forum on Advances in Screening Technologies and

Data Management saw the first mention of the term ‘Ultra-High-Throughput Screening’ in a presentation by Harry Stylli entitled, ‘An Integrated Approach to High-Throughput Screening’. By 1996, uHTS was considered a realistic goal, and 384-well plates were being used in proof-of-principle applications. Around this time, thousands of compounds could be screened a day. In 1996, Evotek, in collaboration with Novartis and SmithKlineBeecham, developed a high-throughput screening system, EVOscreen®, which was eventually launched in 2000.[14]

Based on High-throughput screening instrument build in Merck &Co., Inc. catalysis group, standard procedure of HTS includes following steps: 1) Design experiment in library studio. Hundreds of rational reaction conditions need to be proposed. Solvent combination, additive, catalyst, temperature, pressure, concentrations and all other possible effective factors need to be considered. Software, library studio could help us to design sufficiently and efficiently. 2) Make mixtures using library recipe. After designing experiment, library studio will summarize a recipe for your experiment, which includes amount of chemicals need to be used and adding procedures. Based on this recipe, prepare desired chemicals and mix well as solutions. 3) Prepare reactor. Pour solution to reagent reservoirs, then using multi-channel pipette to transfer desired amount of solution to 96-well or other multi-well reactors. If necessary, current solvent could be evaporated and switched to another

solvent. Then place reactor under desired condition. If it is high pressure reaction, the reactor needs to be placed in a high pressure reaction block, which will be charged with high pressure gas. 4) Results analysis. After reactions finished, part of reaction solution will be transferred to multi-well analytic plate, and diluted with proper solvent. Then place analytic plate in HPLC or other analytic instrument for result analysis.

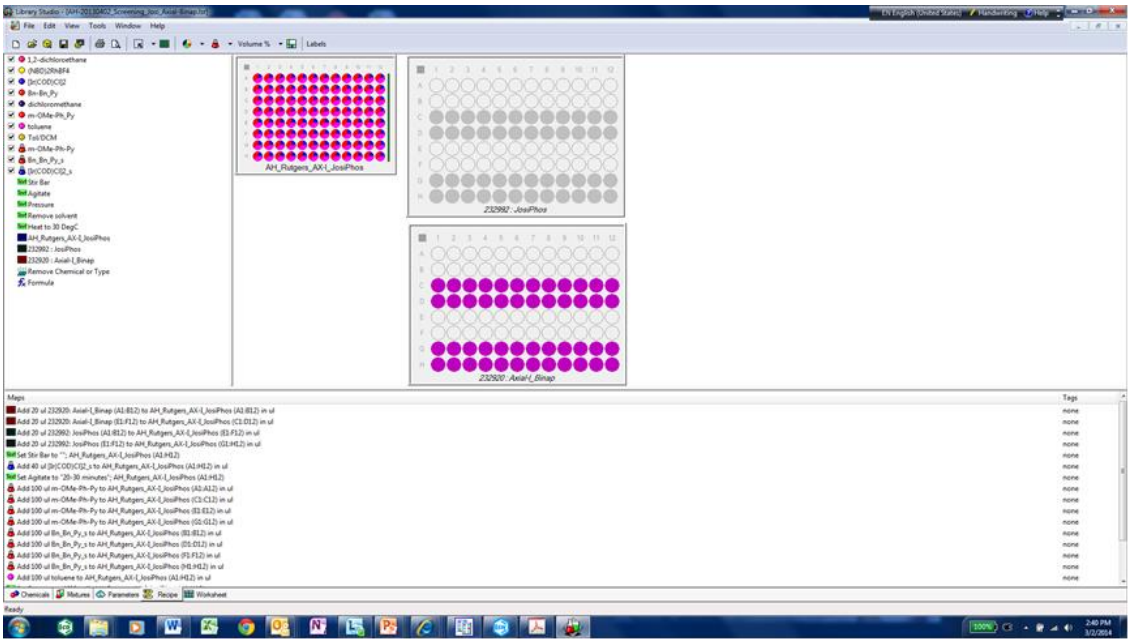

Figure 3.16. Library studio used in HTS

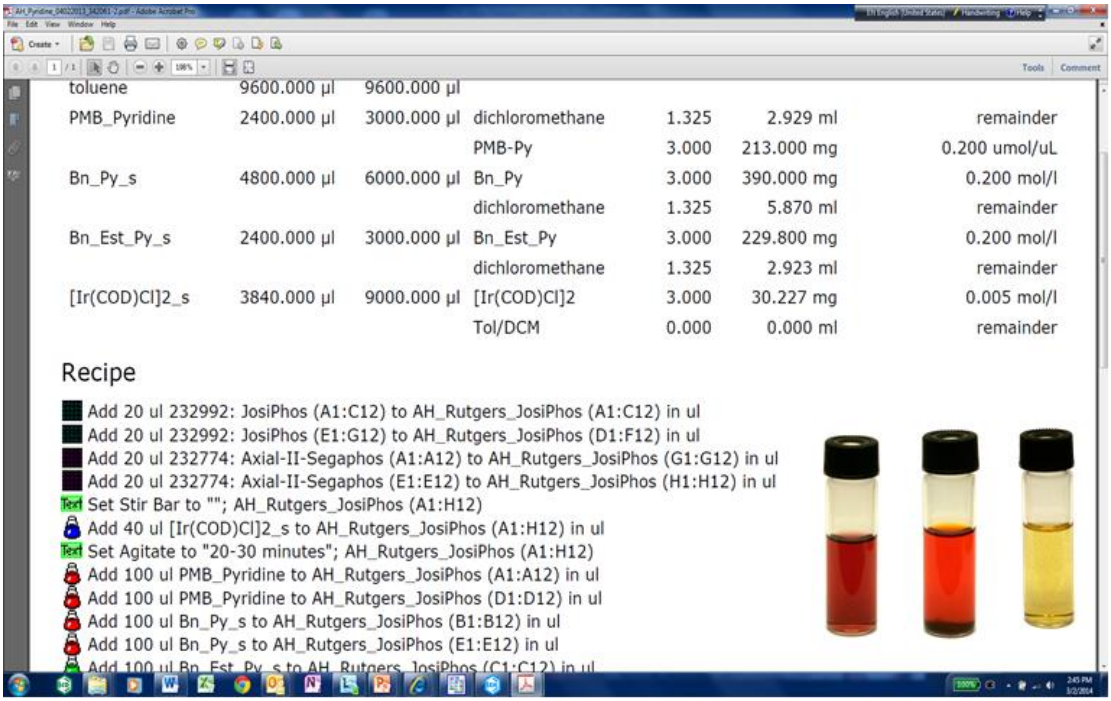

toluene	9600.000 µl	9600.000 µl				
PMB_Pyridine	2400.000 µl	3000.000 µl	dichloromethane	1.325	2.929 ml	remainder
			PMB-Py	3.000	213.000 mg	0.200 umol/uL
Bn_Py_s	4800.000 µl	6000.000 µl	Bn_Py	3.000	390.000 mg	0.200 mol/l
			dichloromethane	1.325	5.870 ml	remainder
Bn_Est_Py_s	2400.000 µl	3000.000 µl	Bn_Est_Py	3.000	229.800 mg	0.200 mol/l
			dichloromethane	1.325	2.923 ml	remainder
[Ir(COD)Cl]2_s	3840.000 µl	9000.000 µl	[Ir(COD)Cl]2	3.000	30.227 mg	0.005 mol/l
			Tol/DCM	0.000	0.000 ml	remainder

Recipe

Add 20 ul 232992: JosiPhos (A1:C12) to AH_Rutgers_JosiPhos (A1:C12) in ul
Add 20 ul 232992: JosiPhos (E1:G12) to AH_Rutgers_JosiPhos (D1:F12) in ul
Add 20 ul 232774: Axial-II-Segaphos (A1:A12) to AH_Rutgers_JosiPhos (G1:G12) in ul
Add 20 ul 232774: Axial-II-Segaphos (E1:E12) to AH_Rutgers_JosiPhos (H1:H12) in ul
Set Stir Bar to ""; AH_Rutgers_JosiPhos (A1:H12)
Add 40 ul [Ir(COD)Cl]2_s to AH_Rutgers_JosiPhos (A1:H12) in ul
Set Agitate to "20-30 minutes"; AH_Rutgers_JosiPhos (A1:H12)
Add 100 ul PMB_Pyridine to AH_Rutgers_JosiPhos (A1:A12) in ul
Add 100 ul PMB_Pyridine to AH_Rutgers_JosiPhos (D1:D12) in ul
Add 100 ul Bn_Py_s to AH_Rutgers_JosiPhos (B1:B12) in ul
Add 100 ul Bn_Py_s to AH_Rutgers_JosiPhos (E1:E12) in ul
Add 100 ul Bn_Est_Py_s to AH_Rutgers_JosiPhos (C1:C12) in ul

Figure 3.17. Library recipe used in HTS

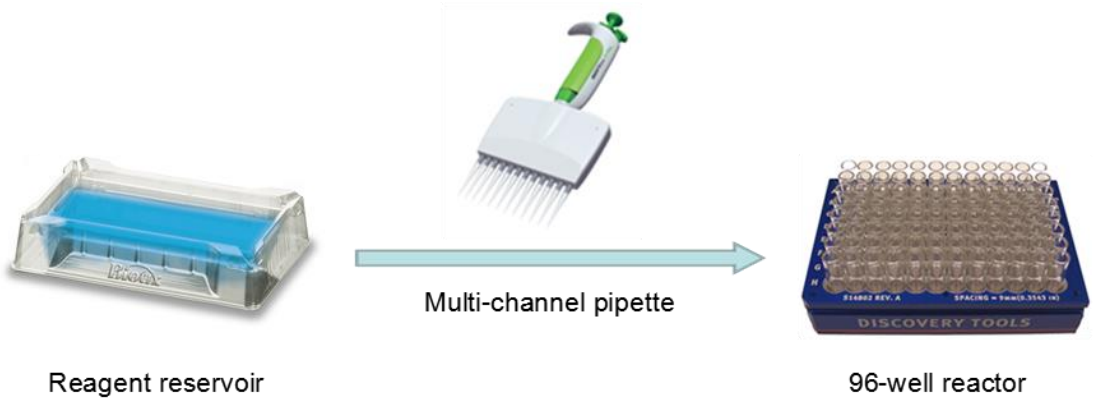

Reagent reservoir

96-well reactor

Figure 3.18. Reactor preparation used in HTS

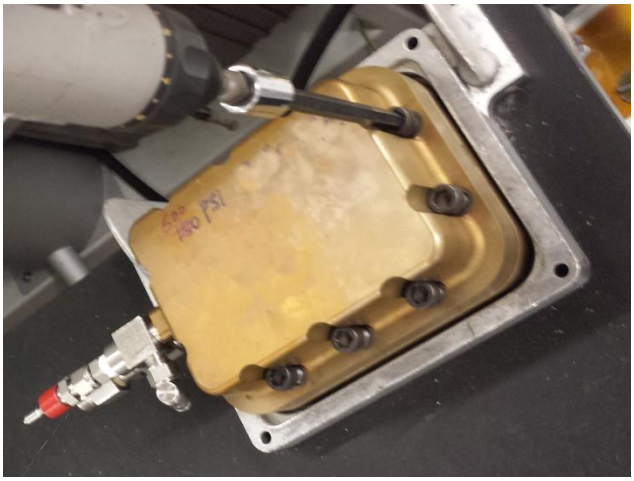

Figure 3.19. High pressure reaction block used in HTS

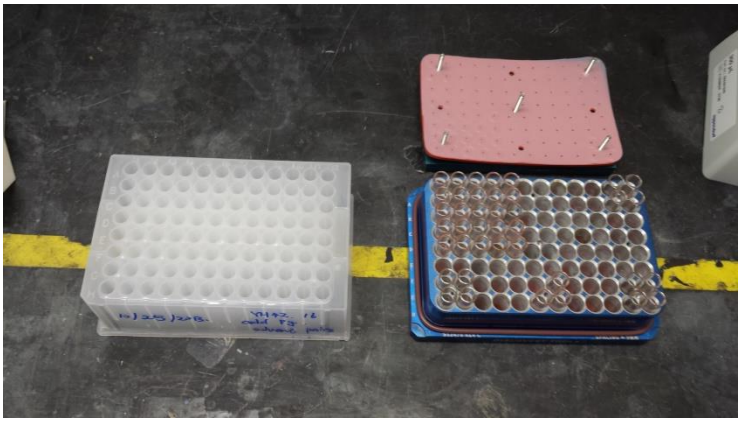

Figure 3.20. Reactor (right) and multi-well analytic plate (left) used in HTS

3.3 Asymmetric hydrogenation of *N*-benzylpyridinium salts

For our initial studies, an *N*-benzyl group was chosen to activate 2-phenylpyridine due to its ubiquity in protecting group chemistry (**Table 3-1**).[15] While simple *N*-benzylpyridinium salts have been demonstrated to be very challenging substrates in asymmetric hydrogenation, we envisioned that an in depth evaluation of ligand architecture with respect to reaction selectivity might

result in the identification of an efficient catalyst. A library of 240 chiral phosphine ligands was evaluated. While the majority of phosphine ligands screened gave <60% ee, several active and selective ligands were discovered. Doubly-oxygenated atropisomeric C2-symmetric bisphosphine ligands, such as SynPhos, SEGPHOS and GarPhos, in conjunction with $[Ir(COD)Cl]_2$ as pre-catalyst, showed good enantioselectivities in the asymmetric hydrogenation of 1 (**Table 3-1**, L7 to L11). The fine-tuning of the GarPhos and SEGPHOS ligands structure also had notable impact on their enantioselectivities, with more sterically encumbered and electron-rich phosphine aryl substituents giving higher enantioselectivities (**Table 3-1**, L8, L9 and L10, L11). In addition, generally higher selectivities were observed with more electron-rich doubly-oxygenated ligand frameworks. When the phosphole-containing MP^2-SEGPHOS (L12) was employed, chiral piperidine 2 (Ar = Ph) was obtained in 96% ee. High ee's also were observed for two other structurally diverse *N*-benzylpyridinium bromides [Ar = 2-(CO_2Me)Ph and 4-(OMe)Ph], suggesting that a general protocol might be achievable. The size of the phosphole substituents was found to be critical (**Table 3-1**, L12 and L13), as evidenced by the increased selectivity when a less sterically encumbered phosphole was employed.

Table 3.1. Selected results of ligand screen for asymmetric hydrogenation of *N*-Alkyl-2-phenylpyridium bromide substrates using iridium catalysts[a-c]

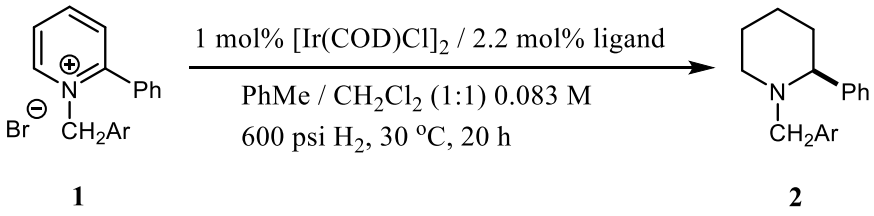

1 **2**

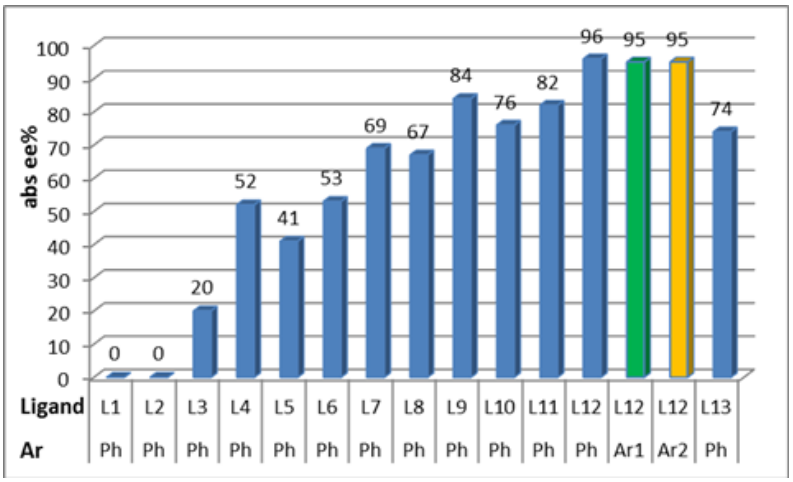

[a] Reactions were carried out using 0.01 mmol of substrate in 0.12 mL of mixed solvent. [b] Absolute enantiomeric excesses were determined by chiral SFC. [c] Ar1 = 2-(CO2Me)Ph, Ar2 = 4-(OMe)Ph.

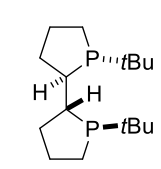

L1:(*S*,*S*,*R*,*R*)-TangPhos

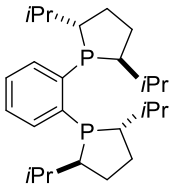

L2: (*R,R*)-*i*Pr-DuPhos

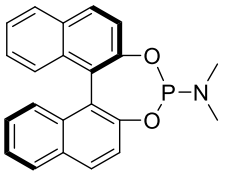

L3: (*R*)-MonoPhos

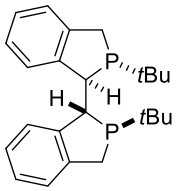

L4: (S_p, R_c)-DuanPhos

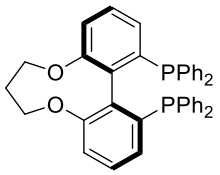

L5:(*S*)-C_3-TunePhos

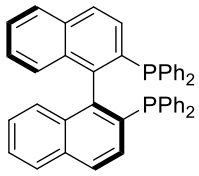

L6: (*S*)-BINAP

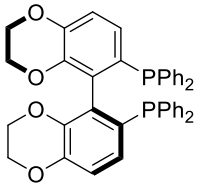

L7: (*S*)-SynPhos

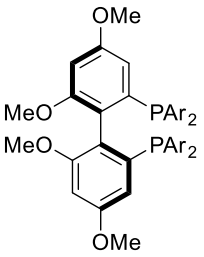

L8, Ar=Ph,(*S*)-GarPhos
L9, Ar=4-OMe-3,5-Di-*t*Bu-C_6H_2 (*S*)-DTBM-GarPhos

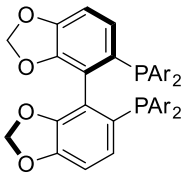

L10: Ar=Ph, (*R*)-SEGPHOS
L11:Ar= Ar=4-OMe-3,5-Di-*t*Bu -C_6H_2-(*R*)-DTBM-SEGPHOS

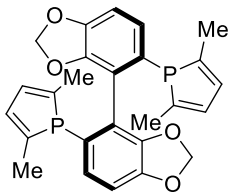

L12: (*R*)-MP^2-SEGPHOS

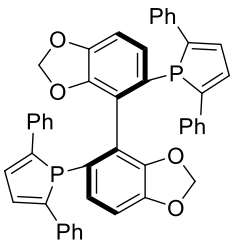

L13: (*R*)-PhP-SEGPHOS

It is worth noting that to the best of our knowledge the results obtained with L12 represent the first reported examples of the use of MP^2-SEGPHOS in a highly efficient asymmetric reaction.[16] A number of unique features of phospholes may contribute to the observed high efficiency and enantioselectivity in the reactions employing MP^2-SEGPHOS as a ligand. Firstly, the previously noted relationship between the selectivity of the asymmetric hydrogenation and donor capacity of the ligand would be further enhanced by the phosphole functionality of MP^2-SEGPHOS (**Scheme 3-9**).[17] Secondly, the rigidity[18] and planarity[19] of the phosphole unit would be expected

to provide a well-defined chiral pocket20 around the reactive site that is substantially different from those seen with other C2-symmetric bis(phosphine) ligands.

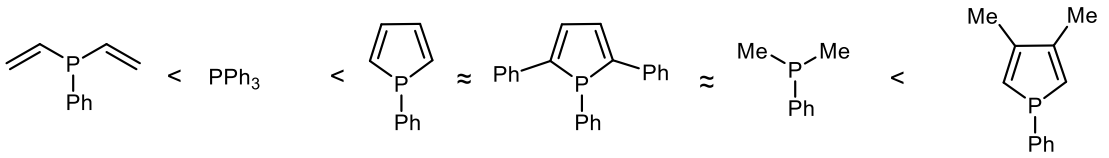

2072 (cm-1)[a] 2070(cm-1)[a] 2068(cm-1)[a] 2060 (cm-1)[a]

[a] Infrared data for $LMo(CO)_5$ complexes.[17] Only the highest energy υ(CO) is given.

Figure 3.21. Order of electron donating ability of phosphorus ligands

Having identified MP^2-SEGPHOS as the most selective ligand of those examined, we next explored the influence of solvent (**Table 3-2**). While many single solvents led to excellent enantioselectivity for substrate 1a, acceptable reactivity was only observed for THF, acetone and 1,2-dichloroethane (DCE) with 2 mol% Ir catalyst. The combination of acetone and DCE proved optimal (**Table 3-2**, entry 10), allowing the Ir catalyst loading to be lowered to 0.5 mol%.

Table 3.2. Solvent screening for asymmetric hydrogenation of *N*-Benzyl-2-phenylpyridium bromide using iridium–(*R*)-MP^2-SEGPHOS catalyst[a]

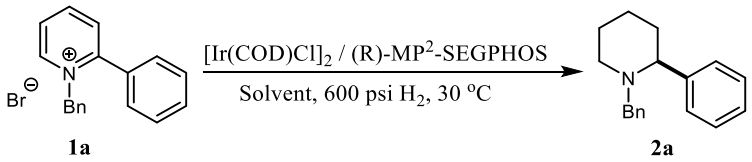

1a **2a**

Entry	Solvent	Conversion (%)[b]	*ee* (%)[b]
1	CH2Cl2	53	93
2	DCE	>99	94
3	EtOAc	57	94
4	Acetone	>99	94
5	Dioxane	62	93
6	Toluene	22	89
7	THF	>99	89
8	MeOH	32	63
9[c]	Acetone	91	86
10[c]	DCE / Acetone 1:1	>99	93
11[c]	DCE	78	95

[a] Reaction conditions: **1a** 0.083 M, [Ir] / ligand / *N*-benzyl-2-phenylpyridium bromide = 2:2.2:100, 20 h. [b] Conversions and enantiomeric excesses were determined by chiral SFC. [c] **1a** 0.025 M, [Ir] / ligand / *N*-benzyl-2-arylpyridium bromide = 0.5:0.55:100, 20 h.

To explore the utility of newly developed Ir–MP^2-SEGPHOS catalytic system, a range of *N*-benzyl-2-substituted pyridium bromide substrates were synthesized and studied under the optimized conditions. The results are summarized in **Table 3-3** (entries 1 to 19). For all chosen 2-arylpyridium substrates, chiral products **2a** to **2m** were obtained in excellent yields and selectivity (90% to 96% ee). The catalytic system worked well for ortho-substituted sterically hindered substrates such as **1d**, **1k** and **1m** (**Table 3-3**, entries 4, 12 and 15), thus highlighting the enhanced reactivity of this system. The enantioselectivities in these cases were only slightly less than

those where the 2-aryl group bore substituents in the *meta* or *para* positions. Significantly, the electronic properties of the 2-aryl group did not exert any noticeable effect on the reaction selectivity. Both electron donating 4-MeO- (1f) and electron withdrawing 4-Cl-(**1i**) and 3,5-F2-phenyl-substituted (1**l**) substrates provided similarly high enantioselectivities (**Table 3-3**, entries 6, 9 and 13). During our study, we observed that some substrates were quite sensitive to the solvent composition (vide supra), requiring adjustment of the ratio to achieve higher reactivity (**Table 3-3**; cf. entries 10, 11; 14, 15). For 2-alkylpyridium substrates, chiral products were obtained with only low to moderate levels of enantioselectivity (**Table 3-3**, entries 16 to 19). While improved enantioselectivity was observed with a sterically bulky substrate (**1o** vs **1n**), the isolated yield dropped significantly due to the lower reactivity (**Table 2**, entries 16 and 17). Notably, tuning the phosphole ligand structure had some impact on the levels of enantioselectivity for the 2-benzylpyridinium substrate (**1p**) (**Table 2**, entries 18 and 19). Using L13, desired product (**2p**) was obtained in 42% ee.

Table 3.3. Iridium-catalysed asymmetric hydrogenation of N-Benzyl-2-substituted-pyridinium salts 1[a]

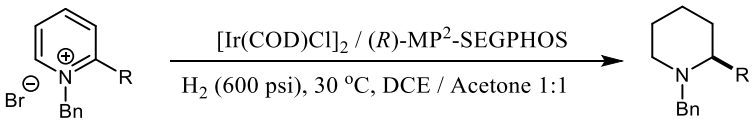

1 **2**

Entry	R	Product	Yield (%)[b]	ee (%)[c]
1	C_6H_5 (**1a**)	**2a**	97	96
2	3-MeC_6H_4 (**1b**)	**2b**	99	96
3	4-MeC_6H_4 (**1c**)	**2c**	93	93
4	2-$MeOC_6H_4$ (**1d**)	**2d**	90	90
5	3-$MeOC_6H_4$ (**1e**)	**2e**	99	96
6	4-$MeOC_6H_4$ (**1f**)	**2f**	95	94
7	4-Ac(H)NC_6H_4 (**1g**)	**2g**	97	95
8	4-tBuC_6H_4 (**1h**)	**2h**	96	93
9	4-ClC_6H_4 (**1i**)	**2i**	96	95
10	4-PhC_6H_4 (**1j**)	**2j**	86	90
11[d]	4-PhC_6H_4 (**1j**)	**2j**	96	95
12	2,4-$Cl_2C_6H_3$ (**1k**)	**2k**	94	90
13	3,5-$F_2C_6H_3$ (**1l**)	**2l**	95	96
14	2-naphthyl (**1m**)	**2m**	12	93
15[e]	2-naphthyl (**1m**)	**2m**	88	94
16[e]	Me (**1n**)	**2n**	81	33
17[e]	*i*-Pr (**1o**)	**2o**	24	69
18[f]	Bn (**1p**)	**2p**	99	9
19[f, g]	Bn (**1p**)	**2p**	94	42

[a] Reaction conditions: **1** 0.025 M, [Ir] / ligand / *N*-benzyl-2-arylpyridium bromide = 0.5:0.55:100, 20 h. [b] Yields are isolated yields. [c] Enantiomeric excesses were determined by chiral SFC or chiral HPLC. [d] DCE / Acetone = 5:1 as solvent. [e] Acetone as solvent. [f] DCE as solvent. [g] **L13** was used as ligand.

To evaluate the practical utility of newly developed method, the asymmetric hydrogenation of *N*-benzyl-2-phenylpyridium bromide **1a** was carried out on 1.5 mmol scale. The desired product **2a** was obtained with 98% isolated yield and 94% ee (**Scheme 3-10**), and the catalyst loading could be reduced to 0.25 mol% (S / C = 400) at this scale. The facile removal of the N-benzyl group was demonstrated through a one-pot asymmetric

hydrogenation followed by deprotection, giving 2-phenylpiperidine in 91% overall yield and 92% ee (**Scheme 3-11**).

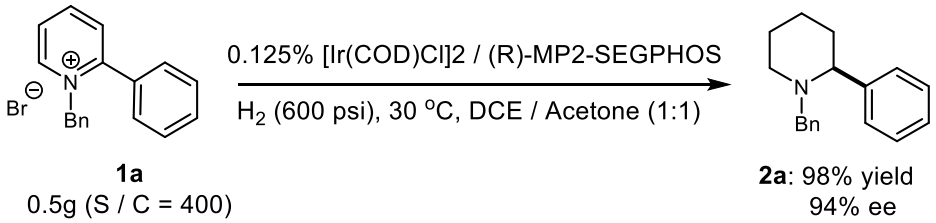

Figure 3.22. Gram scale hydrogenation of *N*-benzyl-2-phenylpyridium bromide

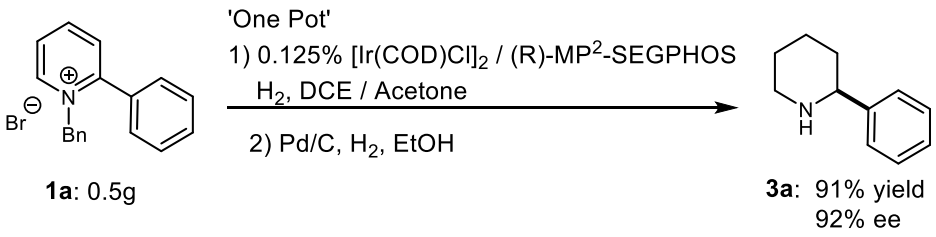

Figure 3.23. One pot reaction to achieve 2-phenylpiperidine

Having established a robust reaction with *N*-benzyl derivatives, we wished to explore the substrate scope with other *N*-alkyl substituents. As shown in Scheme 2, the Ir-phosphole catalyst delivered remarkably high conversion and enantioselectivity with *N*-alkyl substituents as small as Et (**5e**), and even an N-Me pyridinium salt gave the resulting *N*-methylpiperidine product in good yield and 81% ee (**5d**). The (carboethoxy)methyl substituent (**5g**) was also tolerated, giving enantioselectivities comparable to those seen

with benzyl substituents (**5a**); this substituent is particularly interesting due to its utility as a functional group for further elaboration. The nature of the pyridinium counterion had some impact on both the activity and enantioselectivity of the reaction (cf. Scheme 2, **5a** and **5d**). The counterion effect is not yet understood,[21] and we are currently investigating its origin.

Table 3.4. Iridium-catalyzed asymmetric hydrogenation of 2-phenylpyridinium salts 4[a]

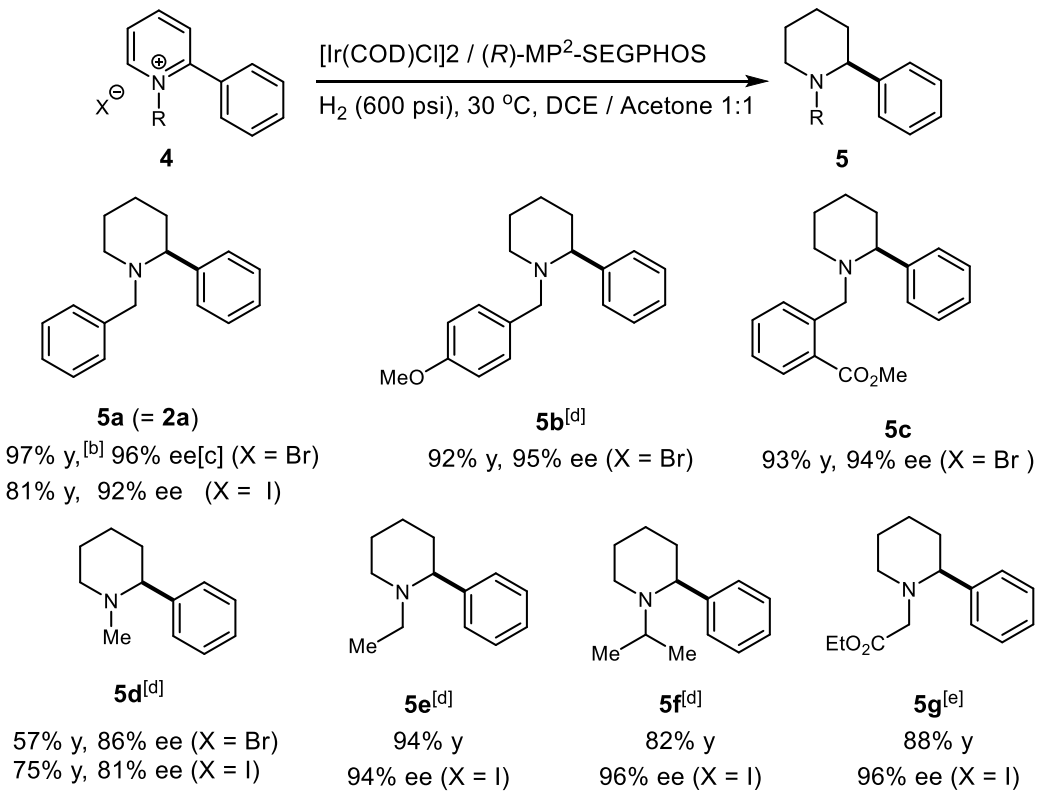

[a] Reaction conditions: **4** 0.025 M, [Ir] / ligand / *N*-Alkyl-2-phenylpyridium bromide = 0.5:0.55:100, 20 h. [b] Yields are isolated yields. [c] Enantiomeric excesses were determined by chiral SFC or chiral HPLC. [d] DCE as solvent. [e] DCE / Acetone = 5:1 as solvent.

In summary, we have developed a highly efficient enantioselective hydrogenation of *N*-alkyl-2-arylpyridinium salts. This protocol represents a significant advance over previous methods in that a directing group is not required. With this constraint removed, this new method tolerates a variety of *N*-benzyl as well as simple *N*-alkyl groups, which greatly increases the scope and applicability of this approach in synthesis. In addition, this work provides the unique example of using a chiral phosphole-based ligand for highly efficient asymmetric catalysis. The unique electronic and structural aspects of the phosphole unit should inform future ligand design for asymmetric catalysis.

3.4 Other related results

3.4.1 Pressure, temperature, concentration and catalyst loading screening of asymmetric hydrogenation of *N*-Benzyl-2-phenylpyridium bromide

To achieve optimized reaction condition of asymmetric hydrogenation of *N*-Benzyl-2-phenylpyridium bromide, potential effective factors including pressure, temperature, starting material concentration and catalyst loading have been studied.

Table 3-5 shows that robust enantioselective catalytic system at lower H_2 pressure (300 psi). Variety of conditions provided similar enantioselectivities (**Table 3-5,** Entry 1-10). Lower catalyst loading (0.1% mol) or lower temperature (30 ^{o}C) lead to lower conversions. Higher pressure (600 psi) or higher

temperature (50 ^{o}C) improves conversion but ee% drops. Solvent plays an important role in this reaction.

Table 3.5. Pressure, temperature, concentration and catalyst loading screening of asymmetric hydrogenation of *N*-Benzyl-2-phenylpyridium bromide[a]

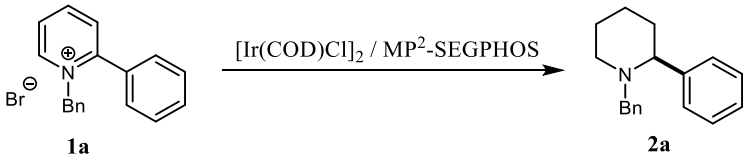

1a 2a

Entry	Pressure/Temp.	Cat. Loading %mol	Conc. (M)	Solvent	Conversion (%)[b]	Ee (%)[b]
1	300 psi/50 ^{o}C	0.5	0.1	Acetone	99	94
2	300 psi/50 ^{o}C	0.5	0.25	Acetone	98	94
3	300 psi/50 ^{o}C	0.1	0.1	Acetone	87	94
4	300 psi/50 ^{o}C	0.1	0.25	Acetone	92	94
5	300 psi/50 ^{o}C	0.5	0.1	Ace/EtOH=1:2	99	94
6	300 psi/50 ^{o}C	0.1	0.1	Ace/EtOH=1:2	36	93
7	300 psi/30 ^{o}C	0.5	0.1	Acetone	97	93
8	300 psi/30 ^{o}C	0.1	0.1	Acetone	9	-
9	300 psi/30 ^{o}C	0.5	0.1	Ace/EtOH=1:2	50	95
10	300 psi/30 ^{o}C	0.1	0.1	Ace/EtOH=1:2	7	-
11	600 psi/50 ^{o}C	0.5	0.1	Acetone	99	90
12	600 psi/50 ^{o}C	0.1	0.1	Acetone	99	91
13	600 psi/50 ^{o}C	0.5	0.1	Ace/EtOH=1:2	-	89
14	600 psi/50 ^{o}C	0.1	0.1	Ace/EtOH=1:2	49	91
15	1200 psi/50 ^{o}C	0.5	0.1	Acetone	99	89
16	1200 psi/50 ^{o}C	0.1	0.1	Acetone	99	90
17	1200 psi/50 ^{o}C	0.5	0.1	Ace/EtOH=1:2	99	90
18	1200 psi/50 ^{o}C	0.1	0.1	Ace/EtOH=1:2	84	90
19	1200 psi/30 ^{o}C	0.5	0.1	Acetone	96	90
20	1200 psi/30 ^{o}C	0.1	0.1	Acetone	31	92
21	600 psi/30 ^{o}C	0.5	0.025	Ace/DCE=1:2	99	96

[a] Reaction conditions: **1a** 0.083 M, [Ir] / ligand / *N*-benzyl-2-phenylpyridium bromide = 2:2.2:100, 20 h. [b] Conversions and enantiomeric excesses were determined by chiral SFC.

3.4.2 Acetone self-reduction liability study

After solvent screening, we find out the combination of acetone : dichloroethane = 1:1 is the best solvent pair. Acetone is a ketone, which is easily to be reduced by some iridium catalyst. To study the acetone self-reduction liability, we use GC to detect the corresponding reductive product isopropanol. The GC condition is:

Column: RTX-624, 20m x 0.18mm, 1.0 µm film; constant Flow =2.0ml/min. Temperature Program: 35 ^{o}C for 5min 20 ^{o}C/min to 240 ^{o}C and hold at 240 ^{o}C for 5min. Injector: 220°C; split 250:1; Detector: FID at 220°C; Hydrogen flow=40 ml/min; Air flow=450 ml/min; Make up gas =40 ml/min Helium. Injection Volume: 1µL.

Five conditions have been studied:

A1: 0.025 M pyridinium salt, 0.5 mol% catalyst loading, DCE/Acetone = 1/1.

A2: 0.025 M pyridinium salt, 0 mol% catalyst loading, DCE/Acetone = 1/1.

A3: No pyridinium salt, 0.5 mol% catalyst loading, DCE/Acetone = 1/1.

A4: 0.025 M pyridinium salt, 0.5 mol% catalyst loading, DCE/IPA = 1/1.

A5: 0.025 M pyridinium salt, 0.5 mol% catalyst loading, DCE.

Based on **Table 3-6,** it indicates that no acetone reduction observed under our optimized catalytic reaction condition. Only the reduction of *N*-Benzyl-2-phenylpyridium bromide carried out.

Table 3.6. Acetone self-reduction liability study

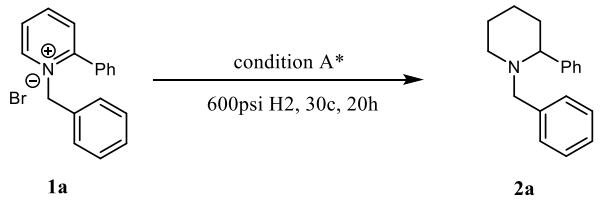

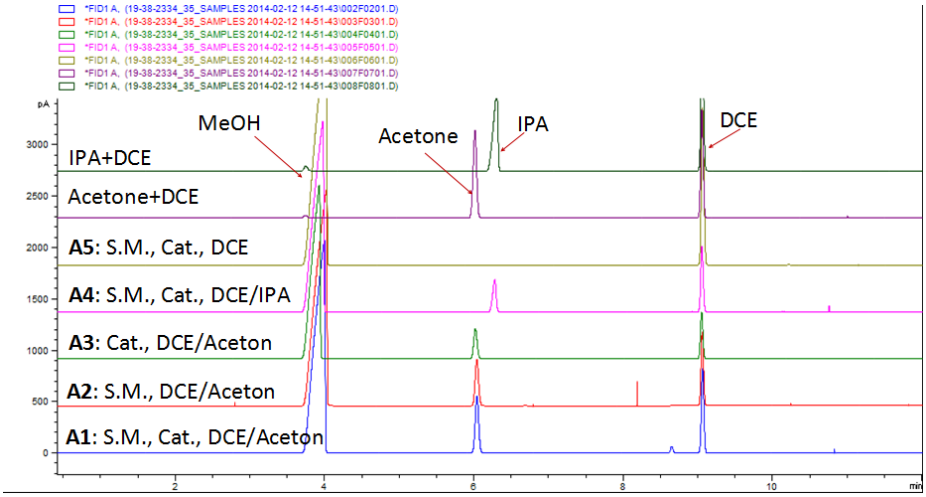

3.4.2 Other screenings

Table 3.7. JosiPhos ligands screening for asymmetric hydrogenation of *N*-Benzyl-2-phenylpyridium bromide [a]

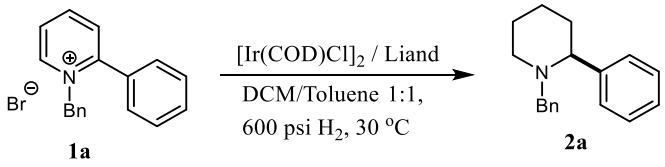

Entry	Ligand[b]	*ee* (%)[c]
1	SL-J001-1	-43%
2	SL-J002-1	-4%
3	SL-J004-1	50%
4	SL-J006-1	-29%
5	SL-J204-1	-18%
6	SL-J013-1	11%
7	SL-J212-1	-83%
8	SL-J017-1	-4%
9	SL-J025-1	-37%
10	SL-J052-1	44%

11	SL-J008-1	8%

[a] Reaction conditions: **1a** 0.083 M, [Ir] / ligand / *N*-benzyl-2-phenylpyridium bromide = 2:2.2:100, 22 h. [b] Due to confidential issue, only part of ligands can be displayed. [c] Conversions and enantiomeric excesses were determined by chiral SFC.

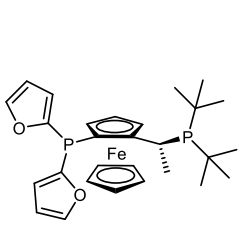

SL-J212-1

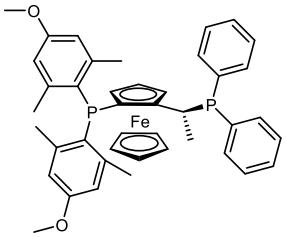

SL-J452-1

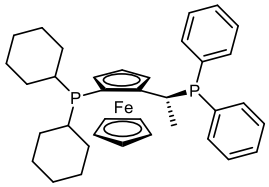

SL-J004-1

Table 3.8. Axial type ligands screening for asymmetric hydrogenation of *N*-Benzyl-2-phenylpyridium bromide [a]

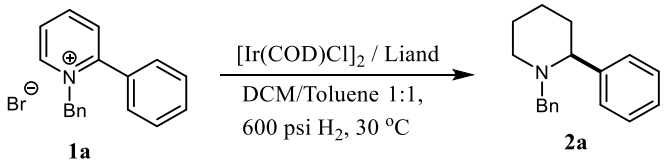

1a **2a**

Entry	Ligand[b]	*ee* (%)[c]
1	G1 MP2-SEGPHOS	96%
2	G5 SL-A 107-1	84%
3	G7 SL-A 121-1	82%
4	H6 DTBM-Garphos	84%
5	B9 DTBM-SEGPHOS	82%
6	B7 SL-A 109-2	79%
7	B06 SEGPHOS	76%

[a] Reaction conditions: **1a** 0.083 M, [Ir] / ligand / *N*-benzyl-2-phenylpyridium bromide = 2:2.2:100, 22 h. [b] Due to confidential issue, only part of ligands can be displayed. [c] Conversions and enantiomeric excesses were determined by chiral SFC.

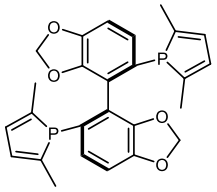

G1 MP2-SEGPHOS

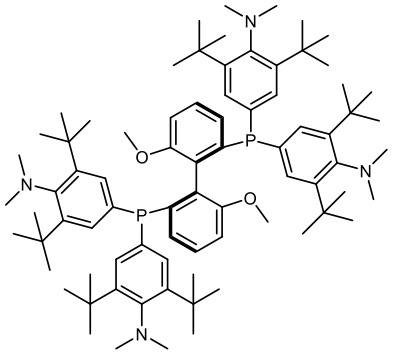

G5 SL-A 107-1

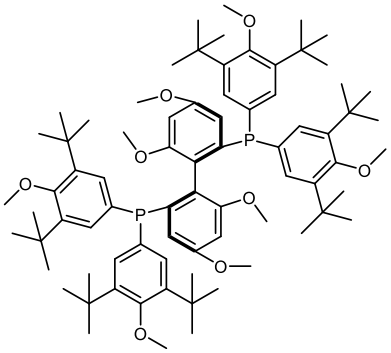

H6 DTBM-Garphos

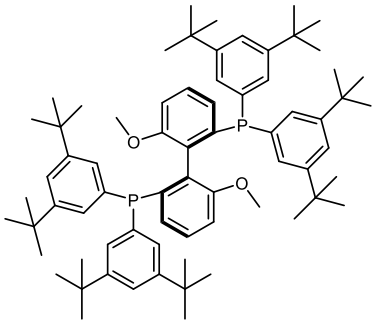

G7 SL-A 121-1

Table 3.9. JosiPhos ligands screening for asymmetric hydrogenation of 1-(4-methoxybenzyl)-2-phenylpyridin-1-ium bromide[a]

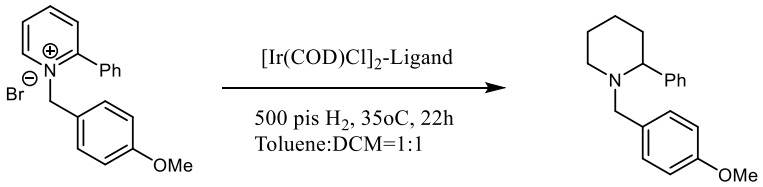

6 7

Entry	Ligand[b]	*ee* (%)[c]
1	SL-J001-1	NA
2	SL-J002-1	NA
3	SL-J004-1	-68%
4	SL-J006-1	NA
5	SL-J204-1	NA
6	SL-J013-1	NA
7	SL-J212-1	75%
8	SL-J017-1	-3%
9	SL-J025-1	44%
10	SL-J052-1	-68%
11	SL-J008-1	NA

[a] Reaction conditions: **6** 0.083 M, [Ir] / ligand / 1-(4-methoxybenzyl)-2-phenylpyridin-1-ium bromide = 2:2.2:100, 22 h. [b] Due to confidential issue, only part of ligands can be displayed. [c] Conversions and enantiomeric excesses were determined by chiral SFC.

Table 3.10. JosiPhos ligands screening for asymmetric hydrogenation of *N*-(2-CO_2*i*Pr)benzylpyridinium bromide[a]

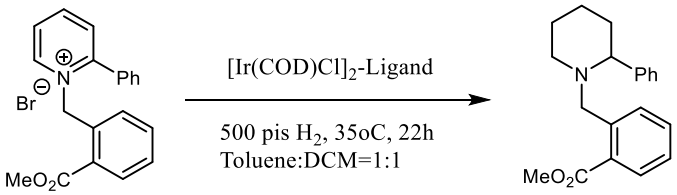

8 **9**

Entry	Ligand[b]	*ee* (%)[c]
1	SL-J001-1	-61%
2	SL-J002-1	10%
3	SL-J004-1	70%
4	SL-J006-1	-9%
5	SL-J204-1	-37%
6	SL-J013-1	9%
7	SL-J212-1	-68%
8	SL-J017-1	-7%
9	SL-J025-1	-6%
10	SL-J052-1	66%
11	SL-J008-1	7%

[a] Reaction conditions: **8** 0.083 M, [Ir] / ligand / *N*-(2-CO_2*i*Pr)benzylpyridinium bromide = 2:2.2:100, 22 h. [b] Due to confidential issue, only part of ligands can be displayed. [c] Conversions and enantiomeric excesses were determined by chiral SFC.

Table 3.11. Axial type ligands screening for asymmetric hydrogenation of *N*-(2-CO_2*i*Pr)benzylpyridinium bromide[a]

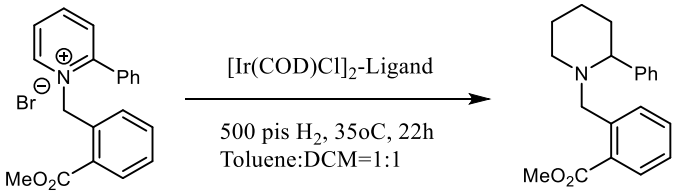

8 **9**

Entry	Ligand[b]	*ee* (%)[c]
1	C01 TMBTP	-61%
2	B06 SEGPHOS	10%
3	F04 DM-SEGPHOS	70%

[a] Reaction conditions: **8** 0.083 M, [Ir] / ligand / *N*-(2-CO_2*i*Pr)benzylpyridinium bromide = 2:2.2:100, 22 h. [b] Due to confidential issue, only part of ligands can be displayed. [c] Conversions and enantiomeric excesses were determined by chiral SFC.

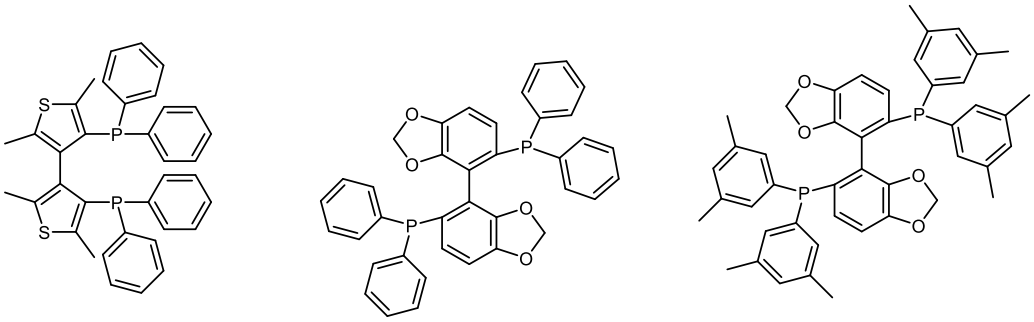

C01 TMBTP B06 SEGPHOS F04 DM-SEGPHOS

Table 3.12. Asymmetric hydrogenation of 1-benzyl-5-methyl-2-phenylpyridin-1-ium bromide[a]

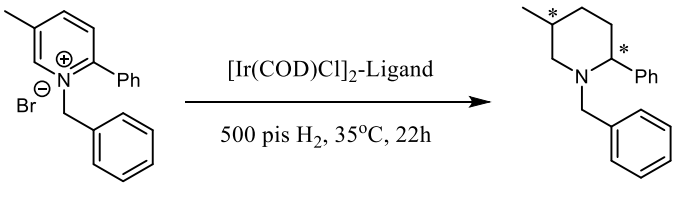

10 **11**

Entry	Ligand	Solvent	dr	ee-1 (%)[b]	ee-2 (%)[b]
1	MP^2-SEGPHOS	Ace/DCE=1:1	2.32	88	84
2	MP^2-SEGPHOS	DCE	2.25	93	84
3	MP^2-SEGPHOS	Acetone	2.43	93	84
4	P^3-SEGPHOS	Ace/DCE=1:1	0.66	47	75
5	P^3-SEGPHOS	DCE	0.67	52	77
6	P^3-SEGPHOS	Acetone	0.46	32	44

[a] Reaction conditions: **10** 0.083 M, [Ir] / ligand / *N*-benzyl-2-phenylpyridium bromide = 2:2.2:100, 20 h. [b] Conversions and enantiomeric excesses were determined by chiral SFC.

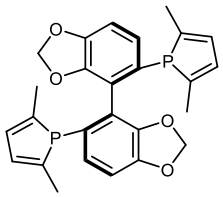

MP^2-SEGPHOS

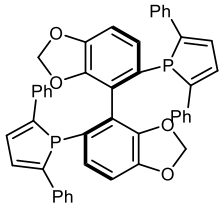

P^3-SEGPHOS

Table 3.13. Asymmetric hydrogenation of 1-benzyl-3-methyl-2-phenylpyridin-1-ium bromide[a]

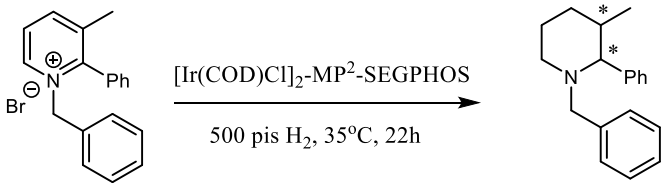

12 **13**

Entry	Solvent	Conversion[b]	ee (%)[b]
1	Ace/DCE=1:1	20	12
2	DCE	12	14
3	Acetone	38	5

[a] Reaction conditions: **12** 0.083 M, [Ir] / ligand / *N*-benzyl-2-phenylpyridium bromide = 2:2.2:100, 20 h. [b] Conversions and enantiomeric excesses were determined by chiral SFC. No trans- product was detected.

Table 3.14. Asymmetric hydrogenation of variable pyridinium bromide[a]

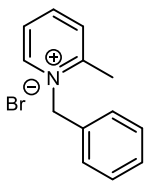

14

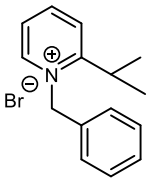

15

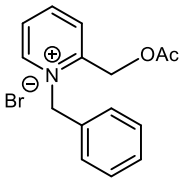

16

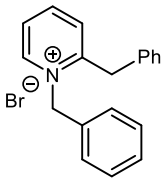

17

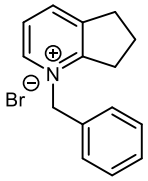

18

Substrate	MP²-SEGPHOS			P³-SEGPHOS		
	Solvent[c]	Conversion[b]	ee (%)[b]	Solvent[c]	Conversion[b]	ee (%)[b]
14	Acetone	95	33	DCE	61	40
15	Acetone	20	69	DCE	61	42
16	Ace/DCE	95	24	Ace/DCE	99	9
17	DCE	99	9	DCE	93	42
18	Ace/DCE	20	12	Acetone	99	22

[a] Reaction conditions: [Ir] / ligand / *N*-benzyl-2-phenylpyridium bromide = 2:2.2:100, 20 h, 30 ^{o}C, 600 psi H_2. [b] Conversions and enantiomeric excesses were determined by chiral SFC. No trans- product was detected. [c] Best solvent after solvent screening.

3.5 Mechanism of Iridium-Catalyzed Asymmetric Hydrogenation of Pyridinium Salts

Among all catalytic systems, iridium catalyst shows its efficiency in direct asymmetric hydrogenation of pyridinium salts.[7-11] Although these successful examples show great potential of asymmetric hydrogenation of pyridinium salts with an iridium catalyst, the mechanism behind this reaction is still unknown for chemists. Reduction of three double bonds makes it complicated products.

3.5.1 Isomerization

To obtain preliminary mechanistic insight, the asymmetric deuteriation of *N*-benzyl-2-phenylpyridium bromide **1** was studied (Eq. 1). The reaction was carried out under a standard condition with D_2. If only three hydrogen gas additions occurred, deuterium percentage at the C-3, -4, -5 and -6 positions should be 50% and at the C-2 should be 100%. However only 6% deuterium at the C-5 was detected while the deuterium incorporated at the C-2, -3, -4, and -6 positions are close to expected results (**Table 3-15**). It indicates that the major proton source for C-5 reduction is not from D_2 (**Table 3-15**). Two potential proton sources except hydrogen gas are acetone and 1, 2-dichloroethane, which are solvents. However, no deuterium was detected from the product when we used deuterated solvents under the same condition with H_2. This suggests these two solvents are not proton source for this hydrogenation. After several control experiments, we found that the residue H_2O in solvents may be the proton source because solvents used in previous experiments were commercial available anhydrous solvents without further dryness.

Table 3.15. Asymmetric hydrogenation of *N*-benzyl-2-phenylpyridium bromide with D_2

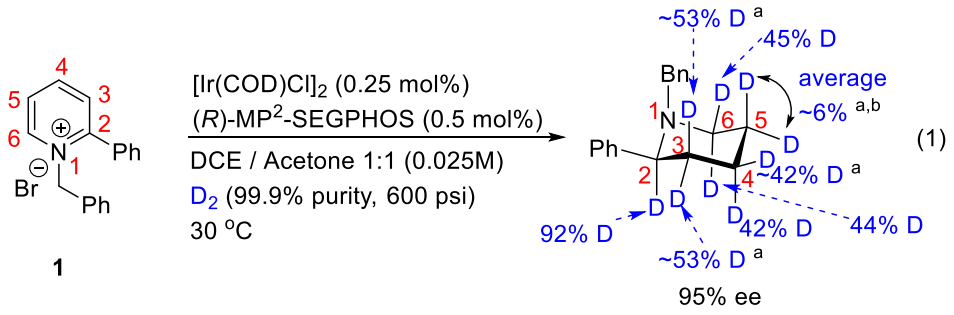

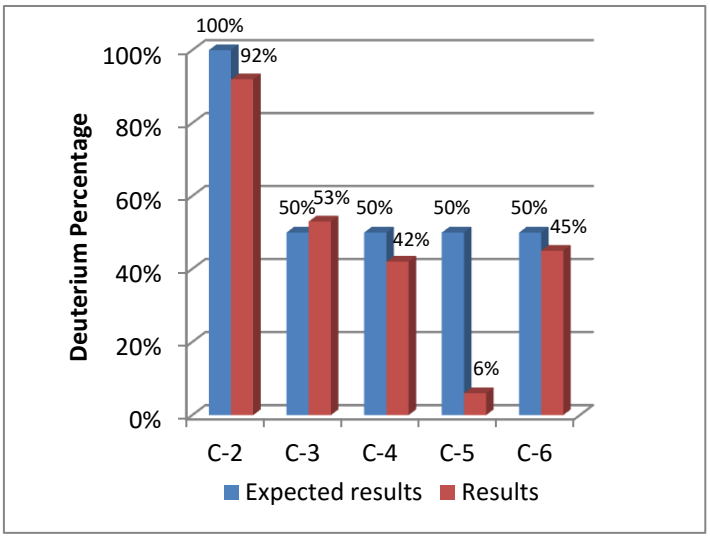

[a] Estimated value; see supporting information for further details. [b] Axial and equatorial proton chemical shifts are overlapped.

The asymmetric hydrogenation of *N*-benzyl-2-phenylpyridium bromide **1** was then carried out with D_2O as an additive (Eq. 2) in further dried solvents. Under these conditions, the deuterium label was incorporated at C-3 and C-5 only, which indicates that water is one of proton sources for reductions at these two carbons. To gain detailed information, different equivalents of D_2O were added. Along the increasing amount of D_2O, deuterium percentages at C-3 and -5 positions increase and increasing rate at C-3 is bigger than the

increasing rate at C-5, which indicates more protonation and deprotonation occurred at C-3.

Table 3.16. Asymmetric hydrogenation of *N*-benzyl-2-phenylpyridium bromide with D_2O

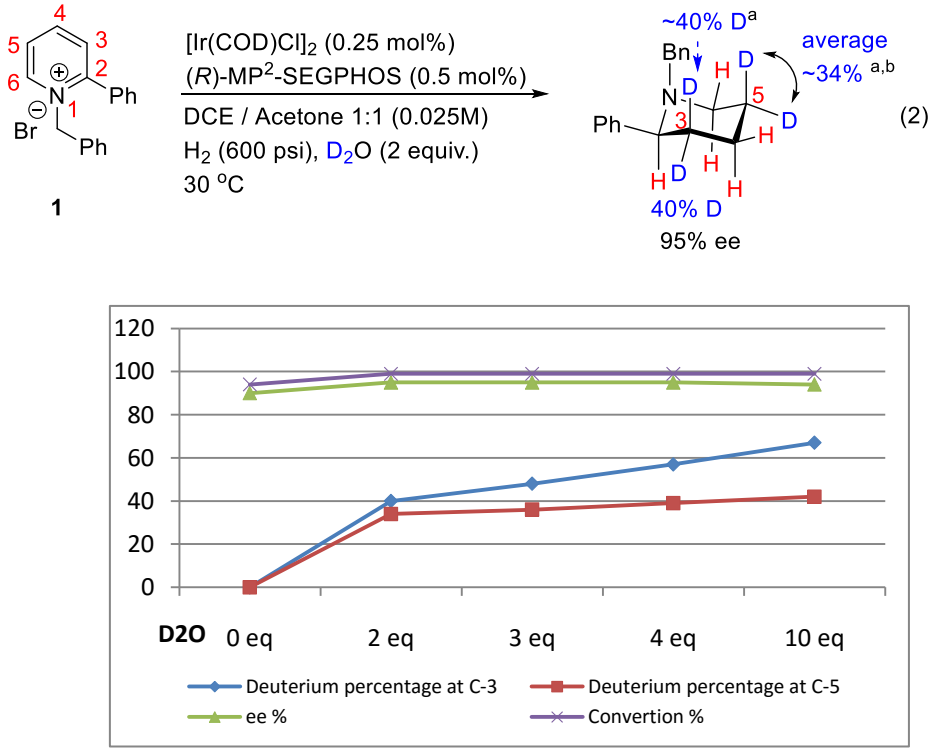

[a] Estimated value; see supporting information for further details. [b] Axial and equatorial proton chemical shifts are overlapped.

While a large amount of deuterium was incorporated at C-3, then why in the asymmetric deuteriation of *N*-benzyl-2-phenylpyridium bromide (Eq. 1), labeled deuterium at C-3 is so close to “expected” value. There are 4 types of proton sources: 1) proton from hydrogen gas; 2) proton from water remaining in solvent; 3) proton from HBr which is part of the product; and 4) proton from proton exchanged water (this proton could either be proton from hydrogen gas

or proton from starting material). At the inception of deuteriation of *N*-benzyl-2-phenylpyridium bromide (Eq. 1), the only proton source for proton exchange is type-two proton. Therefore, deuterium label at C-5 is only 6% because proton at this position has exchanged with H^+ from water. After this first proton exchange and partial product generation, more deuterium exists in the reaction system. When proton exchange undergoes at C-3, deuterium was exchanged with larger possibility. This explains why labeled deuterium at C-3 is more than labeled deuterium at C-5, even close to “expected” value.

Figure 3.24. Four proton sources

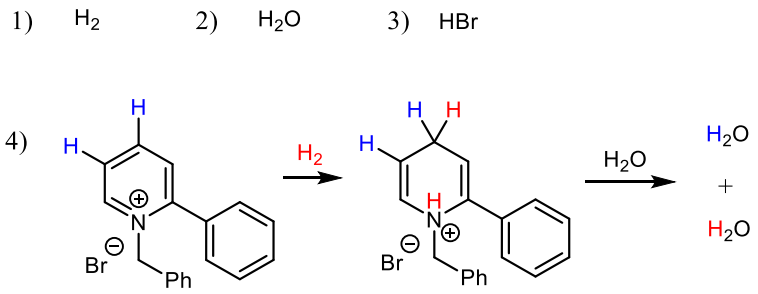

Based on these evidences, two tautomerizations in this reaction are expected (**Scheme 3-12**). After 1,4-hydrogen addition, enamine **19** was generated. **19** would capture one proton to tautomerize into iminium **20**. After second hydrogen addition, enamine **21** was generated. Then **21** would capture another proton to tautomerize into iminium **22**. Reduction of **22** gives the final product. Due to slower reduction rate of tetra-substituted iminium (**22**) compare to the reduction rate of tri-substituted iminium (**21**), second

tautomerization has longer time to undergo a reversible process of protonation and deprotonation, which explains larger deuterium increasing rate at C-3 discussed in hydrogenation of **1** carried out with D_2O as additive.

Figure 3.25. Two tautomerizations

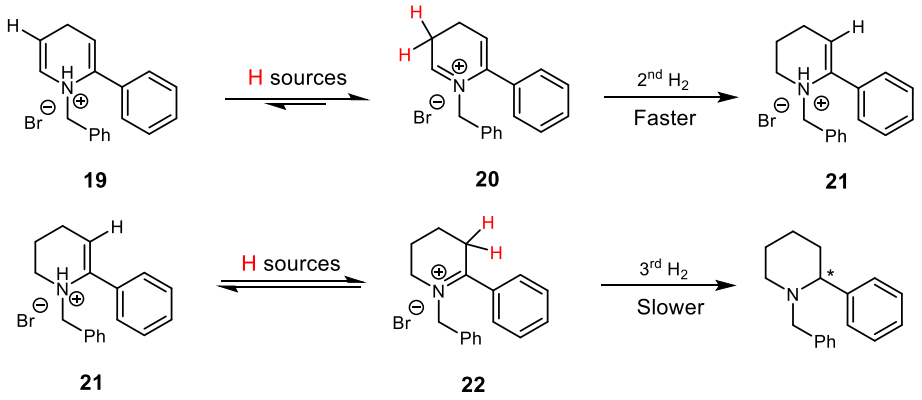

3.5.2 Outer-sphere Mechanism

It was proposed that a challenging in asymmetric hydrogenation of pyridines: substrates that possess strong coordination ability might cause the deactivation of catalysts. Lone electron pair of pyridine will occupy coordination site of catalyst as a δ donor that will lead to no space for substrate to bind with catalyst as a π donor (Scheme *). However, there is one assumption for this issue: this hydrogenation undergoes inner sphere pathway. To test this assumption, pyridines were added as additives. Different amount of 2,6-lutidine, *t*Bu-lutidine and 2-phenyl pyridine were charged. However, no significant changes in conversion or enantioselectivity were detected. Even if one equivalent of 2-phenyl pyridine was added (additive : catalyst = 400:1),

hydrogenation could run smoothly and 97% conversion with 93% ee were obtained. This indicates previous assumption was wrong. Asymmetric hydrogenation of pyridinium by iridium/bisphosphine catalyst should undergo an outer sphere pathway.

Table 3.17. Asymmetric hydrogenation of *N*-benzyl-2-phenylpyridium bromide with additives.

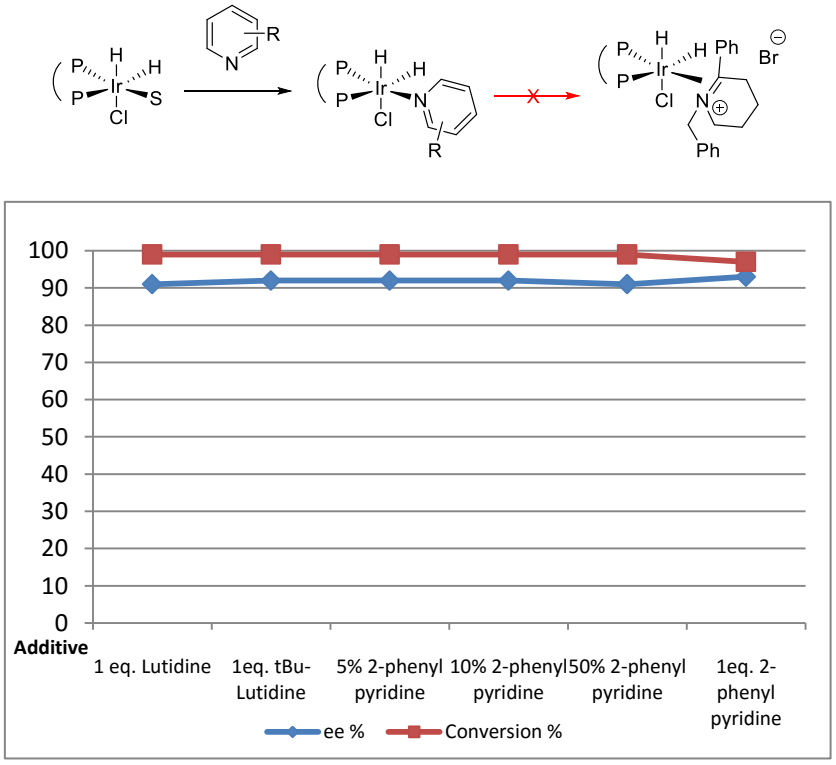

3.5.3 Intermediate

Due to three double bonds in pyridine ring, intermediates with one or two double bonds may be generated during the reaction progress. Carrying reaction with shorter reaction time gives small new peak on HPLC. But after chromatography separation, it gave a mess. It indicated the intermediate may decompose during separation. To confirm that the HPLC peak is an intermediate, not a side product, several experiments were conducted.

Figure 3.26. Intermediate in Asymmetric hydrogenation of *N*-benzyl-2-phenylpyridium bromide

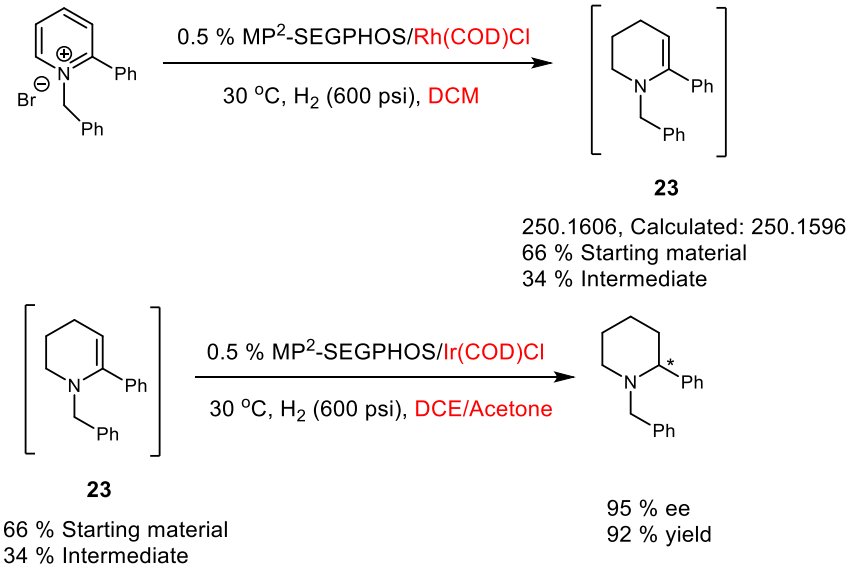

To obtain more intermediate for separation and NMR study. Different metal sources and solvents are screened. We found that hydrogenation with Rh(COD)Cl/MP^2-SEGPHOS in dichloromethane provides the largest amount of intermediate. 34% intermediate and 66% starting material was detected by HPLC. It seems Rh catalyst could not catalyze the last transformation. Subsequent electrospray ionization mass spectroscopic analysis of the

mixture solution showed peak at m/z+ 250.1606, which agreed with the enamine intermediate. The NMR spectrum of the mixture solution also confirms the enamine intermediate. The solvent of mixture solution was then removed in glove box, and Ir(COD)Cl/MP^2-SEGPHOS and DCE/acetone were added as same as previous hydrogenation condition. After hydrogenation, desired piperidines product was obtained with 95% ee and 92 % isolated yield, which indicated that this enamine is the intermediate.

Noteworthy, when carrying out this reaction with commercial available (not further died) acetone/DCE, a new intermediate was detected, HRMS showed peak at m/z+ 268.1694, which implied an addition of water. From C^{13}-NMR, we could find peak belongs to carbonyl group around 200. Due to instability, clean proton NMR is unable to achieve. But all evidences supported ketone compound **24** as an intermediate.

Figure 3.27. Intermediate transformation

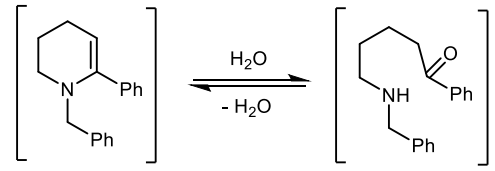

23
(M+H): 250.1606
Calculated: 250.1596

24
(M+H): 268.1694
Calculated: 268.1701

To confirm this, we try to synthesize **24**. Amide **25** was reacted with phenylmagnesium bromide to afford **24**. UPLC, HRMS and crude NMR all

support this product is same as the intermediate in hydrogenation. After removing solvent in glove box, original hydrogenation condition was charged, and product was detected by UPLC. Then we could confirm that ketone **24** is one of the intermediate in the hydrogenation of *N*-benzyl-2-phenylpyridium bromide, especially when water exists.

Figure 3.28. Synthesis of intermediate

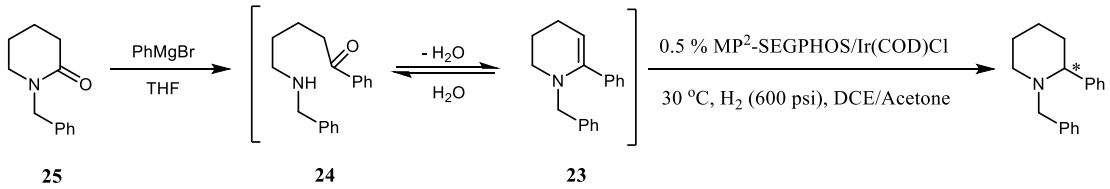

3.5.4 Kinetic Studies of Mechanism

Three issues were challenging us when we did kinetic study: 1) Concentrations are detected under high pressure. We used the remote IR sensor to monitor the intense of characteristic peak of starting material, which is 1640 cm^{-1}; 2) Solubility of *N*-benzyl-2-phenylpyridium bromide is quite small in organic solvents. Then high reaction temperature is required to increase solubility. However, even at 50 ^{o}C, the maximum concentration is 0.04 mmol/ml, which is quite low for IR sensor; 3) Only small amount of intermediate exists, it is impossible to detect it.

Then we carried out the hydrogenation of N-benzyl-2-phenylpyridium bromide at 50 ^{o}C with 0.5% mol iridium catalyst, under 300 psi of hydrogen gas in dichloroethane/acetone. Concentration of starting material was sketched following, which is a straight line. This revealed that the first step of hydrogenation is zero order to the concentration of starting material. By changing the loading (concentration) of iridium catalyst from 0.5% mol to 1% mol, to 2% mol and to 4% mol, the results suggested the first step of hydrogenation is first order with concentration of iridium catalyst.

Figure 3.29. Kinetics – Time Course

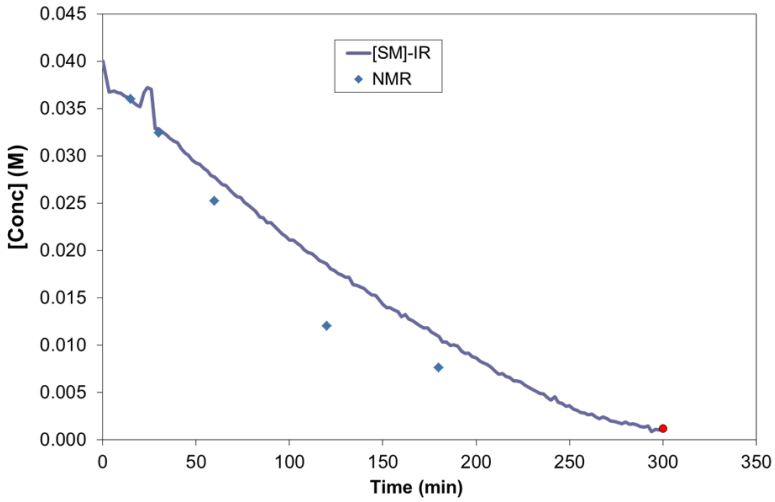

3.5.5 Suggested mechanism of hydrogenation of *N*-benzyl-2-phenylpyridium bromide

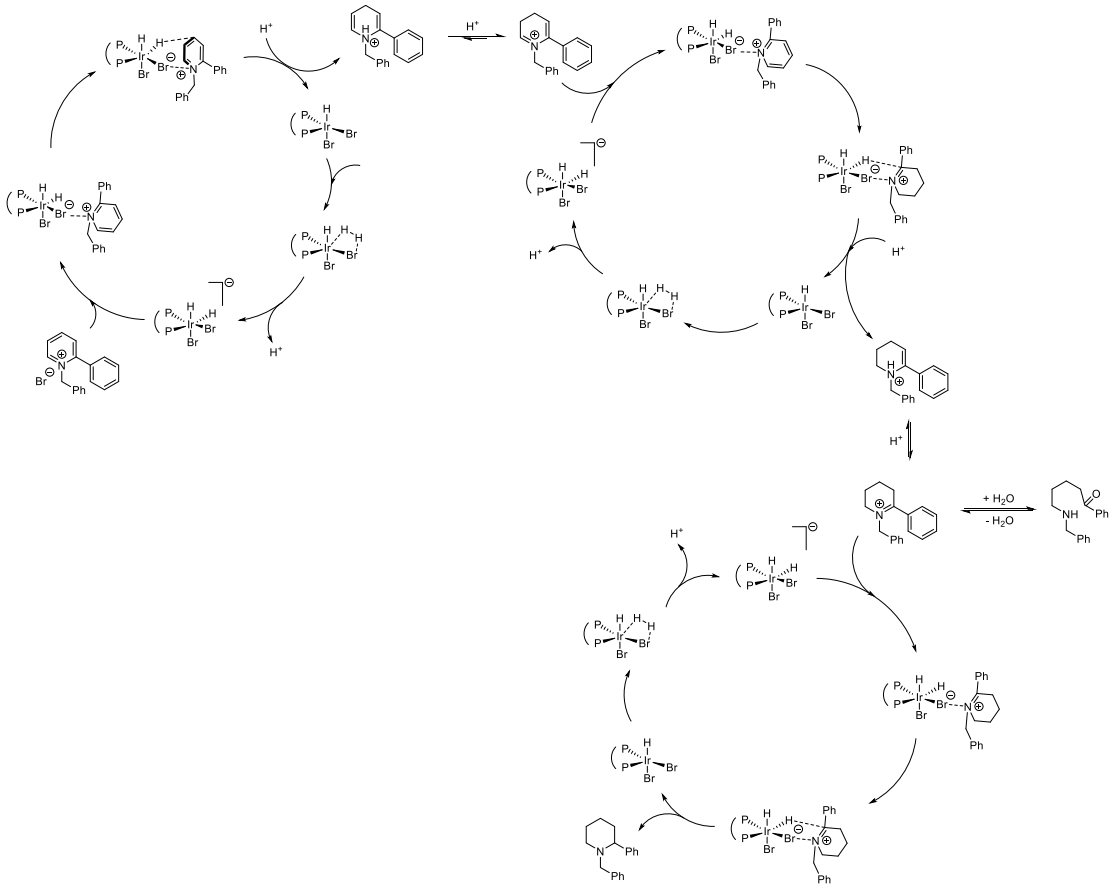

3.6 Experiment Section

3.6.1 General remarks

All reactions were performed in the nitrogen-filled glovebox or under nitrogen using standard Schlenk techniques unless otherwise noted. Column

chromatography was performed using Sorbent silica gel 60 (230 – 450 mesh). ^{1}H NMR, and ^{13}C NMR spectral data were obtained from Bruker 400 MHz spectrometers or Varian 500 MHz spectrometers. Chemical shifts are reported in ppm. Enantiomeric excess values were determined by chiral HPLC on an Acquity H-class (Waters Corp., milford, MA) or chiral SFC on an Acquity UPC2 (Waters Corp., milford, MA). All new products were further characterized by HRMS. A positive ion mass spectrum of sample was acquired on a Micromass 70-VSE mass spectrometer with an electron ionization source.

3.6.2 Typical procedure for the synthesis of 2-arylpyridine[1]

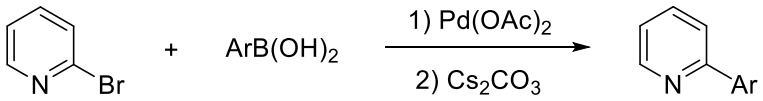

A Schlenk flask containing a magnetic stir bar was charged sequentially with $Pd(OAc)_2$ (0.074 g, 0.33 mmol), dppf (0.19 g, 0.34 mmol), 2-bromopyridine (0.79 g, 5 mmol), aryl boronic acid (6 mmol), and degassed dioxane (20 ml). The mixture was stirred at room temperature for 15 min. A solution of Cs_2CO_3 (3.26 g, 10 mmol) in 5 ml of degassed H_2O was added. The mixture was heated to reflux for 3 h. The organic layer was separated and extracted with EtOAc twice, and the combined organic extracts were dried over Na_2SO_4 and concentrated in vacuo. Purification was performed by a silica gel column, eluted with hexane/EtOAc to give desired products.

3.6.3 Typical procedure for the synthesis of pyridinium salts

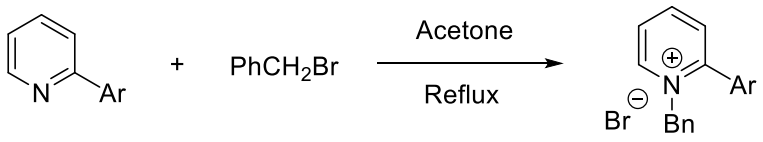

Pyridinium salts were synthesized according to the known literature method by the reaction of pyridine derivatives and benzyl bromide in acetone.[2]

General Procedure: A mixture of 2-substituted pyridine (10 mmol), benzyl bromide (12 mmol) and 5.0 ml acetone was heated at reflux for 40 h. The resulting precipitate was collected and rinsed with acetone to give the solid product which was directly used for the hydrogenation. If the desired product was not precipitated, the reaction mixture was purified by column chromatography on silica gel using CH2Cl2/MeOH (20:1) to give the desired products (47-87%).

3.6.4 Parallel Hydrogenation Screening Procedure

In a nitrogen-filled glovebox, ligands and metal sources were placed into 96 hydrogenation vials. 0.05 ml CH_2Cl_2 was added to each vials and stirring for 30 min. Then *N*-benzyl-2-phenylpyridium bromide dissolved in CH_2Cl_2 was added to each vial. Solvent was removed under reduced pressure in glovebox. Then desired solvent or solvent pairs were added. The vials were placed in a parallel hydrogenation block and following three hydrogen purges, pressurized

to 600 psi at 30 ^{o}C for 20 h. Selectivities and conversions were determined by direct sampling of the reaction mixture on SFC.

3.6.5 Scope of Asymmetric Pyridinium Salt Reductions

In a nitrogen-filled glovebox, MP^{2}-SEGPHOS (4.58 mg, 0.0099 mmol) and $[Ir(COD)Cl]_2$ (3.07 mg, 0.00457 mmol) were placed into a vial and stirring for 30 min in acetone (7.2 ml). Pyridinium salts (0.05 mmol) were placed into 4 ml hydrogenation vials. 0.2 ml catalyst solution and remaining solvent were added. The vials were placed in a parallel hydrogenation block and following three hydrogen purges, pressurized to 600 psi at 30 ^{o}C for 20 h. After carefully releasing the hydrogen, selectivities were determined by direct sampling of the reaction mixture on SFC or HPLC. Then saturated sodium carbonate was added and the mixture was stirred for 15-30 min. The organic layer was separated and extracted with CH_2Cl_2 twice, and the combined organic extracts were dried over Na_2SO_4 and concentrated under vacuum. Purification was performed by a silica gel column, eluted with hexane/EtOAc to give desired product.

3.6.6 Remove the Derivative Benzyl Protecting Group

After asymmetric hydrogenation of pyridinium salt (1.38 mmol), hydrogen gas was released from hydrogenation block. Solvent was evaporated under reduced pressure. 5 wt% Pd/C (20 wt%) and EtOH (20 ml) was charged. Then block was charged with 200 psi of H_2 without hydrogen purge. The

hydrogenation was performed at 40 ^{o}C for 20 h and the hydrogen was released carefully. The solvent was then removed and the residue was purified by column chromatograph to give the corresponding product, which reacted with trifluoroacetic anhydride to yield the corresponding trifluoroacetamide, and then analyzed by chiral HPLC.

3.6.7 Asymmetric Pyridinium Salt Reductions with D_2

In a nitrogen-filled glovebox, MP^2-SEGPHOS (4.58 mg, 0.0099 mmol) and $[Ir(COD)Cl]_2$ (3.07 mg, 0.00457 mmol) were placed into a vial and stirring for 30 min in acetone (7.2 ml). Pyridinium salts (0.05 mmol) were placed into 4 ml hydrogenation vials. 0.2 ml catalyst solution and remaining solvent were added. The vials were placed in a parallel hydrogenation block and following three D_2 purges, pressurized to 600 psi at 30 ^{o}C for 20 h. After carefully releasing the hydrogen, selectivities were determined by direct sampling of the reaction mixture on SFC or HPLC. Then saturated sodium carbonate was added and the mixture was stirred for 15-30 min. The organic layer was separated and extracted with CH_2Cl_2 twice, and the combined organic extracts were dried over Na_2SO_4 and concentrated under vacuum. Purification was performed by a silica gel column, eluted with hexane/EtOAc to give desired product.

3.6.8 Deuterium Content Quantification By NMR

Deuterium incorporation during hydrogenation was quantified by 1D ^{1}H spectrum and qualitatively verified by 2D multiplicity-edited HSQC spectrum. Integration was calibrated with the methylene protons (8) from the benzyl group. The two protons of position 5 are degenerated and their chemical shifts also overlap with that of proton 3axial; Equatorial protons of positions 3 and 4 also coincide. For these overlapping signals, quantification was made based on the assumption that the deuterium ratio is similar for both protons on the same methylene group. This assumption is valid according to multiplicity-edited HSQC. The blue contours represent signals from methylene CH_2 while the red contours represent signals from methylene CHD or methine CH. For positions 4 and 6, CHD is clearly predominant for both axial and equatorial protons, while on position 3 and 5, CH_2 is the major form as manifested by blue contours immediately to the downfield of the red CHD signals due to a small isotopic shift. The intensity ratio of red vs blue contours approximates of the D/H ratio of the corresponding germinal position.

1-benzyl-2-phenylpiperidine (2a): 97% yield, 96% ee, white solid. The

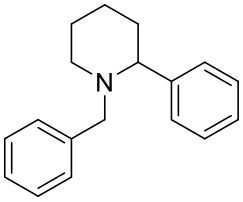

compound data were in good accordance with the literature.[3] ^{1}H-NMR (400 MHz, $CDCl_3$): δ 1.30-1.43 (m, 1H), 1.52-1.67 (m, 3H), 1.70-1.83 (m, 2H), 1.87-1.98 (dt, J_1=3.4 Hz, J_2=11.5 Hz, 1H), 2.80 (d, J=13.2 Hz, 1H), 2.92-3.00 (m, 1H), 3.10 (dt, J_1=2.6 Hz, J_2=11.2 Hz, 1H), 3.76 (d, J=13.8 Hz, 1H), 7.16-7.28 (m, 6H), 7.32 (t,

J=7.7 Hz, 2H), 7.45 (d, *J*=7.5 Hz, 2H). ^{13}C-NMR (400 MHz, $CDCl_3$): δ 25.3, 26.0, 37.0, 53.4, 59.8, 69.2, 126.5, 126.9, 127.5, 128.0, 128.5, 128.7, 139.9, 145.7. Enantiomeric excess was determined by SFC: OJ-3 column (150*4.6 mm), 200 Bar, 40 ^{o}C, CO_2/MeOH with 25 mM IBA=95:5 (0-4 min), 60:40 (4-6.4 min), 35:65 (6.4-6.5 min), 3 ml/min. HRMS calcd for C18H22N+: 252.1747, found: 252.1751.

1-benzyl-2-(m-tolyl)piperidine (2b): 99% yield, 96% ee, yellow oil,

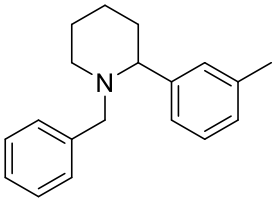

unknown compound. ^{1}H-NMR (400 MHz, $CDCl_3$): δ 1.31-1.40 (m, 1H), 1.56-1.66 (m, 3H), 1.75-1.79 (m, 2H), 1.89-1.95 (dt, J_1=3.6 Hz, J_2=14.4 Hz, 1H), 2.35 (s, 3H), 2.79 (d, *J*=13.5 Hz, 1H), 2.96 (d, *J*=11.3, 1H), 3.06 (dd, J_1=2.3 Hz, J_2=10.9 Hz, 1H), 3.77 (d, *J*=13.5 Hz, 1H), 7.03 (d, *J*=7.2 Hz, 1H), 7.17-7.26 (m, 8H). ^{13}C-NMR (400 MHz, $CDCl_3$): δ 21.5, 25.3, 26.0, 36.9, 53.4, 59.8. 69.3, 124.6, 126.5, 127.6, 128.0, 128.8, 137.9, 139.9, 145.7. Enantiomeric excess was determined by HPLC: Chiralpak AD-RH column (150*4.6 mm), MPA: 5 mM $Na_2B_4O_7$ pH=9.2, MPB: Acetonitrile, 80 % MPB isocratic at flow rate=1.0 ml/min. HRMS calcd for C19H24N+: 266.1903, found: 266.1905.

1-benzyl-2-(p-tolyl)piperidine (2c): 93% yield, 97% ee, yellow solid,

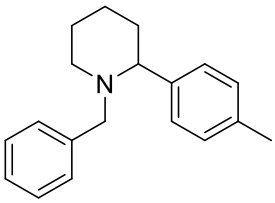

unknown compound. ^{1}H-NMR (500 MHz, CD_3CN): δ

1.35-1.42 (m, 1H), 1.49-1.61 (m, 3H), 1.69-1.76 (m, 2H), 1.89-1.95 (m, 1H), 2.32 (s, 3H), 2.78 (d, *J*=13.5 Hz, 1H), 2.87 (d, *J*=11.47, 1H), 3.10 (d, *J*=10.33 Hz, 1H), 3.67 (d, *J*=13.59 Hz, 1H), 7.15-7.36 (m, 9H). ^{13}C-NMR (400 MHz, $CDCl_3$): δ 21.1, 25.3, 26.1, 29.7, 37.0, 53.4, 59.7, 68.9, 126.5, 127.4, 128.0, 128.7, 129.2, 136.4, 139.9, 142.7. Enantiomeric excess was determined by SFC: OJ-3 column (150*4.6 mm), 200 Bar, 40 ^{o}C, CO_2/MeOH with 25 mM IBA=95:5 (0-4 min), 60:40 (4-6.4 min), 35:65 (6.4-6.5 min), 3 ml/min. HRMS calcd for C19H24N+: 266.1903, found: 266.1908.

1-benzyl-2-(2-methoxyphenyl)piperidine (2d): 90% yield, 95% ee, yellow

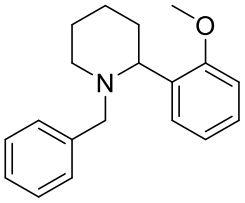

solid, unknown compound. ^{1}H-NMR (500 MHz, CD_3CN): δ 1.37-1.40 (m, 1H), 1.45-1.51 (m, 2H), 1.60-1.62 (m, 1H), 1.70-1.76 (m, 2H), 1.95-1.98 (m, 1H), 2.81 (d, *J*=13.33 Hz, 1H), 2.90 (d, *J*=11.11 Hz, 1H), 3.69 (d, *J*=13.35 Hz, 2H), 3.81 (s, 3H), 6.98 (dd, J_1=7.88 Hz, J_2=12.54 Hz, 2H), 7.19-7.26 (m, 6H), 7.68 (d, *J*=7.34 Hz, 1H). ^{13}C-NMR (400 MHz, $CDCl_3$): δ 25.3, 26.2, 35.5, 53.7, 55.5, 59.6, 59.9, 110.6, 121.1, 126.4, 127.2, 127.8, 128.0, 133.6, 140.0, 156.8. Enantiomeric excess was determined by SFC: OD-3 column (150*4.6 mm), 200 Bar, 40 ^{o}C, CO_2/IPA with 25 mM IBA=88:12 (0-3 min), 3 ml/min. HRMS calcd for C19H24NO+: 282.1852, found: 282.1859.

1-benzyl-2-(3-methoxyphenyl)piperidine (2e): 99% yield, 98% ee, yellow

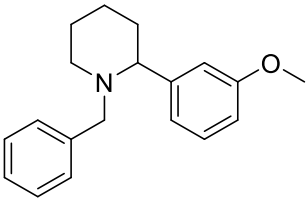

oil, unknown compound. ^{1}H-NMR (400 MHz, $CDCl_3$): δ 1.31-1.38 (m, 1H), 1.55-1.60 (m, 3H), 1.76-1.79 (m, 2H), 1.89-1.96 (ddd, J_1=4.1 Hz, J_2=5.6 Hz, J_3=11.4 Hz,1H), 2.81 (d, J=13.6 Hz, 1H), 2.96 (d, J=11.6 Hz, 1H), 3.08 (dd, J_1=2.4 Hz, J_2=11.0 Hz, 1H), 3.76 (d, J=4.9 Hz, 1H), 3.81 (s, 3H), 6.76 (ddd, J_1=0.9 Hz, J_2=2.6 Hz, J_3=8.2 Hz,1H), 7.02-7.05 (m, 2H), 7.16-7.31 (m 6H). ^{13}C-NMR (400 MHz, $CDCl_3$): δ 25.2, 26.0, 29.7, 36.9, 53.4, 55.2, 59.8, 69.2, 112.4, 112.7, 119.9, 125.5, 128.0, 128.7, 129.4, 139.9, 147.5, 159.9. Enantiomeric excess was determined by SFC: OJ-3 column (150*4.6 mm), 200 Bar, 40 ^{o}C, CO_2/MeOH with 25 mM IBA=95:5 (0-4 min), 60:40 (4-6.4 min), 35:65 (6.4-6.5 min), 3 ml/min. HRMS calcd for C19H24NO+: 282.1852, found: 282.1860.

1-benzyl-2-(4-methoxyphenyl)piperidine (2f): 95% yield, 97% ee, white

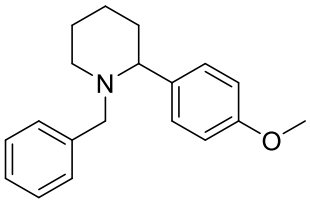

solid, unknown compound. ^{1}H-NMR (400 MHz, $CDCl_3$): δ 1.28-1.41 (m, 1H), 1.54-1.61 (m, 3H), 1.73-1.79 (m, 2H), 1.89-1.95 (dt, J_1=3.9 Hz, J_2=11.4 Hz, 1H), 2.78 (d, J=13.5 Hz, 1H), 2.95 (d, J=11.4 Hz, 1H), 3.05 (dd, J_1=2.8 Hz, J_2=11.0 Hz, 1H), 3.74 (d, J=5.3 Hz, 1H), 3.79 (s, 3H), 6.87 (d, J=8.8 Hz, 2H), 7.16-7.28 (m, 5H), 7.36 (d, J=8.4 Hz, 2H). ^{13}C-NMR (400 MHz, $CDCl_3$): δ 25.3, 26.1, 37.0, 53.4, 55.2, 59.6, 68.5, 113.9, 126.5, 127.9, 128.4, 128.7, 137.8, 140.0, 158.5. Enantiomeric excess was determined by SFC: OJ-3 column (150*4.6 mm),

200 Bar, 40 ^{o}C, CO_2/MeOH with 25 mM IBA=95:5 (0-4 min), 60:40 (4-6.4 min), 35:65 (6.4-6.5 min), 3 ml/min. HRMS calcd for C19H24NO+: 282.1852, found: 282.1858.

N-(4-(1-benzylpiperidin-2-yl)phenyl)acetamide (2g): 97% yield, 95% ee, yellow solid, unknown compound. ^{1}H-NMR (400 MHz, $CDCl_3$): δ 1.32-1.41 (m, 1H), 1.53-1.62 (m, 3H), 1.71-1.78 (m, 2H), 1.89-1.96 (dt, J_1=4.0 Hz, J_2=17.8 Hz, 1H), 2.13 (m, 3H), 2.79 (d, J=13.5 Hz, 1H), 2.95 (d, J=11.4 Hz, 1H), 3.07 (dd, J_1=2.0 Hz, J_2=10.8 Hz, 1H), 3.74 (d, J=13.5 Hz, 1H), 7.18-7.54 (m, 10H). ^{13}C-NMR (400 MHz, $CDCl_3$): δ 14.1, 22.7, 24.5, 25.2, 25.9, 29.4, 31.9, 36.9, 53.3, 59.7, 68.6, 120.2, 126.6, 127.9, 128.0, 128.7, 136.7, 139.6, 141.7, 168.4. Enantiomeric excess was determined by HPLC: Chiralcel OJ-RH column (150*4.6 mm), MPA: 5 mM $Na_2B_4O_7$ pH=9.2, MPB: Acetonitrile, 37 % MPB isocratic at flow rate=1.0 ml/min. HRMS calcd for C20H25N2O+: 309.1961, found: 309.1968.

1-benzyl-2-(4-(tert-butyl)phenyl)piperidine (2h): 96% yield, 96% ee, white solid, unknown compound. ^{1}H-NMR (400 MHz, $CDCl_3$): δ 1.25-1.40 (m, 10H), 1.58-1.63 (m, 3H), 1.75-1.78 (m, 2H), 1.91 (ddd, J_1=4.7 Hz, J_2=7.6 Hz, J_3=11.4 Hz,1H),

2.78 (d, *J*=13.6 Hz, 1H), 2.95 (d, *J*=11.3 Hz, 1H), 3.07 (dd, J_1=2.6 Hz, J_2=11.0 Hz, 1H), 3.78 (d, *J*=13.6 Hz, 1H), 7.18-7.37 (m, 9H). ^{13}C-NMR (400 MHz, $CDCl_3$): δ 25.3, 26.1, 31.5, 34.4, 37.0, 53.5, 59.8, 68.9, 125.3, 126.5, 127.0, 128.0, 128.7, 140.1, 142.5, 149.6. Enantiomeric excess was determined by SFC: OZ-3 column (150*4.6 mm), 200 Bar, 40 ^{o}C, CO_2/MeOH with 25 mM IBA=97:3 (0-2 min), 3:40-60:40 (2-4 min), 60:40 (4-10 min), 3 ml/min. HRMS calcd for C22H30N+: 308.2373, found: 308.2375.

1-benzyl-2-(4-chlorophenyl)piperidine (2i): 96% yield, 98% ee, yellow solid, unknown compound. ^{1}H-NMR (400 MHz, $CDCl_3$): δ 1.26-1.41 (m, 1H), 1.50-1.59 (m, 3H), 1.72-1.79 (m, 2H), (dt, J_1=3.6 Hz, J_2=11.4 Hz, 1H), 2.8 (d, *J*=13.6 Hz, 1H), 2.96 (d, *J*=11.5 Hz, 1H), 3.09 (dd, J_1=2.5 Hz, J_2=11.0 Hz, 1H), 3.71 (d, *J*=13.5 Hz, 1H), 7.17-7.40 (m, 9H). ^{13}C-NMR (400 MHz, $CDCl_3$): δ 25.1, 25.9, 37.0, 53.3, 59.8, 68.4, 126.6, 128.0, 128.6, 128.7, 128.8, 132.3, 139.5, 144.3. Enantiomeric excess was determined by SFC: OJ-3 column (150*4.6 mm), 200 Bar, 40 ^{o}C, CO_2/MeOH with 25 mM IBA=95:5 (0-4 min), 60:40 (4-6.4 min), 35:65 (6.4-6.5 min), 3 ml/min. HRMS calcd for C18H21NCl+: 286.1357, found: 286.1361.

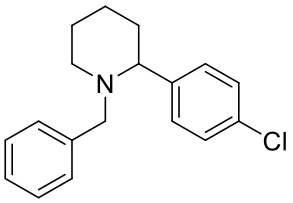

2-([1,1'-biphenyl]-4-yl)-1-benzylpiperidine (2j): 96% yield, 94% ee, white solid, unknown compound. ^{1}H-NMR (400 MHz, $CDCl_3$): δ 1.37-1.43 (m, 1H), 1.62 (m, 3H), 1.80-1.82 (m, 2H), 1.96 (m, 1H), 2.85 (d, *J*=11.8 Hz, 1H), 3.00 (d, *J*=8.7 Hz, 1H), 3.16 (d, *J*=8.2 Hz, 1H), 3.83 (d, *J*=10.0 Hz, 1H), 7.21-7.59 (m, 14H). ^{13}C-NMR (400 MHz, $CDCl_3$): δ 25.2, 26.0, 29.7, 37.0, 53.4, 59.9, 68.9, 126.6, 127.1, 127.3, 127.9, 128.1, 128.7, 139.8, 141.1. Enantiomeric excess was determined by SFC: AD-3 column (150*4.6 mm), 200 Bar, 40 ^{o}C, CO_2/IPA with 25 mM IBA=78:22 (0-4 min), 3 ml/min. HRMS calcd for C24H26N+: 328.2060, found: 328.2066.

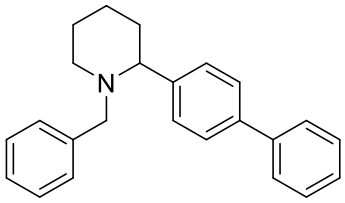

1-benzyl-2-(2,4-dichlorophenyl)piperidine (2k): 94% yield, 93% ee, yellow solid, unknown compound. ^{1}H-NMR (400 MHz, $CDCl_3$): δ 1.36-1.42 (m, 2H), 1.55-1.63 (m, 2H), 1.78-1.83 (m, 2H), 2.00 (dt, J_1=2.9 Hz, J_2=11.6 Hz, 1H), 2.89 (d, *J*=13.7 Hz, 1H), 2.99 (d, *J*=11.4 Hz, 1H), 3.67 (m, 2H), 7.2-7.39 (m, 7H), 7.55 (d, *J*=8.4 Hz, 1H). ^{13}C-NMR (400 MHz, $CDCl_3$): δ 24.9, 25.8, 35.1, 53.3, 59.6, 63.4, 126.7, 127.7, 128.1, 128.6, 129.1, 129.7, 132.5, 133.7, 139.1, 141.3. Enantiomeric excess was determined by SFC: OJ-3 column (150*4.6 mm), 200 Bar, 40 ^{o}C, CO_2/MeOH with 25 mM IBA=95:5 (0-4 min), 60:40 (4-6.4

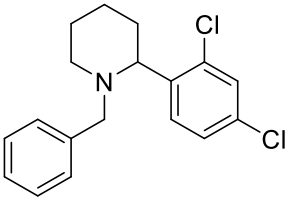

min), 35:65 (6.4-6.5 min), 3 ml/min. HRMS calcd for C18H20NCl2+: 320.0967, found: 320.0974.

1-benzyl-2-(3,5-difluorophenyl)piperidine (2l): 95% yield, 98% ee, white solid, unknown compound. ^{1}H-NMR (400 MHz, $CDCl_3$): δ 1.28-1.39 (m, 1H), 1.48-1.61 (m, 3H), 1.73-1.78 (m, 2H), 1.92 (dt, J_1=3.3 Hz, J_2=11.6 Hz, 1H), 2.83 (d, J=13.5 Hz, 1H), 2.95 (d, J=13.4 Hz, 1H), 3.10 (dd, J_1=2.6 Hz, J_2=11.0 Hz, 1H), 3.73 (d, J=13.5 Hz, 1H), 6.65 (tt, J_1=2.4 Hz, J_2=8.9 Hz, 1H), 7.00 (dd, J_1=2.1 Hz, J_2=8.5 Hz, 2H), 7.19-7.30 (m, 5H). ^{13}C-NMR (400 MHz, $CDCl_3$): δ 24.9, 25.8, 36.8, 53.1, 60.0, 68.6, 101.9, 102.2, 102.5, 109.9, 110.2, 126.8, 128.1, 128.6, 139.2, 150.2, 161.9, 164.5. Enantiomeric excess was determined by HPLC: Chiralpak OJ-RH column (150*4.6 mm), MPA: 5 mM $Na_2B_4O_7$ pH=9.2, MPB: Acetonitrile, 60% (0-10 min), 70% (10-13 min) MPB isocratic at flow rate=1.0 ml/min. HRMS calcd for C18H20NF2+: 288.1558, found: 288.1565.

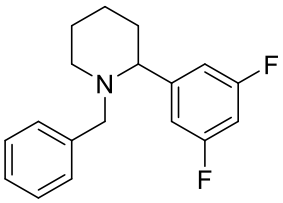

1-benzyl-2-(naphthalen-2-yl)piperidine (2m): 88% yield, 94% ee, yellow solid, unknown compound. ^{1}H-NMR (400 MHz, $CDCl_3$): δ 1.35-1.43 (m, 1H), 1.59-1.61 (m, 3H), 1.76-1.82 (m, 2H), 1.93-2.01 (m, 1H), 2.85 (d, J=13.5 Hz, 1H), 3.01 (d, J=13.5 Hz, 1H), 3.29 (dd, J_1=2.6 Hz, J_2=10.8 Hz, 1H), 3.79 (d, J=13.5 Hz,

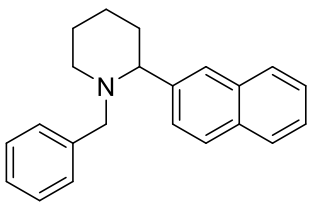

1H), 7.15-7.26 (m, 5H), 7.39-7.64 (m, 2H), 7.68-7.87 (m, 5H). ^{13}C-NMR (400 MHz, $CDCl_3$): δ 25.3, 26.1, 29.5, 36.9, 53.4, 59.9, 69.3, 125.4, 125.7, 125.9, 126.2, 126.6, 127.7, 128.0, 128.3, 128.8, 132.9, 133.6, 139.7, 143.3. Enantiomeric excess was determined by SFC: OJ-3 column (150*4.6 mm), 200 Bar, 40 ^{o}C, CO_2/MeOH with 25 mM IBA=95:5 (0-4 min), 60:40 (4-6.4 min), 35:65 (6.4-6.5 min), 3 ml/min. HRMS calcd for C22H24N+: 302.1903, found: 302.1909.

1-benzyl-2-methylpiperidine (2n): 81% yield, 33% ee, colorless solid. The

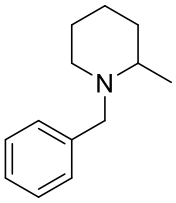

compound data were in good accordance with the literature.[4] ^{1}H-NMR (400 MHz, $CDCl_3$): δ1.21 (d, J = 6.4 Hz, 3H), 1.27-1.54 (m, 4H), 1.64-1.70 (m, 2H), 1.97 (td, J = 11.6, 3.6 Hz, 1H), 2.29-2.35 (m, 1H), 2.76 (dt, J_1=3.9 Hz, J_2=11.4 Hz, 1H), 3.19 (d, J =13.4 Hz, 1H), 4.00 (d, J = 13.4 Hz, 1H), 7.23-7.36 (m, 5H). ^{13}C-NMR (400 MHz, CDCl3) δ 19.9, 24.3, 26.3, 34.9, 52.4, 56.6, 58.7, 126.9, 128.3, 129.4, 139.6. Enantiomeric excess was determined by SFC: OZ-3 column (150*4.6 mm), 200 Bar, 40 ^{o}C, CO_2/MeOH with 25 mM IBA=99:1 to 60:40 (0-5 min), 60:40 (5-8 min), 3 ml/min. HRMS calcd for C13H20N+: 190.1596, found: 190.1598.

1-benzyl-2-isopropylpiperidine (2o): 24% yield, 69% ee, colorless solid. The

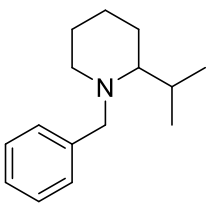

compound data were in good accordance with the literature.[5]

^{1}H-NMR (400 MHz, $CDCl_3$): δ 0.91-0.94 (m, 6H), 1.21-1.31 (m, 2H), 137-1.44 (m, 2H), 1.58-1.62 (m, 1H), 1.72-1.75 (m, 1H), 1.91-1.97 (m, 1H), 1.99-2.02 (m, 1H), 2.21-2.29 (m, 1H), 2.81 (dtd, J_1=1.5 Hz, J_2=3.6 Hz, J_3=3.8 Hz, J_4=11.9 Hz, 1H), 3.09 (d, J=13.4 Hz, 1H), 4.10 (d, J=13.4 Hz, 1H), 7.19-7.34 (m, 5H). ^{13}C-NMR (400 MHz, $CDCl_3$): δ 16.0, 20.2, 23.5, 27.6, 52.7, 56.6, 66.5, 126.5, 128.1, 128.8, 140.4. Enantiomeric excess was determined by SFC: OZ-3 column (150*4.6 mm), 200 Bar, 40 ^{o}C, CO_2/MeOH with 25 mM IBA=99:1 to 60:40 (0-5 min), 60:40 (5-8 min), 3 ml/min. HRMS calcd for C15H24N+: 218.1909, found: 218.1905.

1,2-dibenzylpiperidine (2p): 99% yield, 42% ee, colorless solid. The

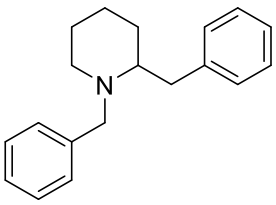

compound data were in good accordance with the literature.[6] ^{1}H-NMR (400 MHz, $CDCl_3$): δ 1.22-1.36 (m, 2H), 1.48-1.56 (m, 3H), 1.58-1.66 (m, 1H), 2.22 (m, 1H), 2.60 (m, 2H), 2.64-2.69 (m, 1H), 2.77 (m, 1H), 3.17 (d, J= 9.8 Hz, 1H), 3.49 (d, J= 13.6 Hz, 1H), 4.05 (d, J= 13.6 Hz, 1H), 7.16-7.38 (m, 10H). ^{13}C-NMR (400 MHz, $CDCl_3$): δ 22.5, 25.4, 29.4, 50.9, 58.6, 61.8, 125.8, 126.7, 128.2, 128.3, 128.9, 129.4, 139.8, 140.5. Enantiomeric excess was determined by SFC: OJ-3 column (150*4.6 mm), 200 Bar, 40 ^{o}C, CO_2/MeOH with 25 mM IBA=95:5 (0-4 min), 60:40 (4-8 min), 3 ml/min. HRMS calcd for C19H24N+: 266.1909, found: 266.1917.

2-phenylpiperidine (3a): 91% yield, 92% ee, yellow oil. The compound

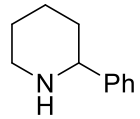

data were in good accordance with the literature.[7] ^{1}H-NMR (400 MHz, $CDCl_3$): δ 1.48-1.90 (m, 6H), 2.79 (m, 1H), 3.19 (d, *J*=11.0 Hz, 1H), 3.58 (d, *J*=11.2 Hz, 1H), 7.20-7.38 (m, 5H). ^{13}C-NMR (400 MHz, $CDCl_3$): δ 25.4, 25.9, 35.0, 47.8, 62.4, 126.6, 127.0, 128.4, 145.6. Enantiomeric excess was determined by GC: Beta-390 column, 140 ^{o}C, 1 ml/min, 45 min.

1-(4-methoxybenzyl)-2-phenylpiperidine (5b): 96% yield, 95% ee, yellow

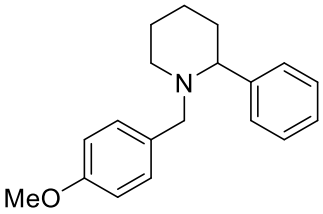

solid. The compound data were in good accordance with the literature.[8] ^{1}H-NMR (500 MHz, CD_3CN): δ 1.39-1.44 (m, 1H), 1.48-1.65 (m, 3H), 1.74-1.77 (m, 2H), 1.93-1.95 (m, 1H), 2.76 (d, *J*=13.3 Hz, 1H), 2.90-2.92 (d, *J*=11.65 Hz, 1H), 3.13-3.16 (dd, J_1=2.53 Hz, J_2=11.04 Hz, 1H), 3.61-3.63 (d, *J*=13.25 Hz, 1H), 3.78 (m, 3H), 6.85-6.88 (t, *J*=5.74 Hz, 2H), 7.18 (d, *J*=8.4 Hz, 2H), 7.27 (t, *J*=7.35 Hz, 1H), 7.38 (t, *J*=7.72 Hz, 2H), 7.50 (d, *J*=7.29 Hz, 2H). ^{13}C-NMR (400 MHz, $CDCl_3$): δ 25.3, 26.0, 37.0, 53.2, 55.2, 59.1, 69.1, 113.4, 126.8, 127.5, 128.5, 129.8, 131.7, 145.8, 158.4. Enantiomeric excess was determined by SFC: OJ-3 column (150*4.6 mm), 200 Bar, 40 ^{o}C, CO_2/MeOH

with 25 mM IBA=95:5 (0-4 min), 60:40 (4-6.4 min), 35:65 (6.4-6.5 min), 3 ml/min. HRMS calcd for C19H24NO+: 282.1852, found: 282.1863.

methyl 2-((2-phenylpiperidin-1-yl)methyl)benzoate (5c): 93% yield, 94.4% ee, white solid, unknown compound. ^{1}H-NMR (500 MHz, CD_3CN): δ 1.43-1.49 (m, 1H), 1.61-1.65 (m, 3H), 1.80-1.83 (m, 2H), 2.03 (dd, J_1=11.27 Hz, J_2=15.2 Hz, 1H), 2.87 (d, *J*=11.5 Hz, 1H), 3.28 (d, *J*=11.4 Hz, 1H), 3.40 (d, *J*=15.8 Hz, 1H), 3.78-3.81 (m, 4H), 7.23 (t, *J*=7.30 Hz, 1H), 7.31 (t, *J*=7.45 Hz, 3H), 7.45 (d, *J*=7.58 Hz, 2H), 7.53 (t, *J*=7.57 Hz, 1H), 7.70 (d, *J*=7.72 Hz, 1H), 7.85 (d, *J*=7.80 Hz, 1H). ^{13}C-NMR (400 MHz, $CDCl_3$): δ 25.3, 26.1, 37.1, 51.8, 54.0, 56.9, 69.4, 125.9, 126.8, 127.4, 128.4, 129.1, 129.7, 130.0, 131.7, 142.0, 145.5, 168.3. Enantiomeric excess was determined by SFC: OJ-3 column (150*4.6 mm), 200 Bar, 40 ^{o}C, CO_2/MeOH with 25 mM IBA=95:5 (0-4 min), 60:40 (4-6.4 min), 35:65 (6.4-6.5 min), 3 ml/min. HRMS calcd for C20H24NO2+: 310.1802, found: 310.1812.

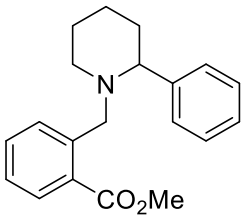

1-methyl-2-phenylpiperidine (5d): 75% yield, 81% ee, white oil. The compound data were in good accordance with the literature.[9] ^{1}H-NMR (400 MHz, $CDCl_3$): δ 1.35 (m, 1H), 1.6 (m, 4H), 1.7 (m, 3H), 1.8 (m, 1H), 1.99 (s, 3H), 2.1 (m, 1H), 2.75 (m, 1H), 3.10 (d,

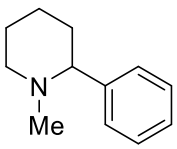

J=8.4 Hz, 1H), 7.2-7.4 (m, 5H). ^{13}C-NMR (400 MHz, $CDCl_3$): δ 25.0, 26.2, 35.9, 44.5, 57.6, 71.1, 126.9, 127.4, 128.7, 144.8. Enantiomeric excess was determined by HPLC: OJ-3R column (150*4.6 mm), MeCN/5mM $Na_2B_4O_7$ (PH~9.2, aq)=80:20, 1mL/min. HRMS calcd for C12H18N+: 176.1434, found: 176.1436.

1-ethyl-2-phenylpiperidine (5e): 94% yield, 94% ee, white solid, unknown

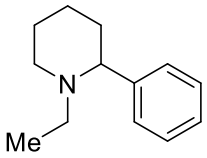

compound. ^{1}H-NMR (400 MHz, $CDCl_3$): δ 1.19-1.31 (m, 4H), 1.50 (m, 1H), 1.56-1.65 (m, 4H), 1.89-2.00 (m, 2H), 2.46 (dd, J_1=7.1 Hz, J_2=12.7 Hz, 1H), 2.95 (d, *J*=10.8 Hz, 1H), 3.10 (d, *J*=10.4 Hz, 1H), 7.16-7.25 (m, 5H). ^{13}C-NMR (400 MHz, $CDCl_3$): δ 11.0, 25.2, 26.1, 29.7, 36.6, 49.1, 52.6, 68.8, 126.7, 127.5, 128.3. Enantiomeric excess was determined by HPLC: OJ-3R column (150*4.6 mm), MeCN/5mM $Na_2B_4O_7$ (PH~9.2, aq)=80:20, 1mL/min. HRMS calcd for C13H20N+: 190.1590, found: 190.1599.

1-isopropyl-2-phenylpiperidine (5f): 82% yield, 96% ee, white solid. The

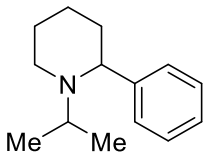

compound data were in good accordance with the literature.[10] ^{1}H-NMR (400 MHz, $CDCl_3$): δ 0.70 (t, *J*=7.4 Hz, 3H), 1.33-1.39 (m, 3H), 1.53-1.70 (m, 5H), 1.84 (m, 1H), 2.03 (dt, J_1=3.4 Hz, J_2=11.5 Hz, 1H), 2.36 (ddd, J_1=7.1 Hz, J_2=9.6 Hz, J_2=12.6 Hz, 1H), 2.98 (dd, J_1=2.7 Hz, J_2=11.0 Hz, 1H), 3.17 (d, *J*=11.2 Hz, 1H), 7.21-7.33

(m, 5H). ^{13}C-NMR (400 MHz, $CDCl_3$): δ 11.8, 19.2, 25.2, 26.2, 36.8, 53.3, 57.3, 69.2, 126.6, 127.5, 128.3, 145.6. Enantiomeric excess was determined by SFC: Column Lux 4 Cellulose (150*4.6 mm), 200 Bar, 40 ^{o}C, CO_2/MeOH with 25 mM IBA=70:30, 3 ml/min. HRMS calcd for C14H22N+: 204.1747, found: 204.1755.

ethyl 2-(2-phenylpiperidin-1-yl)acetate (5g): 82% yield, 96% ee, yellow solid,

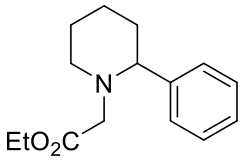

unknown compound. ^{1}H-NMR (400 MHz, $CDCl_3$): δ 1.18-1.26 (m, 3H), 1.37-1.44 (m, 1H), 1.60-1.79 (m, 5H), 2.49 (dt, J_1=4.1 Hz, J_2=11.1 Hz, 1H), 2.89 (d, J=16.7 Hz, 1H), 3.09 (d, J=11.4 Hz, 1H), 3.22 (d, J=16.7 Hz, 1H), 3.43 (dd, J_1=2.6 Hz, J_2=11.0 Hz, 1H), 4.08 (m, 2H), 7.23-7.35 (m, 5H). ^{13}C-NMR (400 MHz, $CDCl_3$): δ 14.2, 25.0, 26.1, 36.2, 53.9, 56.5, 60.0, 66.9, 127.2, 127.7, 128.5, 144.1, 171.2. Enantiomeric excess was determined by HPLC: OJ-3R column (150*4.6 mm), MeCN/5mM $Na_2B_4O_7$ (PH~9.2, aq)=80:20, 1mL/min. HRMS calcd for C14H20NO2+: 234.1489, found: 234.1495.

Cis-1-benzyl-3-methyl-2-phenylpiperidine: 28% yield, 12% ee, white solid,

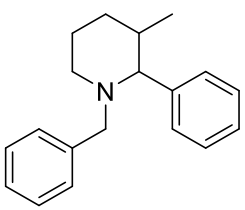

unknown compound. ^{1}H-NMR (400 MHz, $CDCl_3$): δ 0.80 (d, J =7.0 Hz, 3H), 1.30 (m, 1H), 1.59-1.62 (m, 2H), 1.72-1.75 (m, 1H), 1.82-1.88 (m, 2H), 2.72 (d, J =14.0 Hz, 1H), 2.91

(dt, J_1=3.21 Hz, J_2=11.1 Hz, 1H), 3.33 (d, J =3.3Hz, 1H), 3.84 (d, J =14.0 Hz, 1H), 7.12-7.29 (m, 10H). ^{13}C-NMR (400 MHz, CDCl3) δ 14.1, 21.0, 32.3, 35.6, 54.1, 60.1, 71.7, 126.4, 126.5, 127.9, 128.1, 128.4, 128.5, 140.2, 143.2. Enantiomeric excess was determined by SFC: OJ-3 column (150*4.6 mm), 200 Bar, 40 ^{o}C, CO_2/MeOH with 25 mM IBA=95:5 (0-4 min), 60:40 (4-6.4 min), 35:65 (6.4-6.5 min), 3 ml/min.. HRMS calcd for C19H24N+: 266.1909, found: 266.1912.

Reference:

1. For selected reviews, see: a) P. D. Bailey, P. A. Millwood, P. D. Smith, *Chem. Commun.* **1998**, 633; b) F. Glorius, *Org. Biomol. Chem.* **2005**, *3*, 4171; c) D.-S. Wang, Q.-A. Chen, S.-M. Lu, Y.-G. Zhou, *Chem. Rev.* **2012**, *112*, 2557.
2. [2] For a review and selected examples, see: a) T. C. Nugent, Ed. *Chiral Amine Synthesis*, Wiley-VCH, Weinheim, **2010**; b) Y. Zhang, Y.-B. Liu, Y. Li, S.-G. Ma, L. Li, J. Qu, D. Zhang, X.-G. Chen, J.-D. Jiang, S.-S. Yu, *J. Nat. Prod.* **2013**, *76*, 1058; c) Z. Peng, J. W. Wong, E. C. Hansen, A. L. A. Puchlopek-Dermenci, H. J. Clarke, *Org. Lett.* **2014**, *16*, 860; d) Y. Liu, H. Du, *J. Am. Chem. Soc.* **2013**, *135*, 12968.
3. Z.-S. Ye, M.-W. Chen, Q.-A. Chen, L. Shi, Y. Duan, Y.-G. Zhou, *Angew. Chem. Int. Ed*. **2012**, *51*, 10181; *Angew. Chem*. **2012**, *124*, 10328.
4. F. Glorius, N. Spielkamp, S. Holle, R. Goddard, C.W. Lehmann, *Angew. Chem.Int. Ed*. **2004**, *43*, 2850.
5. For the stepwise reduction of ethyl nicotinate example, see: A. Lei, M. Chen, M. He, X. Zhang, *Eur. J. Org. Chem*. **2006**, 4343.
6. M. Studer, C. Wedemeyer-Exl, F. Spindler, H.-U. Blaser, *Monatsh. Chem*. **2000**, *131*, 1335.
7. X.-B. Wang, W. Zeng, Y.-G. Zhou, *Tetrahedron Lett*. **2008**, *49*, 4922.
8. a) C. Y. Legault, A. B. Charette, *J. Am. Chem. Soc*. **2005**, *127*, 8966; b) C. Y. Legault, A. B. Charette, P. G. Cozzi, *Heterocycles* **2008**, *76*, 1271.

9. M. Chang, Y. Huang, S. Liu, Y. Chen, S. W. Krska, I. W. Davies and X. Zhang, *Angew. Chem., Int. Ed.*, **2014**, *53*, 12761.
10. Y. Kita, A. Iimuro, S. Hida and K. Mashima, *Chem. Lett.*, **2014**, *43*, 284.
11. Mu-Wang Chen, Zhi-Shi Ye, Zhang-Pei Chen, Bo Wu and Yong-Gui Zhou, *Org. Chem. Front.*, **2015**, *2*, 586–589.
12. https://en.wikipedia.org/wiki/High-throughput_screening.
13. https://www.chem.upenn.edu/content/penn-chemistry-upennmerck-high-throughput-experimentation-laboratory
14. Evolution of Ultra-High-Throughput Screening, http://www.labmanager.com/lab-product/2011/11/evolution-of-ultra-high-throughput-screening?fw1pk=2#.Vh0g4_lViko
15. T. W. Greene, P. G. M. Wuts, *Protective Groups in Organic Synthesis*, Wiley-Interscience, New York, **1999**.
16. The only reported use of MP^2-SEGPHOS was for asymmetric hydrogenation of *N*-acetamidocinnamic acid, which gave the product in 60% *ee*, see: H. Shimizu, T. Saito, I. Nagasaki, EP 1419815 A1, **2004**.
17. a) W. Schafer, A. Schweig, G. Markl, H. Hauptmann, F. Mathey, *Angew. Chem. Int. Ed*. **1973**, *12*, 145; *Angew. Chem.* **1973**, *85*, 140; b) Schafer, W.; Schweig, A.; Mathey, F.; *J. Am. Chem. Soc*. **1976**, *98*, 407.
18. The value of the intracyclic CPC angle of phosphole (90.7° for phenylphsphole) is much smaller than normal CPC angles (100°) which indicates that the system is very strained and rigid; see: P. Coggon, A. T. McPhail, *J. Chem. Soc*., *Dalton Trans*. **1973**, 1888.
19. W. Egan, R. Tang, G. Zon, K. Mislow, *J. Am. Chem. Soc.* **1971**, *93*, 6205.
20. For a recent example, see: G. Liu, X. Liu, Z. Cai, G. Jiao, G. Xu, W. Tang, *Angew. Chem. Int. Ed.* **2013**, *52*, 4235.
21. For a review of halide effects in transition metal catalysis, see: K. Fagnou, M. Lautens, *Angew. Chem. Int. Ed*. **2002**, *41*, 26; *Angew. Chem.* **2002**, *114*, 26.